



United Kingdom Becomes Tenth Member of ESO

CATHERINE CESARSKY, *Director General of ESO*

On 8–9 July 2002 the ESO Council meets in London to mark the occasion of the United Kingdom becoming the tenth country to join the European Southern Observatory. Forty years ago, when ESO was created by the governments of Belgium, France, Germany, Netherlands and Sweden, the United Kingdom opted not to become a member, but rather to centre its astronomical observations of the southern sky on a new telescope to be built in collaboration with Australia. The recent United Kingdom's interest in joining ESO arose from ESO's success in creating large optical telescopes, high-performance instrumentation and data handling methods, as well as the prospect of participating in key future projects such as the Atacama Large Millimeter Array (ALMA) and the development of extremely large optical telescopes, where it was recognised that the scale of the projects were such that all European nations would be required to work together if these ambitious projects were to be realised in a timely fashion. The participation of such a highly developed astronomical community as the United Kingdom's will strengthen ESO by its significant contribution of intellectual, technical, and financial resources. As part of its adherence to ESO, the United Kingdom will contribute more than 20 per cent of ESO's annual operational budget, an amount based (as are the other countries' contributions) on its gross domestic product.

Given the mutual benefits of U.K. membership of ESO to both parties, it is

not surprising that the negotiations over the details of U.K. entry were brief. In late 1999, I began informal meetings with Ian Halliday, Chief Executive of PPARC, the British institution responsible for funding astronomy, to discuss the U.K. joining ESO. At first, the U.K. expressed the desire to enter ESO progressively, by "ramping up" an initially small annual contribution to that called for by the ESO Convention, but it was soon recognised that this was unacceptable to ESO. Early in March 2000, when the British Parliament took up the question of the U.K.'s entry, Lord Tansley mentioned in a debate in the House of Lords the discoveries to be expected from astronomers using the VLT, and said, "Unfortunately, none of those astronomers will be British – that is, if this country fails to subscribe with our European partners in the setting-up costs of this incredible telescope. In effect, this will mean that astronomy will hardly be worth pursuing as a career in Britain in the new millennium." An exploratory meeting between members of PPARC and U.K. astronomers with ESO Council members and executives on May 24, 2000 led to an understanding that the U.K. would seek to join ESO as soon as possible, so that British astronomers could participate as fully and swiftly as possible in VLT, VLTi, ALMA, and future large telescope development projects. In addition, the special contribution to cover past investments by ESO would be provided partly in cash and partly in kind. By December 2000, John Taylor, the U.K.'s

Director-General of Research Councils, sent me a letter formally requesting that the United Kingdom become a full member of ESO in mid-2002. A working group was then established to discuss possible in-kind contributions, and the detailed negotiations extended over most of the year 2001. On 15 November 2001, I received a letter from Lord Sainsbury of Turville, the U.K.'s Parliamentary Undersecretary of State for Science, confirming that "the United Kingdom wishes to accede to ESO membership on 1 July 2002, on the mutually agreed terms." These terms include the normal annual subscription, the in-cash portion of the entrance fee, and the in-kind contribution ("which will include delivery of the VISTA [four-metre] telescope, which will be [installed at Paranal and devoted to infrared surveys], ESO access to the Wide-Field Camera on the UK Infrared Telescope [on Mauna Kea], and a programme of e-science"). At the ESO Council meeting on 3 December 2001, the Council unanimously approved a resolution in favour of U.K. accession to ESO. In the UK, this decision has now been ratified by the British Parliament; the necessary letters have been signed and exchanged; and the instrument of accession has been deposited at the Ministry of Foreign Affairs in Paris, as required by the ESO Convention. We can now look forward to a new and fruitful era within ESO, significantly enlarged by the accession of the United Kingdom, and with it a new era for European astronomy.

Status of VLT Second Generation Instrumentation

G. MONNET, ESO

I. The Call for Proposals

In the fall of 2001 and largely based on the June 2001 Workshop "Scientific Drivers for future VLT/VLTI Instrumentation", four main scientific objectives were highlighted by the ESO STC:

(a) A Near-Infrared (1–2.4 μm) Cryogenic Multi-Object Spectrometer ("KMOS") for the study of initial galaxy mass assembly.

(b) A wide-field 3D Optical Spectrometer ("3D Deep-Field Surveyor") for the exploration of the early Universe.

(c) A Medium Resolution Wide-band Spectrometer ("Fast-Shooter"), in particular to catch fast astronomical events from Supernova explosions to gamma ray bursts.

(d) A High-contrast, Adaptive Optics assisted Imager ("Planet Finder") for deep study of nearby stellar environments.

Based on this selection, a "Call for Preliminary Proposals" was issued in November 2001, with the deadline set on 18 February 2002.

II. The Result

The community answered very favorably to the Call for proposals. Indeed, we have received a total of 11 answers from generally large Consortia. Given the very significant work that went into the often quite detailed and in depth proposals, it is gratifying to see that this Call was taken very seriously by our Community. I would like here to thank all proponents for the effort they invested to help maintain the competitiveness of VLT instrumentation.

(a) Near-Infrared Cryogenic Multi-Object Spectrometer ("KMOS")

Three answers were received in total:

- KMOS1 is a cryogenic near-infrared facility, with deployable Integral Field Units feeding an array of identical spectrometers. The project P.I. is Ralf Bender, Universitätssternwarte München (USM) and Max-Planck-Institut für Extraterrestrische Physik (MPE-Garching). The Co-PIs are Reiner Hofmann, MPE-Garching and Ray Sharples, University of Durham. The Consortium also includes the ATC-Edinburgh and the Universities of Oxford and Bristol.

- KMOS2 is a cryogenic imaging, multi-slit and multiple integral field Spectrometer. It uses an NGST-type 4K \times 4K IR array. The Coordinator is Dario

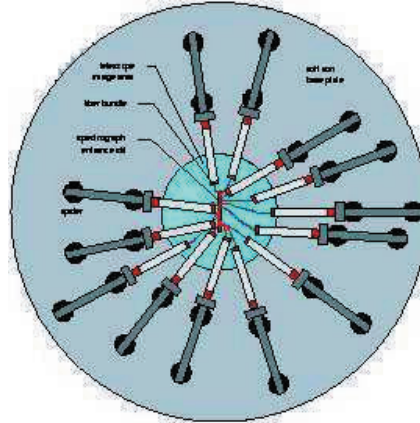


Figure 1: Schematic view of the deployable cryogenic Integral Field Units in the $\sim 8'$ patrol field.

Maccagni, Istituto di Astrofisica Spaziale e Fisica Cosmica – Sezione di Milano (IASF-MI). The local responsables are Jeremy Allington-Smith (IAG-Durham), Olivier Le Fèvre (LAM-Marseille), Jean-Pierre Picat (LAOMP-Toulouse) and Paolo Vettolani (IRA-Bologna).

The cryogenic imaging and multi-slit Spectrometer FLAMINGOS-VLT is proposed by the Department of Astronomy, University of Florida. The P.I. is Richard Elston and the Project Manager Roger Julian. It is a near-clone of the Flamingo-2 instrument currently built by the Team for Gemini-S.

(b) "Wide-Field" 3D Optical Spectrometer

- The Multi Unit Spectroscopic Explorer (MUSE) is a $1' \times 1'$ Integral Field facility in the optical domain – actually a cluster of 24 identical spec-

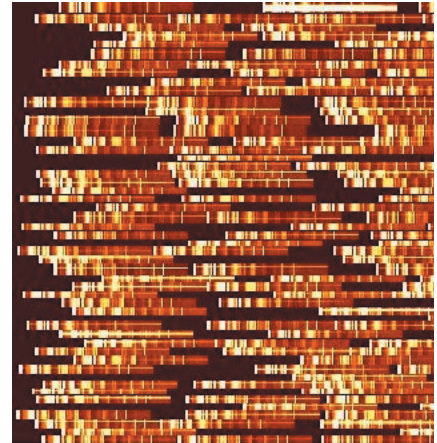


Figure 2: Simulation of multi-slit spectra in the $\sim 8' \times 8'$ field.

trometers fed by a huge image slicer. The project is presented by Roland Bacon, Centre de Recherches Astrophysiques de Lyon (CRAL). The Consortium regroups six Institutes, AIP-Potsdam, CRAL-Lyon; ETH-Zurich; LAM-Marseille; the Physics department of Durham University and the Sterrewacht-Leiden (NOVA program).

- The 3D Wide-Field Optical Spectrometer FAST (Fabry-Perot Spectrometer Tunable) is a $7' \times 7'$ facility, built around the scanning Fabry-Perot concept. The P.I. is Michel Marcelin, Laboratoire d'Astrophysique de Marseille (LAM). The Consortium regroups Bochum University, Byurakan Astrophysical Observatory, the GEPI-Observatoire de Paris, Keele University (UK), LAM-Marseille, Laboratoire d'Astrophysique Expérimentale de Montréal, Max Planck Institut für Astronomie (Heidelberg), Osservatorio di Brera (Milano), Oulu University (Finland),

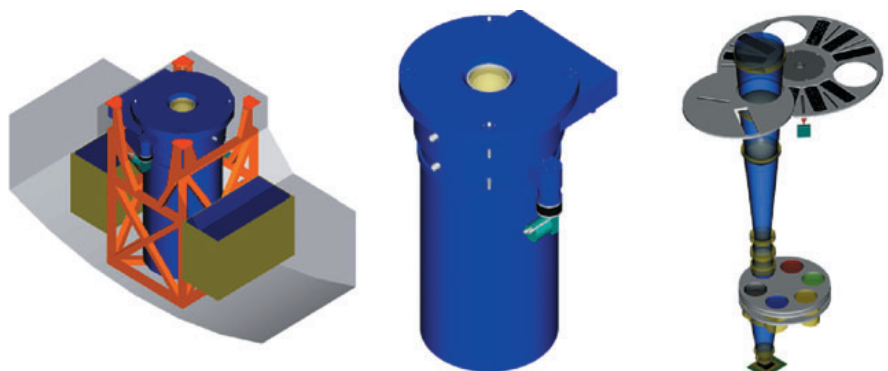


Figure 3: FLAMINGOS-VLT. Left to right: a) mounted on the VLT; b) global view; c) internal functions.

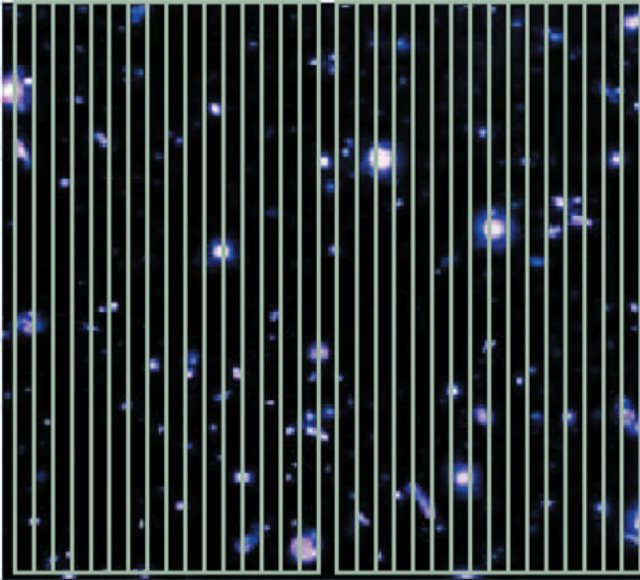


Figure 4: MUSE-like 1' x 1' field overlaid with an Image Slicer grid.

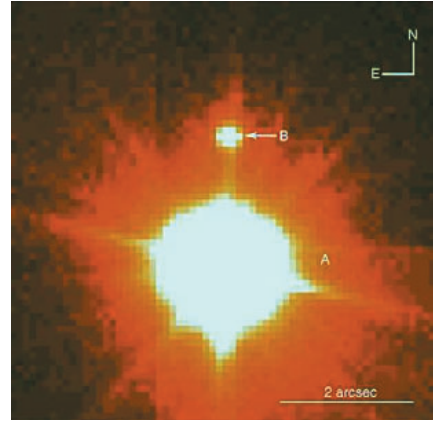


Figure 6: Main goal of the Planet finder is to gain orders of magnitude in the detection of faint sources near a bright star, as compared to this 0.18" FORS2 I band image.

Physical Research Laboratory, Ahmedabad (India) and Université de Montréal. The project scope is quite similar to the so-called Tunable Filter upgrade of FORS1; it however also features a medium resolution ($\sim 10^4$) mode.

(c) *Medium resolution Wide-band Spectrometer ("fast-shooter")*

Four answers were received in total:

- The High Efficiency, Intermediate Dispersion Instrument (HEIDI). The P.I. is Per Kjaergaard Rasmussen, Niels Bohr Institute for Astronomy, Physics & Geophysics (Copenhagen) and the Co-PI Lex Kaper, University of Amsterdam. The Consortium membership also includes Tuola Observatory (FIN), the Universities of Sheffield and Southampton (UK) and ASTRON-Dwingeloo (NL).

- The Fast Instrument Echelle Spectrograph with Triple Arm (FIESTA). The P.I. is Dario Lorenzetti and the project scientist, Fabrizio Fiore, both at the Osservatorio Astronomico di Roma. The Consortium regroups seven Italian Institutes, viz. the Observatories of Bologna (OABo), Brera (OABr), Catania (OACt), Roma (OAR), Padova (OAPd), Palermo (OAPa) and Trieste (OATs).

- The Integral Field Array Spectrophotometry in real Time (IFAST). The P.I. is François Hammer (GEPI-Observatoire de Paris). The Consortium membership also includes APC-Université Paris 7 and the Institut d'Astrophysique de Paris.

- An STJ based Echelle Spectrograph (SES). The P.I. is Mark Cropper, Mullard Space Science Laboratory, University College London. The Consortium also includes ESTEC (NL) and the Universities of Cambridge, St Andrews and Southampton (UK).

The first three proposals feature classical cross-dispersed echelle spectrometers with an entrance slit or a small integral field input. Wavelength separation is done *à la* UVES at the entrance of the instruments to get optimal efficiency. The last one uses a single (echelle) grating, the order separation being done by a 1-D Superconducting Tunnel Junction (STJ) array.

(d) *High-contrast, Adaptive Optics assisted, Imager ("Planet Finder")*

A High-Contrast, Adaptive Optics Aided System for the Direct Detection of Extrasolar Planets (PF1). The P.I. is

Markus Feldt and the Project Manager, Stefan Hippler, both of the Max Planck Institut für Astronomie (Heidelberg). The Instrument Scientist is Raffaele Gratton, Osservatorio Astronomica di Padova. The Consortium includes German Institutes (MPIA-Heidelberg, MPE-Garching, KSO-Tautenburg, AIP-Postdam, AIU-Jena), Italian Institutes (Padova University and Observatories of Padova, Arcetri, Naples and Brera), Dutch Institutes (Leiden Observatory and University of Amsterdam), ETH-Zurich and FCUL-Lisboa.

- A competing project (PF2) is presented by the Laboratoire d'Astrophysique de Grenoble (Anne-Marie Lagrange, P.I.) The Consortium also includes LAM-Marseille, ONERA-Paris, Observatoire de Paris, OCA-Nice and Université de Nice, LAE-Montréal, Durham University, UCL-London, ATC-Edinburgh and Observatoire de Genève.

The two proposals are rather comparable in terms of Adaptive-Optics firmware. On the other hand their scientific line of attack is quite different. The Heidelberg-led group aims at finding planets from their reflected light through high-Strehl imaging in J-H and extremely accurate polarimetry in the I-band. The Grenoble-led group looks in-

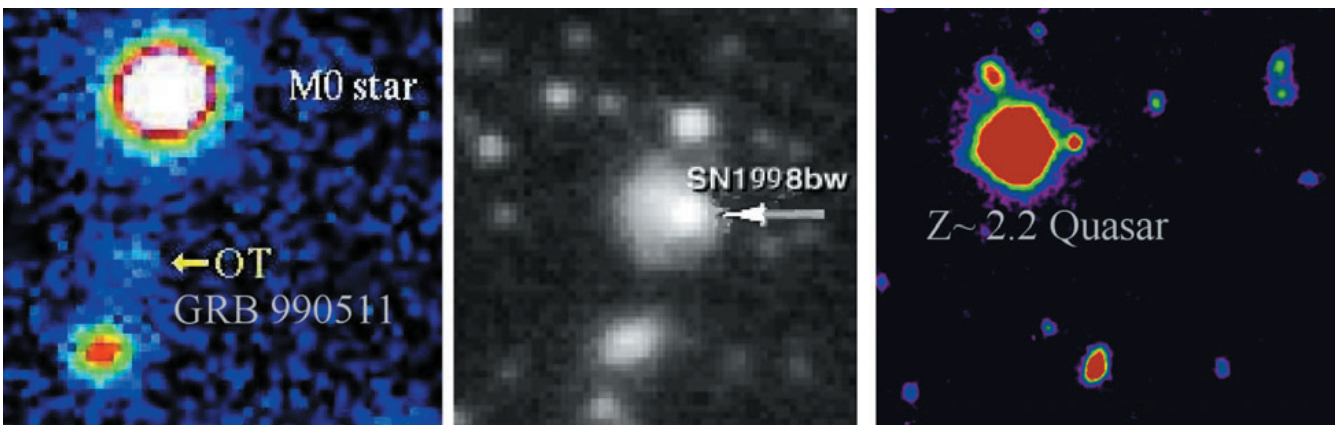


Figure 5: Some types of potential "fast-shooter" targets.

stead at the intrinsic planetary emission in the K and eventually L band.

(e) First Generation Upgrade

In addition, we have received from Jean-François Donati (Observatoire Midi-Pyrénées) a VLT instrument upgrade proposal, aimed at turning UVES into a high-resolution spectro-polarimeter. The Consortium also includes the Landessternwarte Heidelberg, Observatoire de Paris, University of St Andrews and University College London.

III. Next Steps

Following recommendations at the last April STC meeting, we are current-

ly contacting the Project Principal Investigators. The ESO staff responsible for the four domains are respectively A. Moorwood for the KMOS, G. Monnet for the Surveyor, S. D'Odorico for the Fast Shooter (& UVES upgrade), and N. Hubin for the Planet Finder. Following current negotiations with the Consortia, feasibility studies will start soon, with (partial) financing from ESO. On a longer scale, the goal is obviously to get efficient Teams to conduct these huge endeavors.

On the programmatic side, the intention is to initiate in the next 8-year period the development of one second generation instrument per year, starting in 2003. This is of course a rough guide only. The actual rate will depend on the

capital and human resources cost of the selected facilities. It is thus quite appealing that a number of Consortia intend to raise a significant fraction of the capital cost for these expensive facilities.

It may be nevertheless worthwhile to recall that a huge effort still remains to be invested to complete and put into operation the remaining first generation VLT instruments; this is heavily taxing the present capabilities of both ESO and its community for "fast" deployment of these new, exciting, facilities.

In Conclusion, I would like to again extend our deep thanks to all proponents for their valuable contributions.

VLT Quality Control and Trending Services

R. HANUSCHIK, ESO (UVES QC Scientist) and
D. SILVA, ESO (Head Data Flow Operations Group)

Why control quality?

Any observatory worldwide has staff who permanently look into the performance of the instruments and check the quality of the data. ESO's Very Large Telescope has the operational model of a data product facility. This means that it goes beyond the day-to-day performance checks and promises to deliver data of a defined and certified quality.

The Data Flow Operations Group in Garching (DFO, also frequently called QC Garching), provides many aspects of data management and quality control of the VLT data stream. One of the main responsibilities is to assess and control the quality of the calibration data taken, with the goal to know and control the performance of the VLT instruments. Information about the results of this process is fed back to Paranal Science Operations and to the ESO User Community via QC reports and web pages.

The constant flow of raw data from the VLT instruments splits into data streams for the science data and the calibration data. The calibration data stream has two separate components:

- calibrations taken to remove instrument signatures from science data
- calibrations taken for routine daily instrument health checks.

The focus of QC Garching is to process these data and extract Quality Control information. This process of course does not replace the on-site expertise of the Paranal staff. But it goes beyond the usual quick-look, on-the-spot checks and provides a permanent and in-depth knowledge of the instru-

ment status. With the QC parameters routinely collected over years, it is possible to control, predict, and often even improve, the performance of the instruments.

This article describes the Quality Control process for the four presently operational VLT instruments: FORS1+2, ISAAC and UVES. This process will be extended and refined for the next suite of instruments coming soon, VIMOS, NACO, and FLAMES, and ultimately expanded to all VLT instruments.

How to control data quality

The term quality control, though often used, needs some definition. Quality control, as we understand it, implies the control of the following:

- quality of the raw data
- quality of the products and of the product creation process
- performance of the instrument component involved.

Quality control does generally not imply aspects like the monitoring of ambient data (quality of a night), the proper format of FITS headers, or the tracking of programme execution. Responsible for these aspects, being part of Quality Control in a wider sense, are other groups, e.g. Paranal Science Operations, and the User Support Group.

Pipelines. Fundamental in the QC process is the use of automatic data processing packages, the pipelines. Without these, effective quality control of the huge amount of data produced by the Observatory would be impossible. In fact, the primary goal of the data

reduction pipelines is to create calibration products and support quality control. Only after this comes the reduction of science data.

With the large-scale use of data processing pipelines, the Quality Control group has effectively also the function of assessing and improving the accuracy of the pipelines. As a by-product, we provide documentation about the pipeline functions from the user's point of view.

The usual day-to-day workflow of the QC scientists has as primary components: processing the raw data (calibration and science) using the instrument pipeline, performing the quality checks, and selecting the certified products and distributing them.

One might say that the use of the pipeline, once the process has been set up properly, is mainly number-crunching, while the quality checks require expertise.

The QC process. There is a natural three-floor pyramid in the QC process (Figure 1):

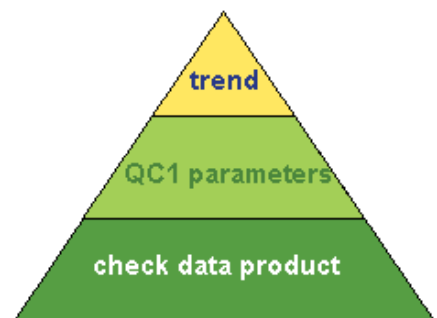


Figure 1. The QC and trending pyramid.

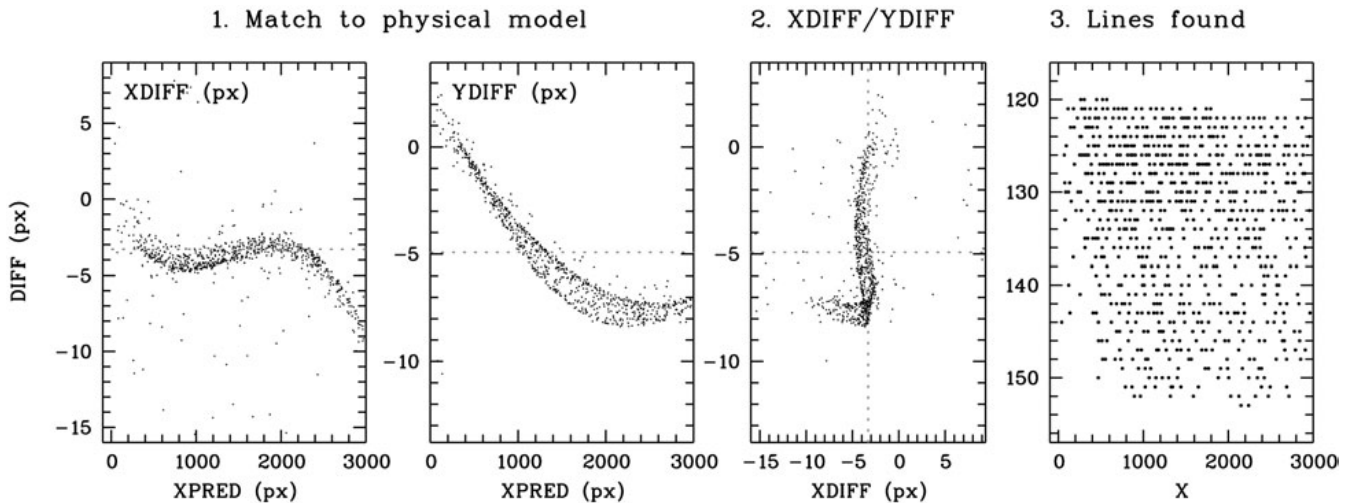


Figure 2. Quality plot for a UVES “formatcheck” frame. Such frames are taken daily to control the proper adjustment of the gratings and cross-dispersers. Main focus here is the proper clustering of the line positions found (boxes 1 and 2 with the difference between predicted and found line positions) and the proper coverage of all orders with identified positions (box 3).

- checking each data product
- measuring and storing a set of QC parameters per product, and
- looking at the long-term behaviour of these parameters.

1. Checking each product. The first, and most fundamental, step in the QC process is done on each pipeline product. Is the frame over/under-exposed? Is it different from the frame taken yesterday? A set of procedures creates displays and graphical information like cross-cuts and histograms. Frequently there is a comparison to a reference frame. Without these procedures, the QC scientist would be blind to data quality. The mere fact that a reduction job was executed without a processing error indicates nothing about data quality.

In practice, after some initial phase when indeed everything is inspected, one usually decides to switch to a ‘confidence mode’ in which, for example, only every third night is inspected in depth, while for the others the trending plots are consulted. This strategy is economic in case of very stable instrument performance, and mandatory with high data rates. Then the ‘human factor’, namely the possible level of concentration, ultimately limits complete product checks.

Figure 2 shows as an example the QC plot for the products of a UVES *formatcheck* frame which is a technical calibration needed by the pipeline to find the spectral format. With an experienced eye, just a second is needed to know from this plot that everything is fine and under control.

QC checks are also done on Paranal, directly after frame acquisition. These on-the-spot inspections are of quick-look character and apply to both raw and product data. They are extremely important to check the actual status of the instrument, especially for those

instruments like UVES which have the data transferred to Garching via airmail.

2. Deriving QC1 parameters. The next step in the QC process is the extraction of QC parameters. These are numbers which describe the most relevant properties of the data product in a condensed form. Since they are in most cases derived through some data manipulation (e.g. by the reduction pipeline), they are called QC1 parameters. This distinguishes them from the QC0 parameters which mainly describe site and ambient properties like seeing, moon phase etc.

Across the instruments, there are always QC1 parameters describing the detector status, i.e. the read noise, the mean bias level, the *rms* of gain variations etc. Other QC1 parameters specific to spectroscopic modes are resolving power, dispersion *rms*, or number of identified lines. Imaging modes are controlled by QC1 parameters like zero-points, lamp efficiency, and image quality.

3. Trending. The top level in the QC pyramid is the trending. Trending is a compilation of QC1 parameters over time, or a correlation of one QC1 parameter against another one. Trending can typically prove that a certain instrument property is stable and working as specified. It can do much more, however. For example, trending can discover the slow degrading of a filter, or aging effects of the detector electronics.

Outliers. Within the trending process, main attention focuses on two extremes: the outliers, and the average data points. Information theory says that outliers transport the highest information content. But not all outliers are relevant for QC purposes. We need to distinguish whether the outlier comes from a bad algorithm setup, from a bad instrument setup, or just from a bad operational setup.

A bad algorithm may, for example, be a wrong code for *rms* determination. Such an outlier would help to improve the code. A bad instrument setup could be a stuck filter wheel with the filter vignetting the light path. A bad operational setup would be a frame labelled as a *flat*, but with the lamp not switched on. In short, evaluation of the trending data is non-trivial and requires judgement.

Finding that a certain QC1 value is stable over months or years may lead one to relax the acquisition rate of the corresponding calibration data. This may be a good idea since we should avoid over-calibration. But one has to bear in mind that for proving stability, one needs a good coverage in time, so it is a good idea to have calibrations done more frequently than their typical variation timescale.

Certification. Once a product file has been QC checked, and its QC1 parameters have been verified to be valid entries, the data enter the delivery channel, which involves ingestion into the master calibration archive, usage for science reduction and distribution to the end users (if taken in Service Mode). By definition, the data are then certified. Rejected data are deleted.

Components controlled

UVES has been operational since April 2000 and was the first instrument with built-in QC procedures as part of the pipeline. So it was possible to measure and collect from the beginning a backbone set of QC1 parameters. This set has been expanded over the last two years and is now almost complete. The two-year baseline forms an asset from which many valuable pieces of information about long-term behaviour can be extracted.

Figure 3. This web interface (<http://www.eso.org/qc/UVES/qc/qc1.html>) connects to the QC1 data of UVES. The user may view trending plots, and download the corresponding ASCII data. A quick-look panel for the current period links to all current trending plots, i.e. those which are relevant for the present instrument health.

Trending

With the QC1 parameters stored in a database they become available for trending. There is a central QC1 database under development which will host all QC1 parameters and other related information such as plots and trending results.

The QC1 database can be considered as the central memory about the status of each VLT instrument. The goal is to have available all quality information from the complete operational history of the instrument. This also includes information about interventions (e.g. mirror recoating) and replacements (optical components, detectors). Such information is vital for interpretation of trending results. Moreover, with data collected over years, it becomes possible to detect slow degrading effects. Preventive interventions and maintenance can be scheduled properly.

Web pages

As part of the QC process, these results are published on the web. The central Quality Control site is <http://www.eso.org/qc/> which has, per instrument, a link to QC and trending results.

Under the URLs <http://www.eso.org/qc/<INSTR>/qc/qc1.html> (where INSTR is any of UVES, FORS1, FORS2 or ISAAC), one connects to the QC1 database and views trending plots and ASCII data (Fig. 3). Here one also finds detailed documentation about the QC1 parameters.

Our goal is to present knowledge, not

UVES QC monitors the following instrument components (<http://www.eso.org/qc/UVES/qc/qc1.html>):

Component	Property
detector	bias level, read noise, dark current; fringing
gratings	stability of spectral format; resolving power, precision of dispersion solution
slit	slit noise
lamps, filters	FF lamp stability, filter throughput
all components	efficiency

FORS1/2 have the following QC items (<http://www.eso.org/qc/FORS1/qc/qc1.html>, the FORS2 link has replaced "FORS1" by "FORS2"); MOS will be added eventually:

Mode	Property
General Imaging	bias level, read noise, dark current, gain, contamination
Long-Slit Spectroscopy	zeropoints, colour terms, image quality
	dispersion, resolution

ISAAC has the following QC items (<http://www.eso.org/qc/ISAAC/qc/qc1.html>), with the long-wavelength arm being added soon:

Mode	Property
General Imaging (short arm)	dark level, read noise
	Zeropoints

just information. Take as an example the trending of the UVES spectral resolving power R . We do not just dump all available numbers per date, but provide a documentation of the measurement process, a selection of trending plots, a correlation with slit width and a comparison to User Manual values.

Some QC and trending highlights

Compensation of UVES thermal drifts. The precision of the UVES spectrograph is limited by ambient temperature changes. A one degree difference causes an effective shift of the gratings by up to 1 pixel in cross-dispersion di-

rection (Figure 4). The daily *formatcheck* frames are compared to a reference frame and used to measure these shifts. Since the QC1 values proved a general stability and a linear slope of the thermal coefficients, a compensation for such drifts was successfully implemented in cross-dispersion direction, and the dispersion direction was corrected.

UVES filter degradation. The monitoring of the exposure level of the UVES flat-field lamps gives control over the lamp and filter status. The filter status is especially significant for the quality of science observations. In July 2001, the transmission of the blue CuSO₄ filter dropped, which was discovered in the trending plot (Figure 5). The replacement of the filter gave the blue efficiency of UVES a boost.

FORS1 image quality. Figure 6 combines input data from pipeline-processed science images from FORS1. It demonstrates that in most cases FORS1 image quality is determined by the seeing and not degraded by potential errors such as telescope guiding.

FORS1 zeropoints. Figure 7 shows the complete history of FORS1 zeropoints in the V band, spanning three years. Zeropoints measure the efficiency of the overall system instrument plus telescope. There have been major interventions (see the caption for details), but perhaps more interesting is the fact that there has been a general loss of efficiency by about 8% per year, due to degrading of the mirror surface.

ISAAC photometric zeropoints. Figure 8 shows the zeropoints derived by the ISAAC pipeline over a half-year period. The sharp rise around MJD-OBS = 52,200 is due to an intervention which included a re-alignment. This improved the instrument efficiency by up to 0.2 mags. The long-term trend is due to degradation, while the short-term scatter in most cases is due to fluctuations of the night quality.

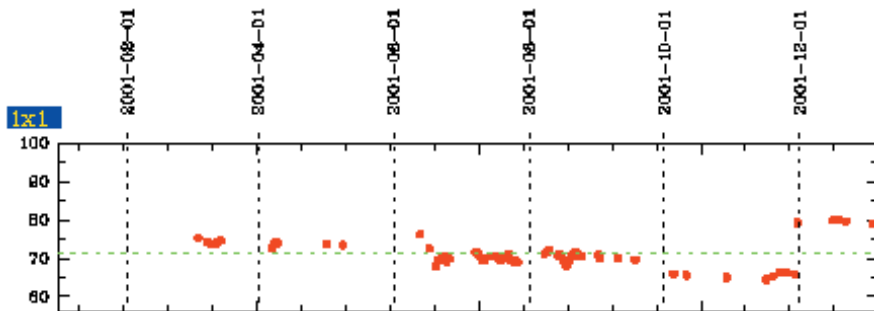


Figure 5. The transmission of the CuSO₄ filter used for reducing scattered light in the blue arm of UVES dropped significantly in July 2001. This was only discovered in November 2001 when the corresponding trending procedure had been established. An inspection of that filter verified its poor state: its coating was partly destroyed by humidity. Its replacement in December 2001 has improved the efficiency considerably, which is clearly visible in the trending plot.

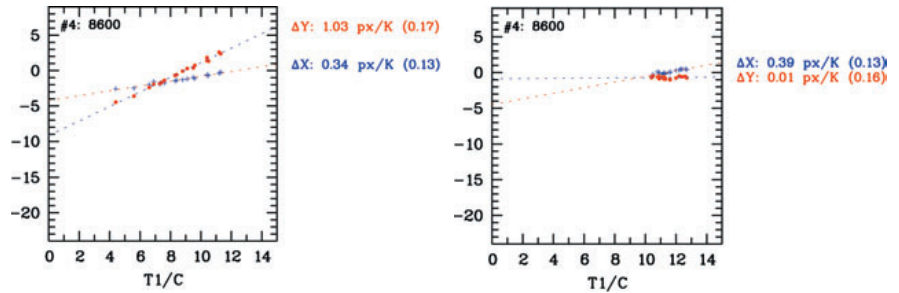


Figure 4. Measured thermally induced drifts of UVES grating #4, without (left), and with (right) thermal compensation in Y direction. The QC1 trending data have been used to establish the coefficients for the automatic compensation of thermal motion in Y (cross-dispersion) direction.

Shared QC

It is obvious that Quality Control must be a shared responsibility between QC Garching and Paranal Science Operations. There are always QC issues which require immediate reaction and intervention. These can only be properly handled on site. With the data airmailed to Garching (which today is the transfer mode for UVES, and soon for all VLT instruments), the typical reaction time on QC issues in Garching is 10 days. This naturally leads to the concept of shared QC which means that part of the QC tasks are done on Paranal (in real time, by daytime astronomer), part in Garching (off-line, by QC scientist).

On-site QC. Basic quality checks on the calibration data are performed by the Paranal daytime astronomer. Just after exposing the raw calibration data and pipeline-processing them into calibration products, the data are inspected visually. The on-line pipelines produce an essential set of QC1 parameters which is fed into a database. Essential are those QC1 parameters relating to fundamental instrument properties which, in case of failure, would jeopardize the usefulness of the science data. Such instrument health parameters are e.g. proper adjustment of gratings and filters, and proper CCD setup.

Off-line QC. The full set of quality checks is applied in Garching – anything which is not time critical, but requires in-depth analysis, pipeline or post-pipeline procedures. This applies also to complex trending analyses requiring extended data sets. Examples are photometric zeropoints which are determined from all standard star data of a night; colour and extinction terms being derived for a whole semester; efficiency curves; sky brightness etc.

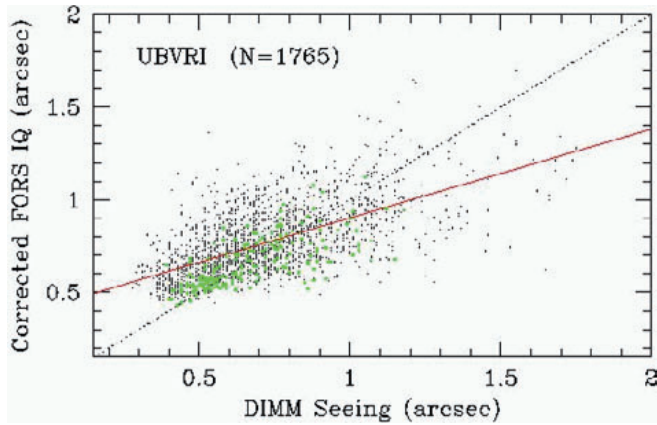
Feedback loops. The exchange of quality information between the two sites with QC activities is especially important. The main feedback channel from QC Garching to Paranal are the web-published trending plots which are updated daily. These monitor the proper function of all QC-checked components. Any anomalies are investigated in detail and reported directly to Paranal.

IOT. The group responsible for studying new results of trending studies, the development of new QC1 parameters or algorithms are the Instrument Operating Teams (IOT). As a vertical structure, these have, per instrument, delegates from each team which is essential for proper operations, i.e. from Science Operations, User Support Group, DFO, Pipeline Development, and Instrumentation. The teams are led by the Instrument Scientist. It is here where all the expertise about a VLT instrument is focused and where the loop between QC results and improvement of instrument performance is closed.

Feedback into calibration plan

An example of successful feedback of the QC process and the instrument operations is the improvement of the Calibration Plan. In principle, calibration data are taken to remove instrumental signature from the science data (“calibrate the science”). In a more general sense, they are taken to know the instrument status (“calibrate the instrument”). Ideally, one would go for the latter goal since this provides the broader knowledge about the instrument while including the requirement to reduce the science data.

Figure 6. Image quality of FORS1 (width of stellar images in arcsec) versus the image quality measured by a seeing monitor (DIMM). Input data have been collected from pipeline-processed FORS1 science images in filters UBVRI. Correction factors have been applied for wavelength and airmass. Green dots mark high-resolution collimator data, black stands for standard-resolution. The broken line indicates FORS IQ = DIMM. The red line is a fit to the data. FORS1 image quality is on average better than DIMM seeing above 0".8.



But in practice this is not even possible for simple instrument modes. For instance, the imaging mode of FORS1 has 5 standard filters with 4 CCD read modes and 2 different collimators. Obtaining a complete set of calibration frames, including twilight flats and standard stars, is practically not possible every night. As a more complex instrument, UVES has 12 standard setups, with roughly 20 different slit widths and 2 CCD modes, and the parameter space becomes forbiddingly large for routinely calibrating all settings.

Therefore, calibration data are usually triggered by the science setups actually used in the night before. To these

are added the daily health check calibrations. On Paranal, an automatic tool is used which collects this information into the daytime calibration queue.

Even this strategy still produces a large calibration overhead both in terms of exposure time and archive disk space. So, after some initial epoch when confidence has been gained that the calibration plan is complete, one may start thinking how to *optimize* the plan. In the case of UVES, it has been shown by the trending studies that the most relevant instrument properties usually show trending timescales much longer than a few days. Based on this experience a three-day memory has

been implemented in the calibration plan, with calibrations for an identical setup being repeated only every three days. The only exception is the wavelength calibration. The health check calibrations are executed daily in order to prove that nothing irregular happens, e.g. an earthquake which would clearly break the long-term trending assumption.

Vision

Our QC process is continuously evolving, to meet the current and future needs of our main customers: Paranal Science Operations and the ESO user community. Here are a few examples.

Although the QC1 parameters computed and controlled by QC Garching are available via our Web pages, they are not easily associated with the calibration products available from the ESO Science Archive. By the end of this year, we hope to have a new QC1 parameter database within the Archive domain. Once this database exists, it should be possible for users to retrieve the QC1 parameters associated with the calibration products they are retrieving from the Archive. This is particularly important in the context of Virtual Observatory development.

The calibration data flowing through QC Garching contains a rich but largely unexploited reservoir of information about Cerro Paranal as a site. QC Garching, in collaboration with other group within ESO, has started several projects to process this information and make it available to our customers. For example, this year we will publish a high signal-to-noise, high resolution sky atlas extracted from many hours of UVES observations, as well as a study of optical sky brightness as a function of lunar phase, lunar distance, time after twilight, etc, derived from FORS data. Possible future projects include the creation of lists of faint, secondary photometric standards for FORS and ISAAC, in collaboration with Paranal Science Operations.

For historical reasons, our QC web pages (<http://www.eso.org/qc>) are implemented in a very heterogeneous way. We are reorganising and revising these pages to make them more homogeneous across instruments, and to make it easier for our users to find the information they need.

Of course, our main priority this year is to establish regular QC operations for the latest VLT instruments: NACO, VIMOS, and FLAMES, as well as extending our process to the VLT Interferometer complex. These instruments introduce many new and complex modes: optical interferometry, adaptive optic imaging, high density multi-object spectroscopy with slits and fibers, and integral field spectroscopy. The underlying, detector based health and wellness QC process are essentially exten-

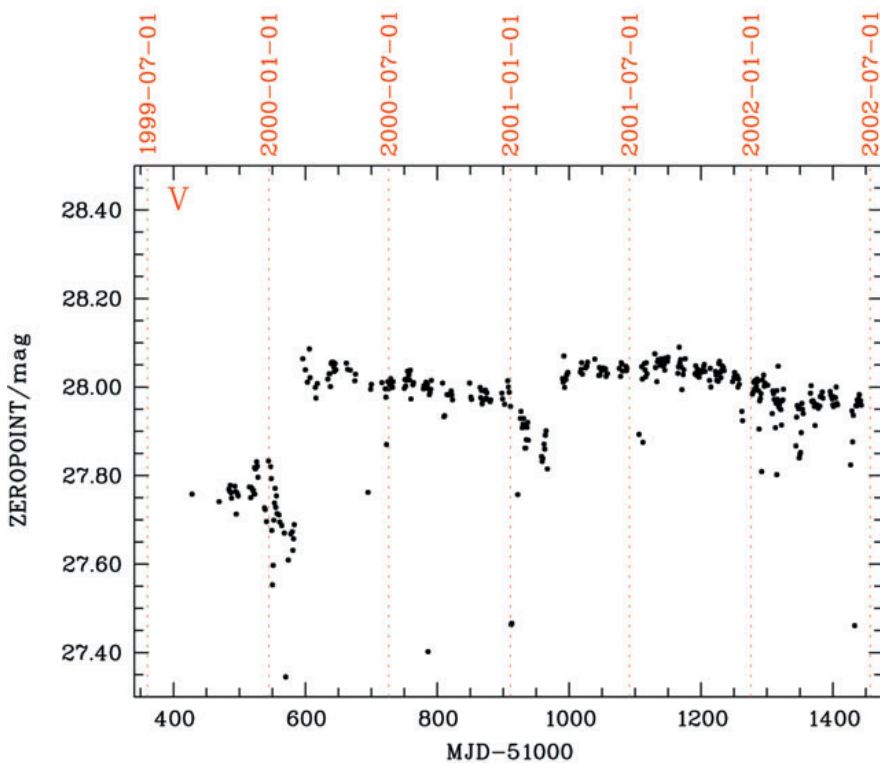


Figure 7. Three years of FORS1 zero-points in the V band. Major interventions, causing steps in the slope, have been mirror recoatings in February 2000 and March 2001, and sudden degrading of the main mirror due to rain in February 2001. The move to UT3/Melipal in August 2001 is invisible in this plot.

sions of our current process, but the development of a higher level QC process will be more challenging.

Last Words: Other DFO Services

In this article, we have focused on our main role: quality control for the VLT data flow. To close, we briefly outline the other services DFO provides to the ESO user community.

As mentioned above, the VLT QC revolves around calibration data. Most quantitative QC is done using calibration products, e.g. dispersion solutions or master flat fields. It is the responsibility of DFO Garching to produce such calibration products and then re-use them in a number of ways. Calibration products are ingested into the ESO Science Archive; they are included in the standard data packages produced for Service Mode users; they are used within the on-line DFS Pipeline system on Paranal; and they are used to produce science data products for Service Modes users.

Another important DFO service is processed Service Mode science data. Science data are only processed when an appropriate pipeline is available. Science pipeline data products are delivered with the understanding that they may not be publication quality in all cases. However, these products can be very useful for making the initial assessment of science data quality and for providing guidance on how to process the delivered science data for a specific application.

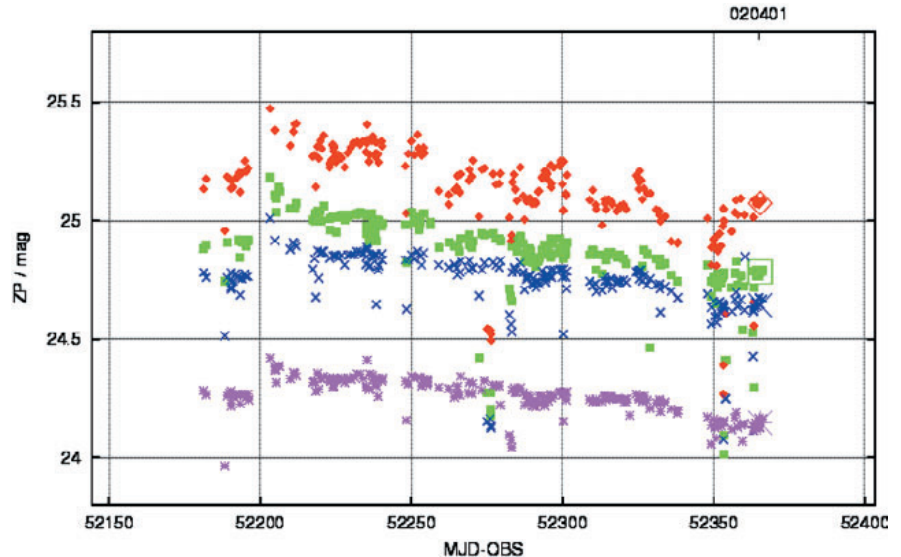


Figure 8. ISAAC photometric zeropoints for Period 68, in photometric bands Js (green squares), J (red diamonds), H (blue crosses), and K (asterisks). Horizontal axis is Julian Date of observation (MJD-OBS), vertical axis is zeropoint in magnitudes. Last civil date of observation on the plot is 2002-04-01.

When a Service Mode run is completed, DFO creates and delivers a standard data package to the run Principal Investigator. This data package contains all the raw science and calibration data, pipeline science and calibration products when available, and a variety of supporting listings and reports. Technical support (e.g. media manufacturing) is provided by the ESO Science Archive team.

Last but not least, DFO maintains extensive documentation about what we do and how we do it, on our QC Web pages: <http://www.eso.org/qc/>. Our detailed descriptions of how sci-

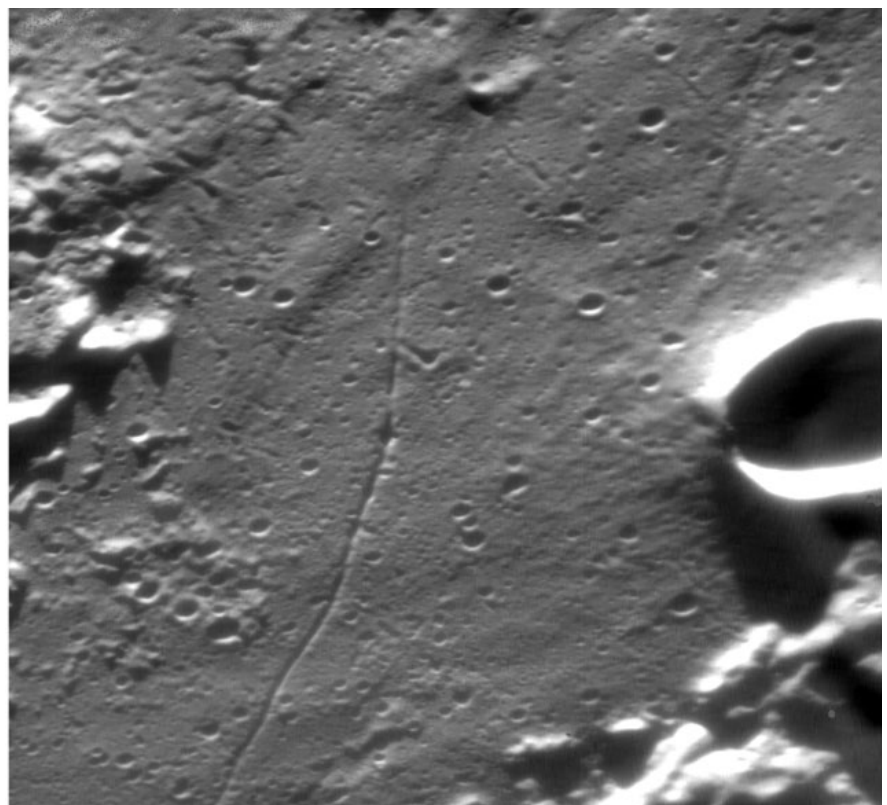
ence and calibration data are processed using the current generation pipelines may be particularly interesting to users.

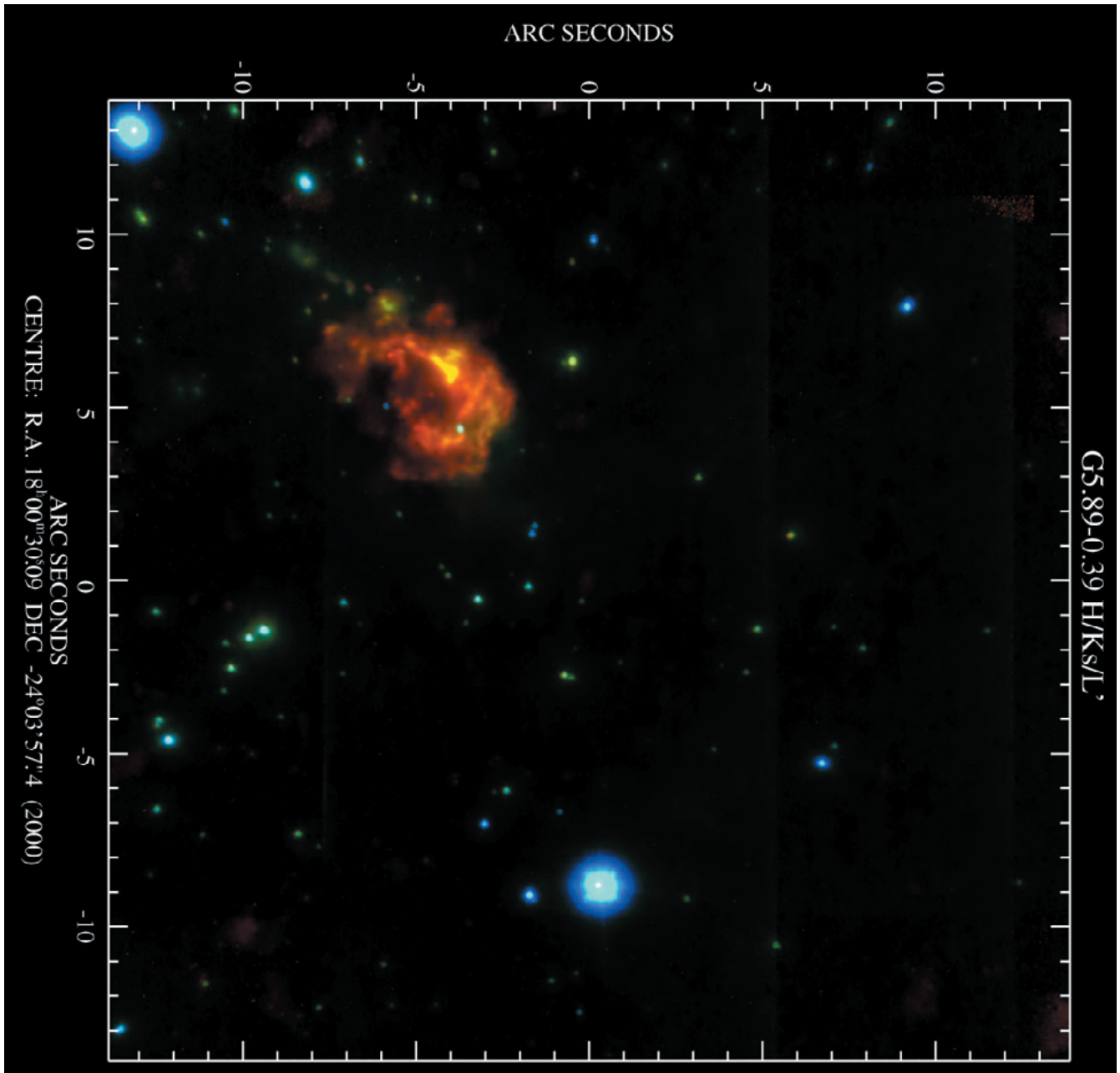
Acknowledgements. The QC process described here is the result of the joint work of the QC Garching team which is constituted, apart from the authors, by Wolfgang Hummel, Roberto Mignani, Paola Sartoretti, and Burkhard Wolff. We also thank our past DFO colleagues Paola Amico, Ferdinando Patat, and Bruno Leibundgut, and all our PSO colleagues, especially Andreas Kaufer.

Recent NAOS-CONICA Images

Walking on the Moon: The ability of NAOS to do wavefront sensing on extended objects was once again demonstrated by closing the AO loop on the peak of a sunlit lunar mountain. This image was obtained with CONICA through a 2.3 micron narrow-band filter and shows details down to 0.1 arcsec (which corresponds to a ground-resolution of 175 metres, quite comparable to the resolution obtained from lunar orbit with the NIR camera aboard the Clementine spacecraft). The NACO image covers a region of about 45×45 km.

(Picture credit: Eric Gendron and the NAOS and CONICA consortia.)





NAOS/CONICA composite colour HKsL' image of the Ultra-compact HII region G5.89-0.39. The diffraction limited image nicely resolves the filamentary structure of the dust shell, which is most prominent in the L' band. At the distance of G5.89-0.39 of 2.6 kpc, the diffraction limited resolution of 60mas in Ks corresponds to 150 A.U. (Picture credit: Markus Feldt and the CONICA and NAOS consortia.)

News from La Silla

L. GERMANY, ESO

FEROS News:

In preparation for moving of FEROS to the 2.2m, a FEROS maintenance mission was completed in February 2002. The old efficiency of FEROS+telescope was confirmed (around 16%), but it was discovered that the sky fiber throughput had substantially degraded with time. We re-adjusted the orientation of the sky fiber+microlens inside the fiber head, so that its beam over-

lapped that of the object fiber at the distance of the secondary mirror. This operation successfully restored the sky fiber throughput to the levels achieved during the original commissioning of FEROS. The sky fiber now receives almost 90% as much light as the object fiber over most of the spectral range.

WFI News:

For users of the WFI, we now have available bad-pixel masks and the

fringing pattern for the lc/lwp filter. You can retrieve these images, learn how they were made and how to use them at the following websites:

Fringing Pattern:
<http://www.ls.eso.org/lasilla/Telescopes/2p2T/E2p2M/WFI/CalPlan/fringing/>

Bad Pixel Masks:
<http://www.ls.eso.org/lasilla/Telescopes/2p2T/E2p2M/WFI/CalPlan/BADPIX/>

Understanding the sources of the X-ray background: VLT identifications in the *Chandra/XMM-Newton* Deep Field South

G. HASINGER¹, J. BERGERON², V. MAINIERI³, P. ROSATI³, G. SZOKOLY¹
and the CDFS Team

¹Max-Planck-Institut für Extraterrestrische Physik, Garching, Germany

²Institut d'Astrophysique, Paris, France

³European Southern Observatory, Garching, Germany

1. Introduction

Deep X-ray surveys indicate that the cosmic X-ray background (XRB) is largely due to accretion onto supermassive black holes, integrated over cosmic time. In the soft (0.5-2 keV) band more than 90% of the XRB flux has been resolved using 1.4 Msec observations with *ROSAT* (Hasinger et al., 1998) and recently 1-2 Msec *Chandra* observations (Rosati et al., 2002; Brandt et al., 2002) and 100 ksec observations with *XMM-Newton* (Hasinger et al., 2001). In the harder (2-10 keV) band a similar fraction of the background has been resolved with the above *Chandra* and *XMM-Newton* surveys, reaching source densities of about 4000 deg⁻². Surveys in the very hard (5-10 keV) band have been pio-

neered using BeppoSAX, which resolved about 30% of the XRB (Fiore et al., 1999). *XMM-Newton* and *Chandra* have now also resolved the majority (60-70%) of the very hard X-ray background.

Optical follow-up programs with 8-10m telescopes have been completed for the *ROSAT* deep surveys and find predominantly Active Galactic Nuclei (AGN) as counterparts of the faint X-ray source population (Schmidt et al., 1998; Lehmann et al., 2001) mainly X-ray and optically unobscured AGN (type-1 Seyferts and QSOs) and a smaller fraction of obscured AGN (type-2 Seyferts). The X-ray observations have so far been about consistent with population synthesis models based on unified AGN schemes (Comastri et al., 1995; Gilli, Salvati & Hasinger, 2001),

which explain the hard spectrum of the X-ray background by a mixture of absorbed and unabsorbed AGN, folded with the corresponding luminosity function and its cosmological evolution. According to these models, most AGN spectra are heavily absorbed and about 80% of the light produced by accretion will be absorbed by gas and dust (Fabian et al., 1998). However, these models are far from unique and contain a number of hidden assumptions, so that their predictive power remains limited until complete samples of spectroscopically classified hard X-ray sources are available. In particular they require a substantial contribution of high-luminosity obscured X-ray sources (type-2 QSOs), which so far have only scarcely been detected. The cosmic history of obscuration and its potential depend-

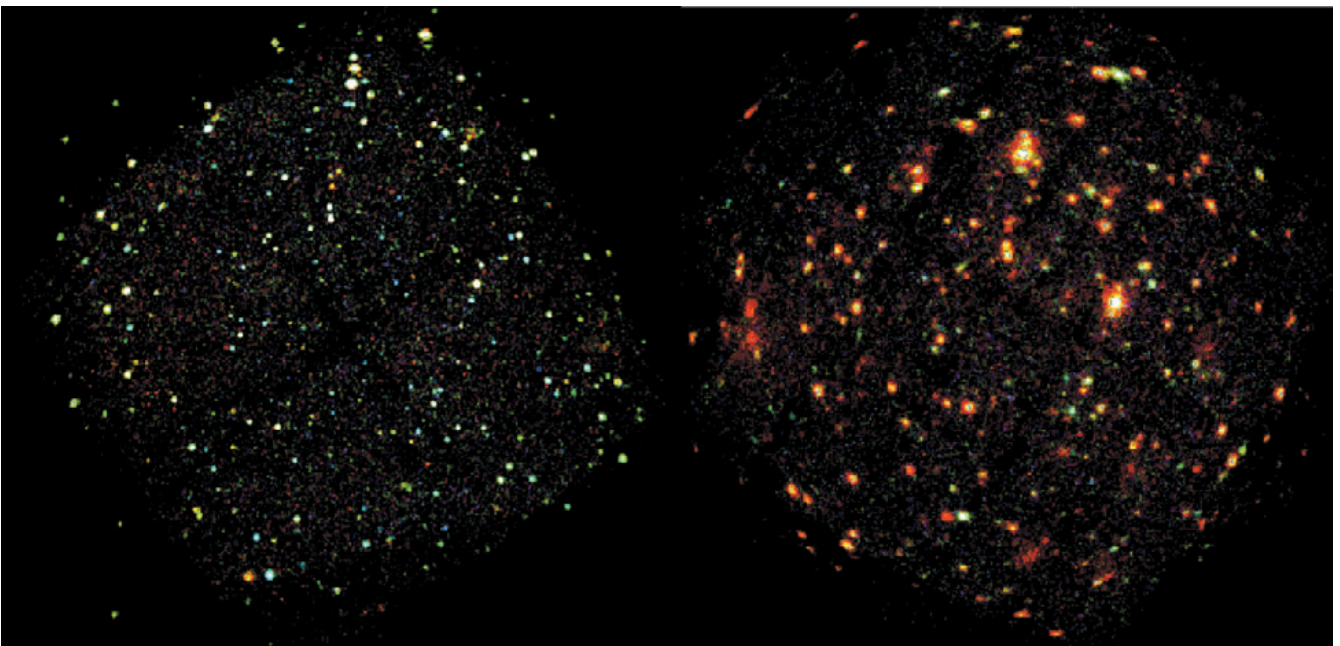


Figure 1: left: Composite image of the *Chandra* Deep Field South of 940 ks (pixel size=0.984", smoothed with a $r=1''$ Gaussian). The image was obtained combining three energy bands: 0.3-1 keV, 1-3 keV, 3-7 keV (respectively red, green and blue). Right: Similar image for the 370 ksec dataset from *XMM-Newton*, roughly to the same scale. The three energy bands are: 0.5-2 keV, 2-4.5 keV, and 4.5-10 keV, respectively. A few diffuse reddish (i.e. soft) sources, associated with groups of galaxies can be seen. The color intensity is derived from the net counts and has not been corrected for vignetting.

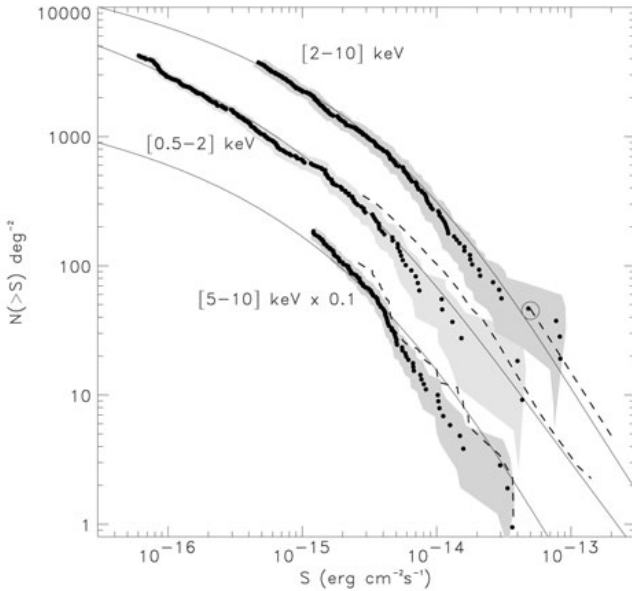


Figure 2: Number counts ($\log N - \log S$) in the soft (0.5–2 keV), hard (2–10 keV) and very hard (5–10 keV) bands from the 1 Megasec observations of the CDFS (Rosati et al., 2002). The grey regions refer to statistical and systematic errors. Solid lines are predictions from model B by Gilli, Salvati & Hasinger (2001).

ence on intrinsic source luminosity remain completely unknown. Gilli et al. e.g. assumed strong evolution of the obscuration fraction (ratio of type-2/type-1 AGN) from 4:1 in the local universe to much larger covering fractions (10:1) at high redshifts (see also Fabian et al., 1998). The gas to dust ratio in high-redshift, high-luminosity AGN could be completely different from the usually assumed galactic value due to sputtering of the dust particles in the strong radiation field (Granato et al., 1997). This might provide objects which are heavily absorbed at X-rays and obscured at optical wavelengths.

After having understood the basic contributions to the X-ray background, the general interest is now focussing on understanding the physical nature of these sources, the cosmological evolution of their properties, and their role in models of galaxy evolution. We know that basically every galaxy with a spheroidal component in the local universe has a supermassive black hole in its centre (Gebhardt et al., 2000). The luminosity function of X-ray selected AGN shows strong cosmological density evolution at redshifts up to 2, which goes hand in hand with the cosmic star formation history (Miyaji et al., 2000). At the redshift peak of optically selected QSO around $z = 2.5$ the AGN space density is several hundred times higher than locally, which is in line with the assumption that most galaxies have been active in the past and that the feeding of their black holes is reflected in the X-ray background. While the comoving space density of optically and radio-selected QSO has been shown to decline significantly beyond a redshift of 2.5 (Schmidt, Schneider & Gunn, 1995; Shaver et al., 1996), the statistical quality of X-ray selected AGN high-redshift samples still needs to be improved (Miyaji et al., 2000). The new *Chandra*

and *XMM-Newton* surveys are now providing strong additional constraints here.

Optical identifications for the deepest *Chandra* and *XMM-Newton* fields are still in progress, however a mixture of obscured and unobscured AGN with an increasing fraction of obscuration at lower flux levels seems to be the dominant population in these samples too (Barger et al., 2001; Rosati et al., 2002; Stern et al., 2002; Szokoly et al., 2002; see below). Interestingly, first examples of the long-sought class of high-redshift, high-luminosity, heavily obscured active galactic nuclei (type-2 QSO) have been detected in deep *Chandra* fields (Norman et al., 2002; Stern et al., 2002) and in the *XMM-Newton* deep survey in the Lockman Hole field (Lehmann et al., 2002).

In this paper we give an update on the optical identification work in the *Chandra* Deep Field South, which thanks to the efficiency of the VLT has progressed furthest among the deepest X-ray surveys.

2. The *Chandra* Deep Field South (CDFS)

The *Chandra* X-ray Observatory has performed deep X-ray surveys in a number of fields with ever increasing exposure times (Mushotzky et al., 2000; Hornschemeier et al., 2000; Giacconi et al., 2001) and has completed a 1 Msec exposure in the *Chandra* Deep Field South (CDFS, Rosati et al., 2002) and a 2 Msec exposure in the Hubble Deep Field North (HDF-N, Brandt et al., 2002). The Megasecond dataset of the CDFS (500 ksec from R. Giacconi’s guaranteed time, augmented by 500 ksec director’s discretionary time) is the result of the coaddition of 11 individual *Chandra* ACIS-I exposures with aimpoints only a

few arcsec from each other. The nominal centre of the CDFS is $\alpha = 03^{\text{h}}32^{\text{m}}28.0^{\text{s}}$, $\delta = -27^{\circ}48'30''$ (J2000). This field was selected in a patch of the southern sky characterized by a low galactic neutral hydrogen column density $N_{\text{H}} = 8 \times 10^{19} \text{ cm}^{-2}$ and a lack of bright stars (see Rosati et al., 2002).

In Figure 1 (left), we show the colour composite *Chandra* image of the CDFS. This was constructed by combining images (smoothed with a Gaussian with $r = 1''$) in three bands (0.3–1 keV, 1–3 keV, 3–7 keV), which contain approximately equal numbers of photons from detected sources. Blue sources are those undetected in the soft (0.5–2 keV) band, most likely due to intrinsic absorption from neutral hydrogen with column densities $N_{\text{H}} > 10^{22} \text{ cm}^{-2}$. Very soft sources appear red. A few extended low surface brightness sources are also readily visible in the image.

The CDFS was also observed with *XMM-Newton* for a total of ~ 500 ksec in July 2001 and January 2002 in guaranteed observation time (PI: J. Bergeron). Due to high background conditions some data were lost and a total of ~ 370 ksec has finally been accumulated. The colour composite image of the *XMM-Newton* dataset is shown in Figure 1 (right), smoothed with a Gaussian with $r = 5''$, using three energy bands (0.5–2 keV, 2–4.5 keV, 4.5–10 keV), thus harder than the *Chandra* image. The analysis of the *XMM-Newton* data is still ongoing, but we can conclude that the hard band sensitivity (5–10 keV) is comparable to the Megasecond *Chandra* image. The EPIC cameras have a larger

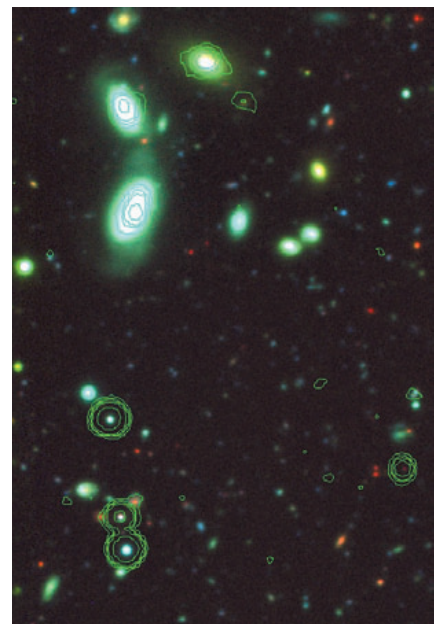
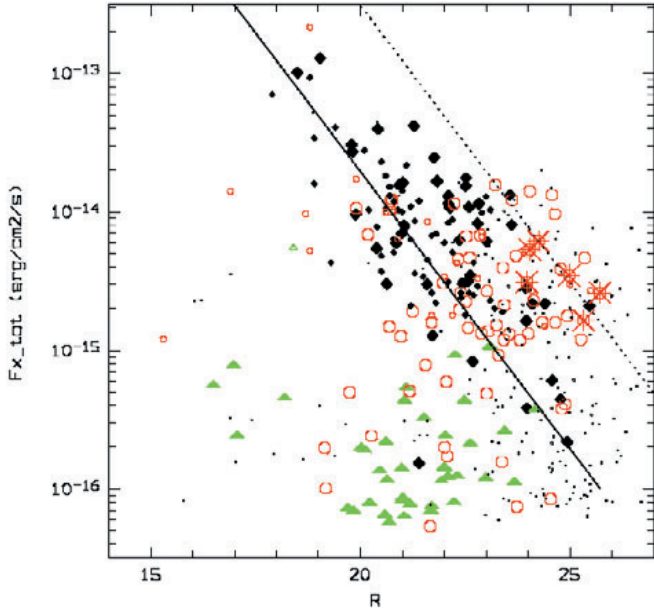


Figure 3: Cutout of a part of the CDFS. A deep FORS R-image has been combined with the EIS WFI B-image and the GOODS ISAAC K-image. X-ray contours are overlaid on the optical/NIR data. The image shows diffuse X-ray emission for the bright galaxies.

Figure 4: X-ray flux versus R-band magnitude for the CDFS sources (large symbols) and the ultra-deep ROSAT survey in the Lockman Hole (small symbols). Objects are coloured according to their X-ray/optical classification (see below): filled black diamonds correspond to type-1 AGN, open red hexagons to type-2 AGN and green triangles to galaxies. The large asterisks indicates type-2 QSOs (see text). Small dots refer to spectroscopically unidentified CDFS sources, the brighter ones of which have photometric redshifts. The solid line corresponds to an X-ray to optical flux ratio of 1, the dashed line is at an optical limit 3 magnitudes fainter.



field-of-view than ACIS, and a number of new diffuse sources are detected just outside the *Chandra* image. X-ray spectroscopy of a large number of sources will ultimately be very powerful with *XMM-Newton* (see Mainieri et al., 2002 for the Lockman Hole).

In Figure 2 (from Rosati et al., 2002), we show the *Chandra* cumulative number counts in three bands: soft, hard and very hard (5–10 keV). The logN-logS distribution shows a significant cosmological flattening in the softer bands, while in the very hard band it is still relatively steep, indicating that those surveys have not yet sampled the redshifts where the strong cosmological evolution of the sources saturates.

3. Optical identifications in the CDFS

Our primary optical imaging was obtained using the FORS1 camera on the ANTU (UT-1 at VLT) telescope. The R band mosaics from these data cover $13.6' \times 13.6'$ to depths between 26 and 26.7 (Vega magnitudes). These data do not cover the full CDFS area and must be supplemented with other observations. The ESO Imaging Survey (EIS) has covered this field to moderate depths in several bands (Arnouts et al. 2001; Vandame et al. 2001). The EIS data have been obtained using the Wide Field Imager (WFI) on the ESO-MPG 2.2 meter telescope at La Silla.

Figure 3 shows *Chandra* X-ray contours in a selected area of the CDFS superposed on a deep BRK multicolour image. The positioning is better than $0.5''$ and we readily identify likely optical counterparts in 85% of the cases (78% for the shallower WFI data). Note the very red object in the lower right,

which is only detected at K. Figure 4 shows the classical correlation between optical (R-band) magnitude and X-ray flux of the CDFS-objects in comparison with the deepest *ROSAT* sur-

vey in the Lockman Hole (Lehmann et al., 2001). Generally the 0.5-2 keV flux is given, however, for *Chandra* sources not detected in the soft band, the 2-10 keV flux is given. Sources are marked according to their optical classification (see below). The *Chandra* data extend the previous *ROSAT* range by a factor of ~ 40 in flux and to substantially fainter optical magnitudes. While the bulk of the type-1 AGN population still follows the general correlation along a constant f_x/f_{opt} line, the type-2 AGN cluster at higher X-ray to optical flux ratios. There is also a new population of normal galaxies showing up at significantly brighter optical magnitudes.

4. VLT optical spectroscopy

Optical spectroscopy has been carried out in ~ 11 nights with the ESO Very Large Telescope (VLT) in the time frame April 2000 - December 2001, using deep optical imaging and low resolution multiobject spectroscopy with the FORS instruments with individual exposure times ranging from 1-5 hours. Some preliminary results including the VLT optical spectroscopy have already been presented (Norman et al., 2002; Rosati et al., 2002). The complete opti-

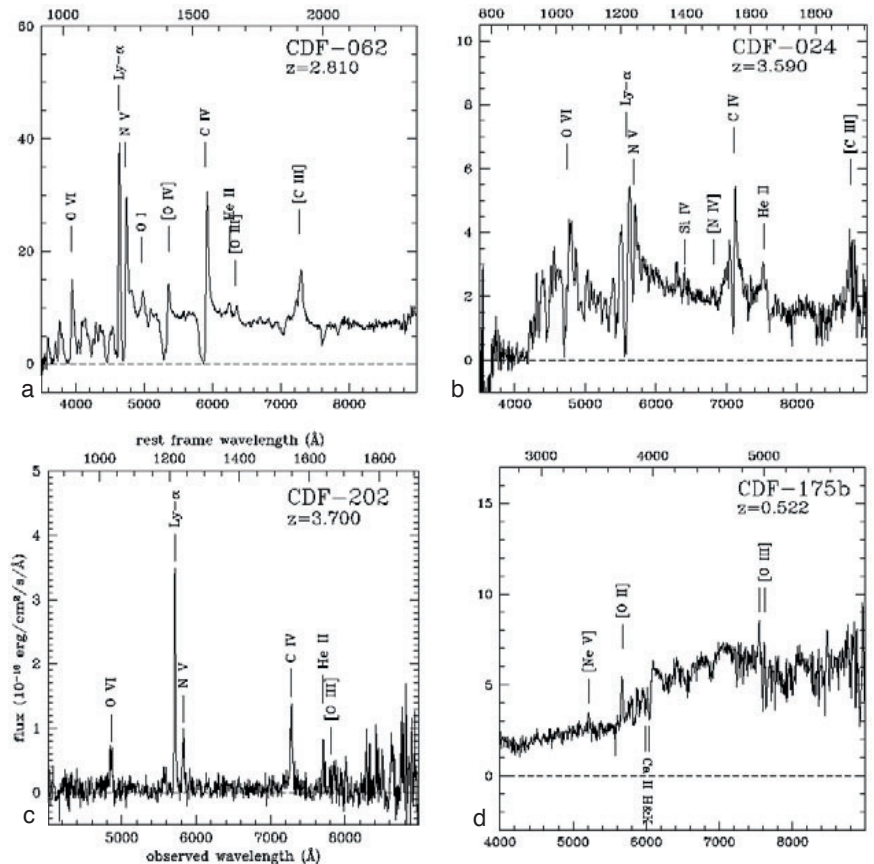


Figure 5: Optical spectra of some selected CDFS sources obtained using multiobject spectroscopy with FORS at the VLT (Szokoly et al., 2002). a: broad absorption line (BAL) QSO CDF-062 at $z=2.822$ (see also Giacconi et al., 2001); b: high-redshift QSO CDF-024 at $z=3.605$, showing strong absorption lines; c: QSO-2 CDF-202 at $z=3.700$ (see Norman et al., 2002); d: Seyfert-2 CDF-175b at $z=0.522$, showing a weak high excitation line of [NeV].

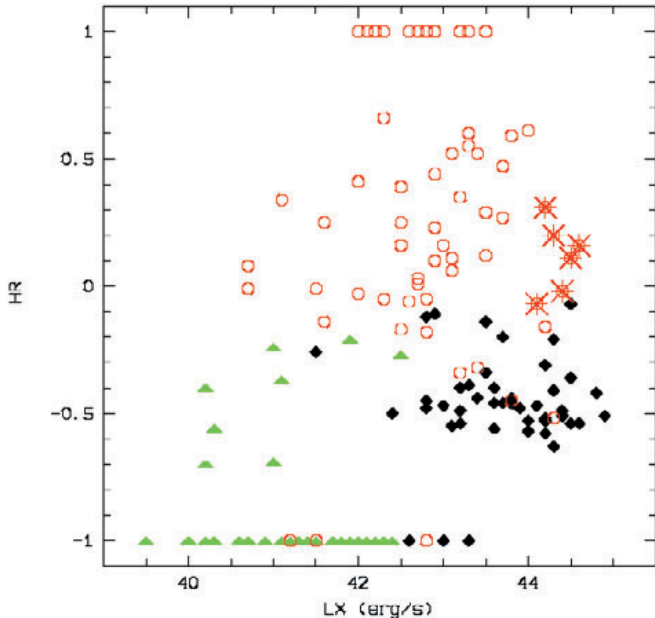


Figure 6: Hardness ratio versus rest frame luminosity in the total 0.5–10 keV band. Symbols as in Figure 4. A critical density universe with $H_0 = 50 \text{ km s}^{-1} \text{ Mpc}^{-1}$ has been adopted. Luminosities are not corrected for possible intrinsic absorption.

cal spectroscopy will be published in Szokoly et al. (2002). Figure 5 shows examples of four VLT spectra of sources with X-ray absorption. The upper two spectra show high-redshift QSOs with restframe-UV absorption features (BAL or mini-BAL QSOs), which both show some indication of intrinsic absorption in their X-ray spectra. The object in the lower left is the famous, highest redshift type-2 QSO detected in the CDFS with heavy X-ray absorption and a $\sim 7 \text{ keV}$ Fe-line in the QSO rest frame (Norman et al., 2002). The spectrum in the lower right shows a Seyfert-2 galaxy with heavy X-ray absorption and an AGN-type luminosity. The latter spectrum is characteristic for the bulk of the detected galaxies, which show either no or very faint high excitation lines indicating the AGN nature of the object, so that we have to resort to a combination of optical and X-ray diagnostics to classify them as AGN (see below). Redshifts could be obtained so far for 169 of the 346 sources in the CDFS, of which 123 are very reliable (high quality spectra with 2 or more spectral features), while the remaining optical spectra contain only a single emission line, or are of lower S/N.

For objects fainter than $R=24$ reliable redshifts can be obtained if the spectra contain strong emission lines. For the remaining optically faint objects we have to resort to photometric redshift techniques. Nevertheless, for a subsection of the sample at off-axis angles smaller than 8 arcmin we obtain a spectroscopic completeness of about 60%.

5. Optical and X-ray classification

Type-1 AGN (Seyfert-1 and QSOs) can be often readily identified by the broad permitted emission lines in their optical spectra. Luminous Seyfert-2 galaxies show strong forbidden emis-

sion lines and high-excitation lines indicating photoionization by a hard continuum source. However, already in the spectroscopic identifications of the *ROSAT* Deep Surveys it became apparent, that an increasing fraction of faint X-ray selected AGN shows a significant, sometimes dominant contribution of stellar light from the host galaxy in their optical spectra, depending on the ratio of optical luminosity between nuclear and galaxy light (Lehmann et al., 2001). If an AGN is much fainter than its host galaxy it is not possible to detect it optically. Many of the counterparts of the faint X-ray sources detected by *Chandra* and *XMM-Newton* show optical spectra dominated by their host galaxy and only a minority have clear indications of an AGN nature (see also Barger et al., 2001). In these cases, the X-ray emission could still be dominated by the active galactic nucleus, while a contribution from stellar and thermal processes (hot gas from supernova remnants, starbursts and thermal halos, or a population of X-ray binaries) can be important as well.

Therefore X-ray diagnostics in addition to the optical spectroscopy can be crucial to classify the source of the X-ray emission. AGN have typically (but not always!) X-ray luminosities above $10^{42} \text{ erg s}^{-1}$ and power law spectra, often with significant intrinsic absorption. Local, well-studied starburst galaxies have X-ray luminosities typically below $10^{42} \text{ erg s}^{-1}$ and very soft X-ray spectra. Thermal haloes of galaxies and the intergalactic gas in groups can have higher X-ray luminosities, but have soft spectra as well. The redshift effect in addition helps the X-ray diagnostic, because soft X-ray spectra appear even softer already at moderate redshift, while the typical AGN power law spectra appear harder over a very wide range of redshifts.

Following Rosati et al (2002), we show in Figure 6 the hardness ratio as a function of the luminosity in the 0.5–10 keV band for 165 sources for which we have optical spectra and rather secure classification (Szokoly et al. in preparation). The hardness ratio is defined as $HR = (H-S)/(H+S)$ where H and S are the net count rates in the hard (2–7 keV) and the soft band (0.5–2 keV), respectively. The X-ray luminosities are not corrected for internal absorption and are computed in a critical density universe with $H_0 = 50 \text{ km s}^{-1} \text{ Mpc}^{-1}$.

Different source types are clearly segregated in this plane. Type-1 AGNs (black diamonds) have luminosities typically above $10^{42} \text{ erg s}^{-1}$, with hardness ratios in a narrow range around $HR \approx -0.5$. This corresponds to an effective $G = 1.8$, commonly found in type-1 AGN. Type-2 AGN are skewed towards significantly higher hardness ratios ($HR > 0$), with (absorbed) luminosities in the range $10^{41-44} \text{ erg s}^{-1}$. Direct spectral fits of the *XMM-Newton* and (some) *Chandra* spectra clearly indicate that these harder spectra are due to neutral gas absorption and not due to a flatter intrinsic slope (see Mainieri et al., 2002). Therefore the unabsorbed, intrinsic luminosities of type-2 AGN would fall in the same range as those of type-1's.

In Figure 6, we also indicate the type-2 QSOs (asterisks), the first one of which was discovered in the CDFS (Norman et al. 2002). In the meantime, more examples have been found in the CDFS and elsewhere (e.g. Stern et al. 2002). It is interesting to note that no high-luminosity, very hard sources exist in this diagram. This is a selection effect of the pencil beam surveys: due to the small solid angle, the rare high luminosity sources are only sampled at high redshifts, where the absorption cut-off of type-2 AGN is redshifted to softer X-ray energies. Indeed, the type-2 QSOs in this sample are the objects at $L_X > 10^{44} \text{ erg s}^{-1}$ and $HR > -0.2$. The type-1 QSO in this region of the diagram is a BAL QSO with significant intrinsic absorption.

About 10% of the objects have optical spectra of normal galaxies (marked with triangles), luminosities below $10^{42} \text{ erg s}^{-1}$ and very soft X-ray spectra (several with $HR = -1$), as expected in the case of starbursts or thermal halos. Those at $L_X < 10^{41.5} \text{ erg s}^{-1}$ and HR larger than -0.7 are at particularly low redshifts. However, a separate subset has harder spectra ($HR > -0.5$), and luminosities $> 10^{41} \text{ erg s}^{-1}$. In these galaxies the X-ray emission is likely due to a mixture of low level AGN activity and a population of low mass X-ray binaries (see also Barger et al., 2001). Therefore the deep *Chandra* and *XMM-Newton* surveys detect for the first time the population of normal starburst

galaxies out to intermediate redshifts (Mushotzky et al., 2000; Giacconi et al., 2001; Lehmann et al., 2002). These galaxies might become an important means to study the star formation history in the universe completely independently from optical/UV, sub-mm or radio observations.

6. The redshift distribution

Figure 7 shows the optical magnitudes of the spectroscopically identified CDFS sources as a function of redshift. There is a segregation between type-1 and type-2 AGN at high redshifts, most likely because the optical light from type-1 AGN contains a significant non-thermal contribution in addition to the host galaxy. Reliable redshifts can be obtained at the VLT typically for objects with $R < 25.5$, however, some incompleteness already sets in around $R = 23$. The CDFS has a spectroscopic completeness of about 60%, which is mainly caused by the fact that about 40% of the counterparts are optically too faint to obtain reliable spectra. Photometric redshift estimates of the remainder of the sources indicate a redshift distribution similar to the spectroscopic one.

The completeness of 60% therefore allows us to compare the redshift distribution with predictions from X-ray background population synthesis models (Gilli, Salvati & Hasinger 2001), based on the AGN X-ray luminosity function and its evolution as determined from the *ROSAT* surveys (Miyaji et al., 2000), which predict a maximum at redshifts around $z = 1.5$. It is interesting to note, that contrary to these expectations, the bulk of the CDFS objects are found at redshifts below 1. The redshift distribution peaks at $z \sim 0.7$, even if the normal star forming galaxies in the sample are removed. This clearly demonstrates that the population synthesis models will have to be modified to incorporate different luminosity functions and evolutionary scenarios for intermediate-redshift, low-luminosity AGN.

In Figure 7 there is an interesting accumulation of redshifts in the range $z = 0.6-0.8$. We obviously have discovered two large-scale structures at redshifts $z = 0.66$ and $z = 0.73$, respectively, which are made up of type-1 and type-2 AGN as well as normal galaxies in roughly the same proportion as observed in the field. The objects in these redshift spikes are distributed across a large fraction of the field, so that they are probably sheet-like structures. At least one of them (at $z = 0.73$) is also seen in the K-band selected galaxy survey of Cimatti et al. (2002) and corresponds to several X-ray clusters in the field. It will be interesting to study the correlation of active galaxies to field galaxies in these sheets and to try to determine the role that galaxy mergers play in the trig-

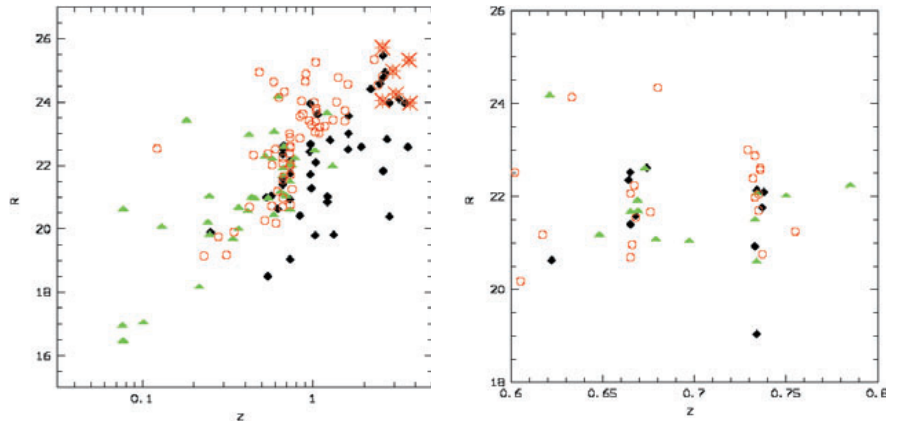


Figure 7: Left: Optical magnitudes as a function of redshift for the CDFS objects. Symbols are as in Figure 4. An accumulation of objects in two redshift bins around $z = 0.7$ (enlarged in the right figure) is due to a large scale structure in the CDFS.

gering of the AGN activity. Finally, there may be a relation between the surprisingly low redshift of the bulk of the *Chandra* sources, the existence of the sheets at the same redshift and the strongly evolving population of dusty starburst galaxies inferred from the ISO mid-infrared surveys (Franceschini et al., 2002).

By no means does the CDFS redshift distribution confirm the prediction by Haiman & Loeb (1999), that a large number (~ 100) QSO at redshifts larger than 5 should be expected in any ultra deep *Chandra* survey. The highest redshift in the CDFS thus far is 3.7, while there are two objects at $z = 4.4$ and $z = 5.2$, respectively, in the HDF-N (Brandt et al., 2002) and one QSO at $z = 4.5$ in the Lockman Hole (Schneider et al. 1998). This suggests a cut-off of the X-ray selected QSO space density at high redshift.

7. Summary and outlook

Deep X-ray surveys have shown that the cosmic X-ray background (XRB) is largely due to accretion onto supermassive black holes, integrated over cosmic time. The findings are consistent with the notion that most larger galaxies contain black holes which have been active in the past. However, the characteristic hard spectrum of the XRB can only be explained if most AGN spectra are heavily absorbed (Comastri et al. 1995). Thus about 80-90% of the light produced by accretion must be absorbed by gas and dust clouds, which may reside in nuclear starburst regions that feed the AGN (Fabian et al., 1998).

The star formation history has been determined in the last years based on optical and UV measurements (Steidel et al., 1999). However, deep submillimeter surveys with SCUBA have revealed the existence of a large population of hitherto undetected dust-enriched galaxies (e.g. Hughes et al. 1998), which may provide the dominant contribution to the star formation rate at

higher redshifts. The spectral shape of the X-ray background may be related to the dust obscuration of the far-infrared sources, which are believed to be the high- z equivalents of the ultra luminous IR galaxies (ULIRGs). For some ULIRGs the presence of heavily obscured AGN has been inferred by *BeppoSAX* (e.g. Vignati et al. 1999). Therefore a relation between the faint X-ray and far-infrared source populations is expected. Indeed, a large fraction of the faint hard *Chandra* and *XMM-Newton* sources have infrared counterparts in deep ISOCAM images (Fadda et al., 2002, Alexander et al., 2002) and the redshift distribution of faint X-ray sources and Mid-IR sources is similar (see above).

The so-far deepest X-ray and SCUBA observations (Hornschemeier et al., 2000) did pick up only very few common objects. Even deeper X-ray images in conjunction with deep surveys at the peak wavelength of the far-infrared background e.g. with SIRTf, are therefore required. The *Chandra* Deep Field South has been selected as one of the deep fields in the SIRTf legacy programme "Great Observatories Origins Deep Survey" (GOODS). GOODS will produce the deepest observations with the SIRTf IRAC instrument at $3.6-8 \mu\text{m}$ and with the MIPS instrument at $24 \mu\text{m}$ and together with the *Chandra* data provide the necessary depth and statistics to finally establish the FIR/X-ray relation.

In addition to the data described here, a large number of supporting observations across a wide range of the electromagnetic spectrum are being carried out or planned. We have proposed to complement the already existing *Chandra* Megasecond observations with two 500 ksec ACIS-I pointings to homogenize and increase the exposure in the GOODS area to 2 Msec. Three small regions in the CDFS have already been observed with HST, which provides excellent morphology of the AGN host galaxies and photometry for the

faintest optical counterparts (Koekemoer et al., 2002). The whole CDFS will soon be covered by an extensive set of pointings with the new Advanced Camera for Surveys (ACS) in BVlz to “near HDF” depth. Following up the deep EIS survey in the CDFS, ESO has started a large program to image the GOODS area with the VLT to obtain deep JHKs images in some 32 ISAAC fields. The first imaging data covering the central 50 arcmin² have recently been made public. Optical spectroscopy across the whole field will be obtained with very high efficiency using VIRMOS on the VLT.

The multiwavelength coverage of the field will be complemented by deep radio data from the VLA at 6 cm (already obtained) and ATCA at 20 cm. The CDFS/GOODS will therefore ultimately be one of the patches in the sky providing a combination of the widest and deepest coverage at all wavelengths and thus a legacy for the future.

References

Alexander D.M., Aussel H., Bauer F.E., et al., 2002, ApJ 568, L85

Arnouts S., Vandame B., Benoist C., et al., 2001, A&A. 379, 740
 Barger, A. J., Cowie, L. L., Mushotzky, R. F., Richards, E. A., 2001, AJ 121, 662
 Brandt W.N., Alexander D.M., Bauer, F.E., Hornschemeier A.E., 2002, astro-ph/0202311
 Cimatti, A., Daddi E., Mignoli M., et al., 2002, A&A 381, L.68
 Comastri, A.; Setti, G.; Zamorani, G.; Hasinger, G., 1995, A&A 296, 1
 Fabian A.C., Barcons X., Almaini O., Iwasawa K., 1998, MNRAS 297, L11
 Fadda D., Flores H., Hasinger G., 2002, A&A 383, 838
 Fiore F., La Franca F., Giommi P., et al., 1999, MNRAS 306, 55
 Franceschini A., Fadda D., Cesarsky C., et al., 2002, ApJ 568, 470
 Gebhardt K., Bender R., Bower G., et al., 2000, ApJ 539, 13
 Giacconi, R., Rosati P., Tozzi P., et al., 2001, ApJ 551, 624
 Gilli, R., Salvati, M., Hasinger, G., 2001, A&A 366, 407
 Granato G.L., Danese L., Francheschini A., 1997, ApJ 486, 147
 Haiman, Z. & Loeb A., 1999, ApJ 519, 479
 Hasinger, G., Burg, R., Giacconi, R., et al., 1998, A&A 329, 482
 Hasinger, G., Altieri, B., Arnaud, M., et al., 2001, A&A 365, 45
 Hornschemeier, A.E., Brandt, W.N., Garmire, G.P., et al., 2000, ApJ 541
 Hughes D.H., Serjeant S., Dunlop J., et al., 1998, Nature 394, 241

Koekemoer A.M., Grogin N.A., Schreier E.J., 2002, ApJ 567, 657
 Lehmann, I., Hasinger, G., Schmidt, M., et al., 2001, A&A 371, 833
 Lehmann I., Hasinger G., Murray S.S., Schmidt M., 2002, astro-ph/0109172
 Mainieri V., Bergeron J., Rosati P., et al., 2002, astro-ph/0202211
 Miyaji, T., Hasinger, G., Schmidt, M., 2000, A&A 353, 25
 Mushotzky, R.F., Cowie L.L., Barger, A.J., Arnaud, K.A., 2000, Nature 404, 459
 Norman C., Hasinger G., Giacconi R., et al. 2002, ApJ 571, 218
 Rosati P., Tozzi P., Giacconi R., et al., 2002, ApJ 566, 667
 Schmidt, M., Schneider, D.P. & Gunn J.E., 1995, AJ 114, 36
 Schmidt, M., Hasinger, G., Gunn, J.E., et al., 1998, A&A 329, 495
 Schneider, D.P., Schmidt, M., Hasinger, G., et al., 1998, AJ 115, 1230
 Shaver P.A. et al., 1996, Nature 384, 439
 Steidel C.C., Adelberger K.L., Giavalisco M., Dickinson M., Pettini M., 1999, ApJ 519, 1
 Stern D., Moran E.C., Coil A.L., et al., 2002, ApJ 568, 71
 Szokoly, G., Hasinger G., Rosati, P. et al., 2002 (in prep.)
 Vandame et al. 2001, astro-ph/0102300
 Vignati P., Molendi S., Matt G., et al., 1999, A&A 349, L57

Using color-magnitude diagrams and spectroscopy to derive star formation histories: VLT observations of Fornax

CARME GALLART¹, Andes Prize Fellow, Departamento de Astronomía, Universidad de Chile, and Department of Astronomy, Yale University

ROBERT ZINN, Department of Astronomy, Yale University

FREDERIC PONT², Departamento de Astronomía, Universidad de Chile

EDUARDO HARDY, National Radio Astronomy Observatory

GIANNI MARCONI, European Southern Observatory

ROBERTO BUONANNO, Osservatorio Astronomico di Roma

1. Star formation and chemical enrichment histories of the Milky Way satellites

During the last decade, the varied star formation histories of the dSph galaxies satellites of the Milky Way have been revealed to us in detail, dramatically changing our perception from the early idea that they were predominantly old systems. Some hints on the presence of, at least, an intermediate-age population had been provided previously by the peculiarity of the variable star populations of dSph galaxies (Norris & Zinn 1975) and the discovery of Carbon stars in Fornax (Demers & Kun-

kel 1979; Aaronson & Mould 1980), Carina (Cannon, Niss & Norgaard-Nielsen 1981) and other dSph (Aaronson, Olszewski & Hodge 1983). However, only in the last few years have these intermediate-age populations been shown beautifully in the wide-field, extremely deep CMDs of a number of dSph galaxies. There is the extreme case of Leo I (Caputo et al. 1999; Gallart et al. 1999a,b), which has formed over 80% of its stars from 6 to 1 Gyr ago, and the intermediate cases of Carina (Smecker-Hane et al. 1996; Hurlley-Keller et al. 1998; Castellani et al. 2001) and Fornax (Stetson et al. 1997; Buonanno et al. 1999), with prominent intermediate-age populations. There are also predominantly old systems like Draco (Aparicio et al. 2001) and Ursa Minor (Carrera et al. 2002).

These CMDs offer qualitative first glances at the star formation histories (e.g. in the case of Carina, one can see that there have been three major events of star formation), but their quantitative determination requires a detailed comparison of the distribution of stars in the CMD with that predicted by model CMDs. CMDs reaching the old main-sequence turnoffs are particularly useful for these comparisons because there are few uncertainties in the theory for this stage of a star's life and there is less age-metallicity degeneracy. We have shown that with this method, it is possible to break the classical age-metallicity degeneracy in stellar populations for systems with low levels of metal enrichment like Leo I (Gallart et al. 1999b). However, in the case of a more complicated chemical

¹Currently: Ramon y Cajal Fellow. Instituto de Astrofísica de Canarias.

²Currently: Observatoire de Genève.



Figure 1: Image of the central field in Fornax obtained by combining the V and FORS1 I images. Cluster 4 is in the bottom left corner. The outline of the WFC2 camera shows the pointing from which the photometry in Figure 2c was obtained. North is up and East is to the left.

evolution, the age-metallicity degeneracy may be more difficult to break (Gallart, Aparicio & Bertelli 2002), and in these cases, obtaining independent constraints on the age-metallicity relationship $Z(t)$ may be key to retrieving unambiguously the star formation history.

Spectroscopic studies that would provide direct information on the metallicities of the stars in these galaxies are scarce, due to the large investment of large-aperture telescope time required. Only a few high dispersion spectroscopic studies of stars in dSph galaxies have been published so far, either from Keck-HIRES (e.g. Shetrone, Côté & Sargent 2001 and references therein) or from VLT-UVES (Bonifacio et al. 2000), and all count the measured stars

by the units. The extraordinary multiplexing capability of FLAMES at the VLT will certainly cause a breakthrough in this field in the near future.

A more economical – though less informative – way of obtaining metallicity information involves low resolution spectroscopy. The Ca II triplet offers the possibility of obtaining global $[\text{Fe}/\text{H}]$ values for individual stars with relatively high precision (≤ 0.2 dex), and this technique has developed into the most popular way of using low-resolution spectra to estimate the abundances of stars in globular clusters and dSph galaxies.

We undertook a study of the star formation and chemical enrichment history of the Fornax dSph galaxy with the twofold approach described above: we

used the VLT with FORS1 to obtain photometry reaching the oldest main-sequence turnoffs and CaII triplet spectroscopy of a sample of red giant branch stars in the same fields. The observations and the main results are described below.

2. Wide field color-magnitude diagrams

We obtained old main-sequence turnoff photometry in three fields at two galactocentric distances in the dSph Fornax, using FORS1 at the VLT. The observations were performed in service mode in July 2000, with the requirement of seeing $\leq 0.6''$, which is key to perform photometry in fields affected by stellar crowding. In some of the frames,

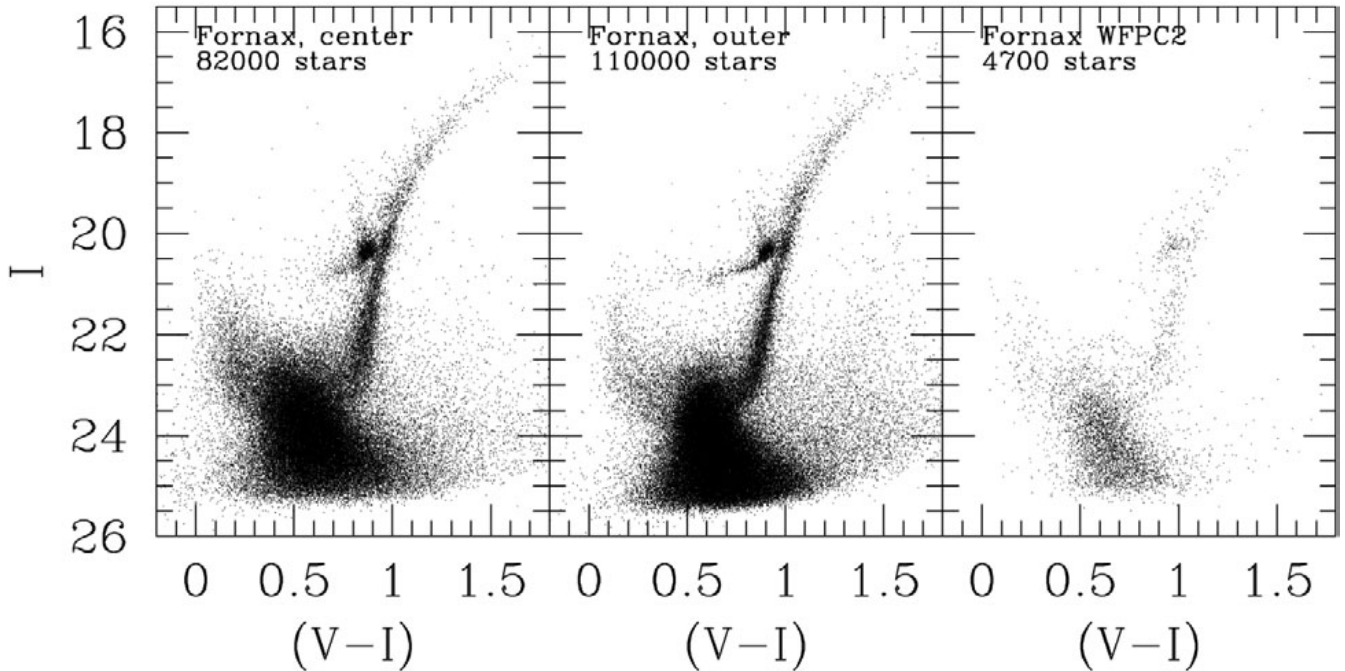


Figure 2: a) CMD for a FORS1 field centred in Fornax; b) composite CMD for the two fields situated about 11 arcmin North; c) WFPC2 CMD of a subset of the central field, shown in Figure 1.

with exposure times as long as 750 sec, the seeing was measured as good as 0.4". In the central field, containing globular cluster Fornax #4, a total of 3650 sec in V and 4700 sec in I were accumulated. The other two fields were situated at about 11 arcmin north of the center of the galaxy, and total integration times were 1850 sec in V and 4600 sec in I. The locations of these off-center fields were chosen by considering the change in surface brightness across Fornax and then selecting fields that would provide measurements of similar numbers of stars in the central field and in the other two fields combined. A composite image combining the V and I frames of the central field is shown in Figure 1, where the outline of the HST WFPC2 camera has been superimposed in the position where HST observations exist. The gain in area allowed by FORS1 at the VLT is key to measuring sufficient numbers of stars in parts of the CMD that are vital for deriving the star formation history, such as the subgiant branch and the horizontal branch.

Figure 2 shows the CMDs at the two galactocentric distances. The CMD in Figure 2a corresponds to the central field, while Figure 2b displays the CMD of the off-center fields. Figure 2c shows the WFPC2 CMD from Buonanno et al. (1999). Note that the depth of the FORS1 CMDs is similar to that of the WFPC2 CMD, but that the number of stars in the former is much larger, thus providing a better representation of the star formation history, not affected by small number statistics. In fact, a tantalizing evidence of bursts of star formation in Fornax was provided by the sparsely populated subgiant branch of

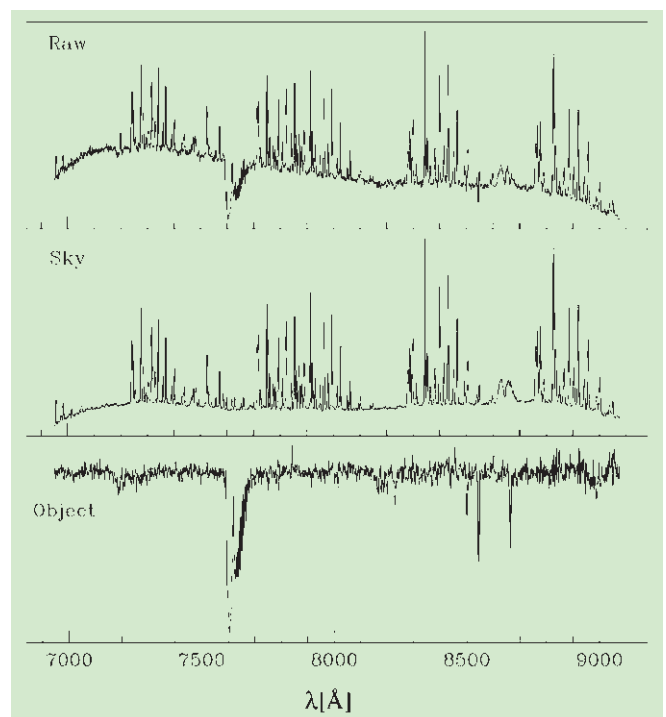
the WFPC2 CMD; the FORS1 CMD, instead, seems to show a smooth distribution of stars in the subgiant branch, that may be indicative of continuous star formation. We are still investigating if we can definitely rule out discrete burst of star formation with the FORS1 data.

Our goal is to derive the complete star formation history in these fields, and test for possible spatial variations, using synthetic CMDs, and the input on $Z(t)$ from the CaII triplet study (see below).

3. Stellar metallicities from the CaII triplet

We obtained CaII triplet spectroscopy for about 100 RGB stars in the central part of Fornax, using FORS1 at the VLT,

Figure 3: Example showing the excellent sky subtraction allowed by the dithering technique in one of our Fornax targets. Top: raw spectrum. The sky emission lines are prominent, with the Ca II triplet lines hardly noticeable under them. Middle: the sky spectrum obtained next to the star spectrum. Bottom: the final sky-subtracted spectrum.



in December 1999. The central wavelength was 7490 Å, dispersion 1.06 Å per pixel, and resolution $R \approx 1530$. The excellent seeing conditions during the observations – most of the time below 0.8" seeing – allowed us to use slitlet widths of 0.7 arcsec. We observed seven fields, with an average of 17 targets per field. For each, two 20-min exposures were acquired on two positions offset along the slit by about 3". This procedure allows the direct subtraction of the sky from the unextracted spectra and very significantly improves the removal of the contamination by night sky emission lines. Short expo-

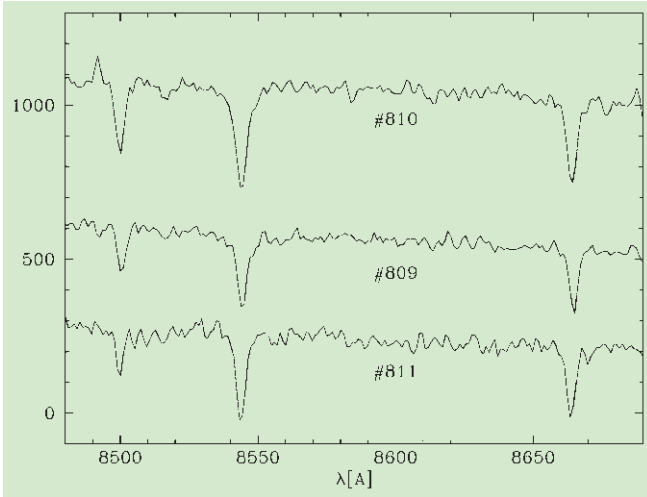


Figure 4: Representative spectra for three stars spanning the luminosity range of our targets.

ures were also obtained on selected red giants of three nearby globular clusters of known metallicity for calibration purposes.

Figure 3 show the excellent sky subtraction that can be achieved with the dithering technique discussed above. Figure 4 shows three examples of the quality of the spectra obtained for one of the brightest, faintest and intermediate-brightness stars in our sample.

We find a large metallicity dispersion in Fornax, with about 20% of the objects having low abundances ($-2.5 \leq [\text{Fe}/\text{H}] \leq -1.3$), and about 35% having abundances greater than 47 Tuc ($[\text{Fe}/\text{H}] = -0.7$). The peak of the metallicity distribution occurs at $[\text{Fe}/\text{H}] \approx -0.9$. The most metal rich stars have Ca II triplet equivalent widths $W(\text{Ca})$ as strong as the average of the metal-richer LMC population in Cole et al. (2000). This allows us to put an upper limit to the metallicity of the stars in Fornax, which lie in a somewhat uncertain area of the $W(\text{Ca})$ - $[\text{Fe}/\text{H}]$ calibration (see Pont et al. 2002 for a thorough discussion of this point).

The combination of the spectroscopic metallicity for each star with its color

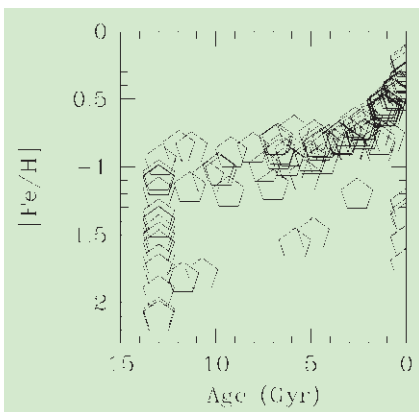


Figure 5: Age-metallicity relation obtained for Fornax from Ca II triplet spectroscopy and RGB photometry. See text for details.

on the RGB provides a constraint on its age, and therefore, a well delineated age-metallicity relation can be obtained, especially for the more metal-rich, young stars. The colors of most metal-rich RGB stars are much bluer than those of an old globular cluster of the same metallicity, and lead to the conclusion that they must be much younger.

Indeed, while for each given metallicity, stars older than ≈ 3 Gyr have a small range in color, the younger stars are substantially and increasingly bluer with decreasing age. In Figure 5 we display a preliminary version of the Fornax age-metallicity relation obtained by Pont et al. (2002).

Finally, using theoretical evolutionary models, we investigated the relation between the stellar population represented in the fraction of the RGB that has been spectroscopically observed, and the total population of the galaxy.

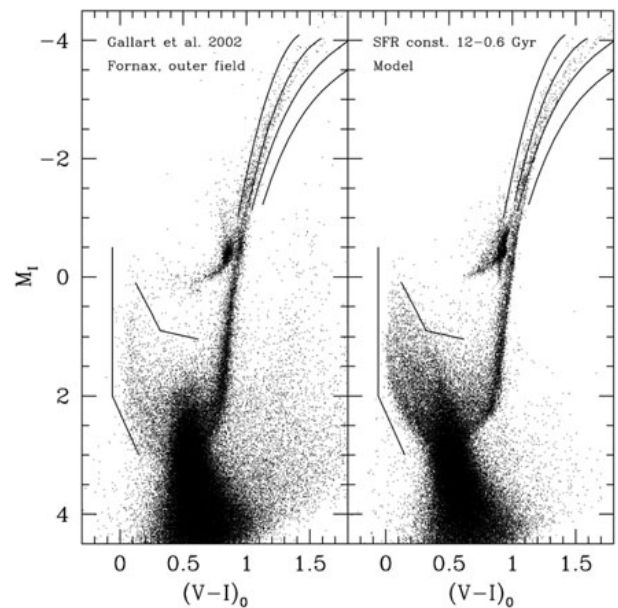
4. Combining Ca II triplet spectroscopy with the color-magnitude diagram: a coherent picture of the Fornax star formation history

The $Z(t)$ shown in Figure 5 was obtained by combining the spectroscopic metallicity with the position of the stars on the RGB. But is our picture com-

patible with parts of the CMD other than the RGB? The Fornax CMD contains numerous features associated with a particular age and metallicity, namely a horizontal branch, an important red clump with a long tail at the bright end, and a main sequence extending to $M_V \sim -0.5$. These features indicate respectively the existence of an old, metal-poor population, a significant intermediate-age population, and a very recent population, as young as ≈ 500 Myr old. All of these are qualitatively compatible with the picture obtained from the RGB and the Ca II triplet, which indicates the need for a substantial amount of young population to account for the blue color of the metal-rich stars.

The locations of these evolutionary phases in the CMD depend on the metallicities and the ages of the stars (thus on $Z(t)$), while the numbers of stars in each phase depend on the lifetime of the phase and the star formation history of Fornax. To test if the derived $Z(t)$ produces stars in the right positions in the CMD, we computed a synthetic model of the Fornax CMD assuming that $Z(t)$ and a constant star formation rate starting 12 Gyr ago and stopping 600 Myr ago, to account for the absence of a very bright main sequence in the CMD. $Z(t)$ was approximated by a linear interpolation between (Gyr $\sim z$) = (15.0, 0.0001), (10.0, 0.0011), (2, 0.0036), (1, 0.0057) and (0, 0.008). We used the synthetic CMD code ZVAR (Bertelli et al. 2002) with the Bertelli et al (1994) generation of Padova stellar evolutionary models. A Kroupa, Tout & Gilmore (1993) IMF has been assumed, and a binary fraction $\beta = 0.25$, with mass fraction $q > 0.7$ and flat IMF for the secondary stars. For a description of these parameters and the way they are used in the ZVAR code, the reader is referred

Figure 6: Observed CMD for the outer Fornax field (left) and model color-magnitude diagram (right) obtained assuming a fit to the $Z(t)$ displayed in Figure 5, a constant star formation rate from 12 to 0.6 Gyr ago, and a given binary fraction (see text for details). A few lines around the upper main sequence, and a few globular cluster RGB loci from Da Costa & Armandroff (1990) have been drawn to guide the eye. Note that the different density of stars in different areas of the CMD may be due to the fact that the star formation rate has been assumed constant (we did not try to model it at this stage). Also the simulation of observational errors is somewhat preliminary and an underestimate of the errors may cause the different width of the main-sequence and the different shape of the red-clump.



to Gallart et al. (1999b). The completeness and error simulation has been performed using a preliminary crowding test table obtained from the deep VLT imaging for Fornax presented in Gallart et al. (2002).

The resulting synthetic CMD is displayed in Figure 6, to the right of the observed CMD. The synthetic CMD successfully reproduces the major morphological features of the observed CMD, namely the RGB, the horizontal branch, the red-clump and the main-sequence. Particularly important is the agreement between locations of the young main-sequence stars (a set of lines have been drawn in both the observed and model CMDs to guide the eye). Its position is very sensitive to metallicity of the stars younger than about 2 Gyr. If their metallicity were lower than that given by the $Z(t)$ relation, for example, lower than $[Fe/H] \leq -0.7$, as one could deduce from the color of the RGB without correction for the young ages of the stars, then the position of this part of the main sequence would be substantially too blue. There is also striking agreement between the model and observed CMDs for the *plume* of stars above the red-clump, which is composed of metal rich young stars (younger than 1 Gyr and with $Z \approx 0.006-0.008$) undergoing their He-burning loop phase of stellar evolution. The most obvious disagreement between the model and the observed CMDs is in the color of the RGB. To illustrate this we have plotted in both diagrams the fiducial RGBs of the globular clusters M15, M2, NGC 1851 and 47

Tuc, from Da Costa & Armandroff (1990). Notice that the model RGB is somewhat redder than the observed one. This disagreement, which is larger for the fainter RGB stars, is known to exist from other comparisons between observations and the Padova stellar evolutionary models. It has no effect on our major conclusion that the $Z(t)$ shown in Figure 5 is compatible with the morphology of the Fornax CMD. A quantitative derivation of the star formation history from a thorough fit of the CMD will add further confidence in the reconstruction of the history of Fornax. It will be presented in Gallart et al. (2002).

Acknowledgements. This research is part of a Joint Project between Universidad de Chile and Yale University, funded partially by the Fundación Andes. C.G. acknowledges partial support from Chilean CONICYT through FONDECYT grant number 1990638. R.Z. was supported by NSF grant AST-9803071 and F.P. by the Swiss National Science Fund and FONDECYT grant number 3000056.

References

- Aaronson, M., Olszewski, E.W. & Hodge, P.W. 1983, *ApJ*, **267**, 271
 Aaronson, M. & Mould, J. 1980, *ApJ*, **240**, 804
 Aparicio, A., Carrera, R. & Martínez-Delgado, D. 2001, *AJ*, **122**, 2524
 Bertelli, G., Bressan, A., Chiosi, C., Fagotto, F. & Nasi, E. 1994, *A&AS*, **106**, 275
 Bertelli, G. et al. 2002, in preparation
 Bonifacio, P., Hill, V., Molaro, P., Pasquini, L., Di Marcantonio, P., & Santin, P. 2000, *A&A*, **359**, 663

- Buonanno, R., Corsi, C.E., Castellani, M., Marconi, G., Fusi Pecci, F. & Zinn, R. 1999, *AJ*, **118**, 1671
 Cannon, R.D., Niss, B. & Norgaard-Nielsen, H.U. 1981, *MNRAS*, **196**, 1
 Caputo, F., Cassisi, S., Castellani, M., Marconi, G., Santolamazza, P. 1999, *AJ*, **117**, 2199
 Carrera, R., Aparicio, A., Martínez-Delgado, D., & Alonso, J. 2002, *AJ*, in press
 Castellani, M., Pulone, L., Ripepi, V., Dall’Ora, M., Bono, G., Brocato, E., Caputo, F., Castellani, V., Corsi, C. 2001, in “Dwarf Galaxies and their environment”, eds. K.S. de Boer, R.-J. Dettmar & U. Klein, Shaker Verlag.
 Cole, A., Smecker-Hane, T.A., Gallagher, J.S. 2000, *AJ*, **120**, 1808
 Da Costa, G. S. & Armandroff, T. E. 1990, *AJ*, **100**, 162
 Demers, S. & Kunkel, W.E. 1979, *PASP*, **91**, 761
 Gallart, C., Aparicio, A., Bertelli, G. 2002, in “Observed HR diagrams and stellar evolution...”, eds. T. Lejeune & J. Fernandes, ASP Conference Series.
 Gallart, C. et al. 1999a, *ApJ*, **514**, 665
 Gallart, C., Freedman, W.L., Aparicio, A., Bertelli, G. & Chiosi, C. 1999b, *AJ*, **118**, 2245
 Gallart, C., Zinn, R., Marconi, G., Hardy, E. & Buonanno, R. 2002, in prep.
 Hurley-Keller, D., Mateo, M. & Nemeč, J. 1998, *AJ*, **115**, 1840
 Kroupa, P., Tout, C.A. & Gilmore, G. 1993, *MNRAS*, **262**, 545
 Norris, J. & Zinn, R. 1975, *ApJ*, **202**, 335
 Pont, F., Zinn, R., Gallart, C., Winnick, R., Hardy, E. 2002, in preparation
 Shetrone, M.D., Côté, P. & Sargent, W.L.W. 2001, *ApJ*, **548**, 592
 Smecker-Hane, T. A., Stetson, P. B., Hesser, J. E. & van den Bergh, D. A. 1996 in *From stars to galaxies...*, eds.
 C. Leitherer, U. Fritze-van Alvensleben & J. Huchra. ASP Conf Ser, **98**, 328
 Stetson, P. B., Hesser, J. E. & Smecker-Hane, T. A. 1998, *PASP*, **110**, 533

The ups and downs of a stellar surface: Nonradial pulsation modelling of rapid rotators

THOMAS RIVINIUS, DIETRICH BAADE, ESO, Garching b. München, Germany

STANISLAV ŠTEFL, Astronomical Institute, Academy of Sciences Ondřejov, Czech Republic,

MONIKA MAINTZ, Landessternwarte Heidelberg, Germany

RICHARD TOWNSEND, University College London, United Kingdom

1. Introduction

Usually one thinks of stars as stable objects, taking at least millions of years to evolve significantly. While it is true that stars take such timescales to age, they need not be “stable” in a static sense over all that time. Many stars in fact undergo pulsations on timescales between minutes and years, as for instance the Be stars Baade, Rivinius and Štefl reported about in a recent *Messenger* issue (No. 107, p. 24). The most obvious pulsation mode is the radial one, where the star becomes bigger and smaller periodically, and like

any expanding/compressing gas also cooler and hotter again. We see these stars varying in brightness and colour, and their spectra cyclically approaching and receding. The well known Mira in the constellation Cetus ($P = 330$ day), or the Cepheids ($P = 1...50$ day), which help in measuring extragalactic distances, are such objects. Stars may not only pulsate radially, however. Imagine a free-floating blob of water in a Space Shuttle, or a big soap bubble. Before reaching a stable spherical shape (or popping) they undergo damped wobbles. This, in a sense, is externally excited non-

radial pulsation (*nrp*) in a multitude of modes.

Nonradially pulsating stars behave similarly. But since these pulsations are excited from inside the star and are going on for millions of cycles, they appear more ordered as most modes are damped, and typically only one or few high-amplitude modes are excited in an *nrp* star. The excitation process resembles a Carnot process (as in an ideal steam engine) where the role of the valve is played by a layer inside the star that turns opaque with increasing temperature due to ionization processes and becomes transparent again during

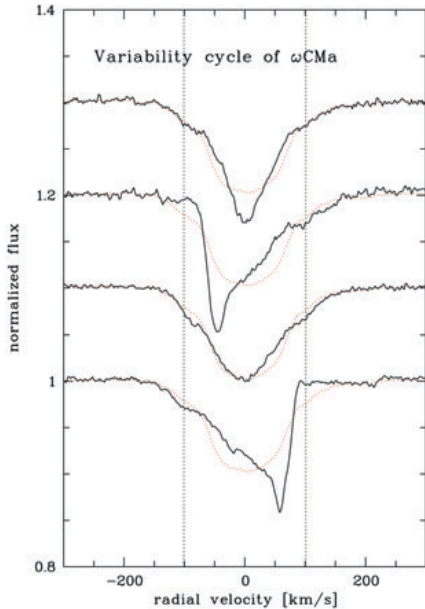


Figure 1: The pulsational variability of ω CMA in the MgII 4481 line. The phase (i.e. time) increases from bottom to top. The mean profile, which is averaged over all pulsation phases, is shown in red, the projected rotation velocity of the star is plotted as dotted lines, shifted to the stellar systemic velocity. The range of variability exceeds the rotational range by about 40 km s^{-1} with a ramp-like form. The line profile variability, well seen also in the asymmetric “spikes” at the most extreme blue and red phases, is among the strongest ever observed.

the following expansion phase. When such a layer is close to the stellar surface, stellar pulsation may be excited. On the stellar surface *nrp* manifests itself as a global wave pattern, which travels along the stellar surface parallel to the equator and causes the periodic behaviour. This global wave pattern can be described by means of quantum numbers ℓ and m , characterizing the number of oscillation nodes along the equator and across it, similar to the two-dimensional oscillations of a drumskin (or of the VLT primary mirror, being exploited for the active optics).

Such *nrp* might be very subtle, as in our Sun, which pulsates in numerous low-amplitude modes with $P = 5 \text{ min}$. In other stars, like the Be stars, however, the induced variability may look so violent, that it was first claimed that, if this were pulsation, the star would be disrupted. In fact, browsing the spectra of the early type Be star ω CMA after the observations taken during the HEROS project (Fig. 1, see also Baade et al., op. cit.), we were convinced that the periodic variability could not be modelled without taking into account also shocks and other non-linear effects. Most notably, the variability can be observed out to higher velocities than the projected stellar rotational velocity, which would normally suggest a

circumstellar origin, and the strong, narrow absorption “spikes” seemed to require severe distortions of the stellar surface (see Fig. 1 for an example). However, as will be shown, these features could be modelled without any additional assumptions with a general-purpose non-radial pulsation modelling code.

Other hypotheses proposed to explain the line profile variability (*lpv*) of Be stars, and especially of ω CMA, include starspots and co-rotating clouds. However, for none of them was a satisfying model able to reproduce the observed variations of more than a single spectral line.

Ever since the discovery of periodic *lpv* in Be stars one has wondered whether it could be the same process that is responsible for building up the circumstellar disk. Since the mass loss modulations of early type stars are not very well understood in general, the identification of the cause of the *lpv* in Be stars also would be a step forward in hot star physics in general.

2. A new model-code

When the HEROS project started, none of the hypotheses introduced above was clearly favoured. At this point, however, a new *nrp* modelling code, the BRUCE/KYLIE-package, was published by Rich Townsend. Several advantages made it the first choice to attempt modelling the *lpv* of ω CMA (and other pulsating Be stars).

For instance, the pulsational surface wave pattern depends not only on ℓ and m , but also on stellar rotational velocity. With increasing rotation, the wave pattern becomes more and more concen-

trated towards the equator. BRUCE, other than most codes before, can compute the surface wave pattern up to the critical rotation limit. It is therefore ideally suited to Be stars, that typically rotate at about 70 to 80% of their critical speed.

Also, BRUCE is one of the few codes optimized for relatively long oscillation periods (i.e. longer than the fundamental radial oscillation mode), for which horizontal motions are the most important. These are called *g*-modes (since gravity is the most important restoring force) and are comparable to water waves in an ocean. Most other codes specialize in short period pulsation modes, where radial motions dominate, called *p*-modes (from pressure) and rather resembling sound waves.

The input parameters required by BRUCE are stellar quantities (mass, temperature, radius, rotation, and inclination), and the pulsational parameters. At first look, this seems to be a disadvantage of the code, because other codes require only the pulsational parameters, but also only compute the variability of the *residuals* from the mean, not the line profiles themselves. However, this is in fact a major advantage, since the variability depends strongly on properties of the spectral line modelled, which in turn are determined by the stellar parameters. The extended wavelength range of echelle data allows one to make use of the differences of individual spectral lines formed at different stellar latitudes to further constrain the model parameters. Therefore, the reproduction of the variability and the mean profile, for as many different lines as possible, not only gives the pulsational parameters, but also the stellar ones.

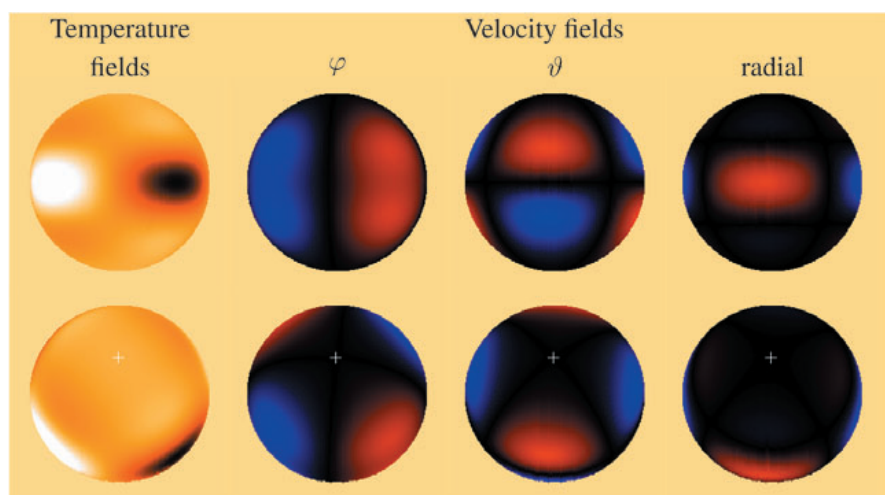


Figure 2: The pulsational variations of the stellar surface as computed by BRUCE for an $\ell = 2$, $m = 2$ mode. This sectorial mode has two node-lines in longitude ($\ell = 2$), thus the *nrp*-pattern repeats twice along the equator. The same model is shown for equator-on (upper row) and almost pole-on orientation, like ω CMA is seen from Earth (lower row, the “+” marks the rotational pole). The radial motions are a factor of almost 10 slower than the horizontal ones, while the ϕ - and θ -amplitudes are about equal. These three velocity fields are co-added and projected onto the line of sight, before KYLIE computes the observed spectrum (see also Fig. 3). The temperature changes are caused by the varying pressure.

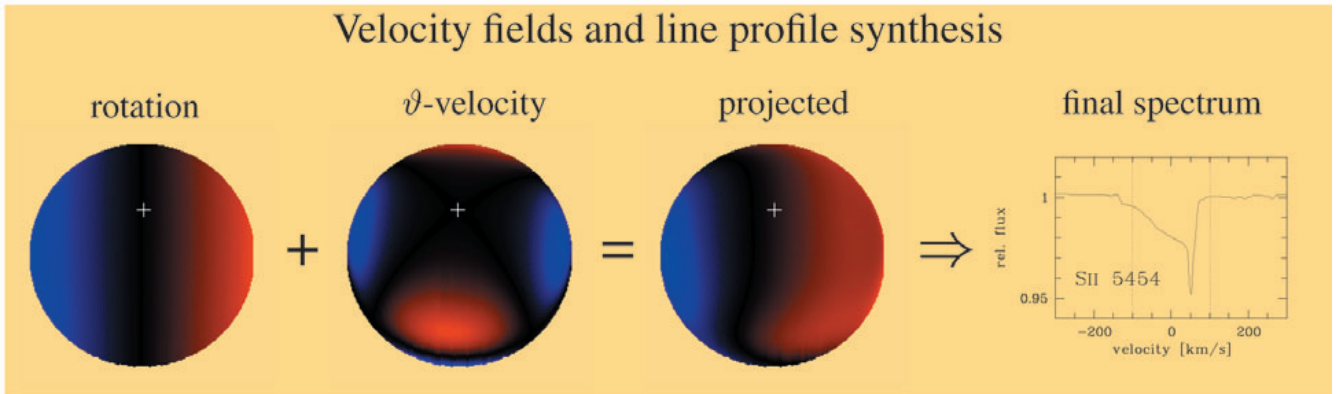


Figure 3: The projected velocity field, as seen from Earth, is dominated by the rotation and the pulsational θ -velocity for a pole-on star. At the approaching limb of the star (blue), the co-added θ -amplitude increases the total approaching velocity, causing the extended ramp on the blue wing of the final spectrum (see also Fig. 1). At the receding limb, rotation and θ -velocity have different signs, thereby reducing the maximal projected velocity. A large part of the receding hemisphere is, therefore, projected into a narrow velocity range, causing the spike. The modelled SiII 5454 line is shown for illustration.

BRUCE computes the surface parameters (such as temperature, gravity, and projected velocity) of the pulsating star for a mesh of about 25,000 points on the visible surface (Fig. 2 has been constructed from the BRUCE output). For each surface point the local spectrum is taken from an input grid of pre-computed data and shifted by the projected velocity. The KYLIE program then co-adds these local spectra to the one that would be observed from Earth.

3. Reproducing spectra

How could this new code help in resolving the seemingly contradictory behaviour of ω CMa? The key is the almost polar inclination of the star. Figure 2 shows the three constituents of the pulsational velocity before projection

onto the line of sight. In the equatorial view, the ϕ -velocity would dominate the visible variability at the stellar limbs. The θ -component is almost perpendicular to the line of sight, and thus suppressed by projection effects in the equatorial view. For a polar orientation of the star, the situation is reversed, however. The θ -velocity is now dominant, while the visibility of the ϕ -component is suppressed. Since the rotational velocity is also in ϕ -direction, it underlies the same projection.

The excess of 40 km s^{-1} , by which the variability is seen beyond the rotational range (such features are also called ramps), is therefore the true maximal velocity of the θ -field. Since this is 40% of the *projected* rotational velocity at the small inclination of ω CMa, it alters the visible line profile sig-

nificantly (see Fig. 3). But it is only about 15% of the *true* rotational velocity, so the physical effects on the stellar surface are much less severe. This way the polar inclination amplifies the contrast of the observed variability for g -mode pulsation.

Figure 3 demonstrates how under these conditions ramps and spikes result from the generic properties of a nonradially oscillating, rotating sphere, without the necessity to customize the model code for the specific case of ω CMa.

The final parameter set to reproduce the spectral variability of ω CMa was searched by computing and testing tens of thousands of models against the observations. The recent Messenger article by Baade et al. (*op. cit.*) has already presented an example of

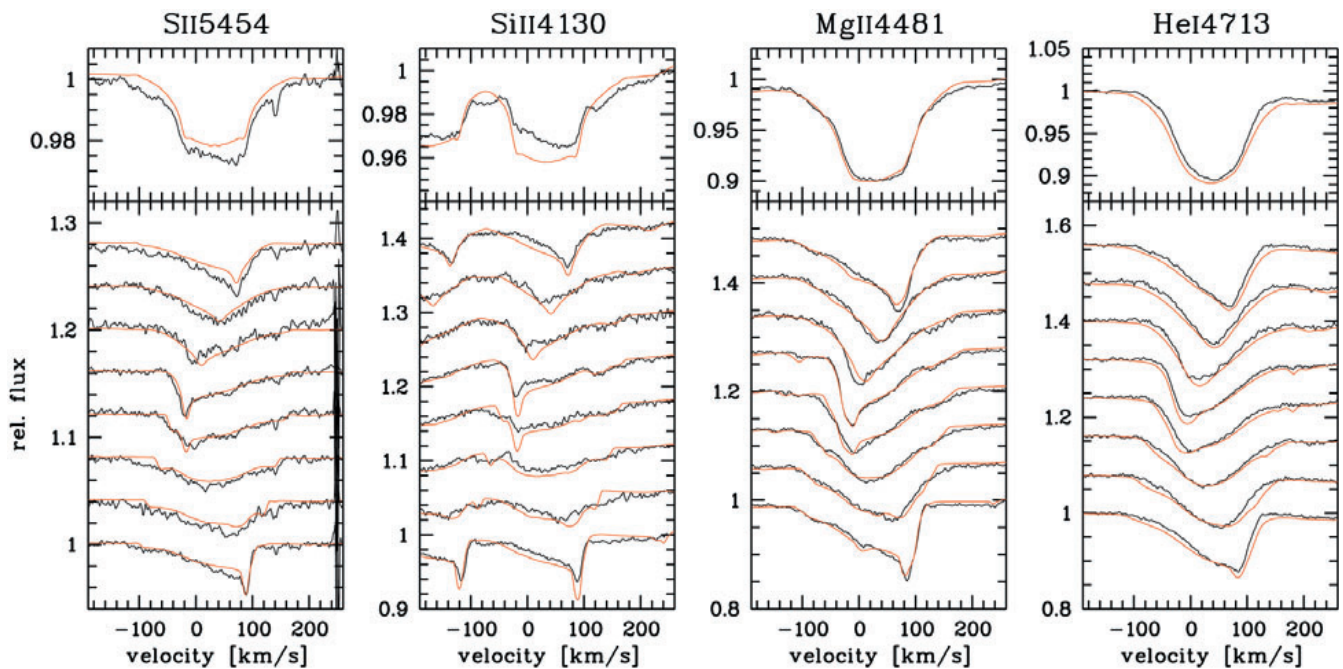


Figure 4: Comparison of observed phase-variations (black) with the modelled ones (red), including line blends. The phase averaged mean spectra are plotted above. The good reproduction, also of the absolute mean line profiles (and their anomalies, like the flat bottoms), demonstrates that the stellar parameters derived by modelling the variability provide a good estimate of the true quantities.

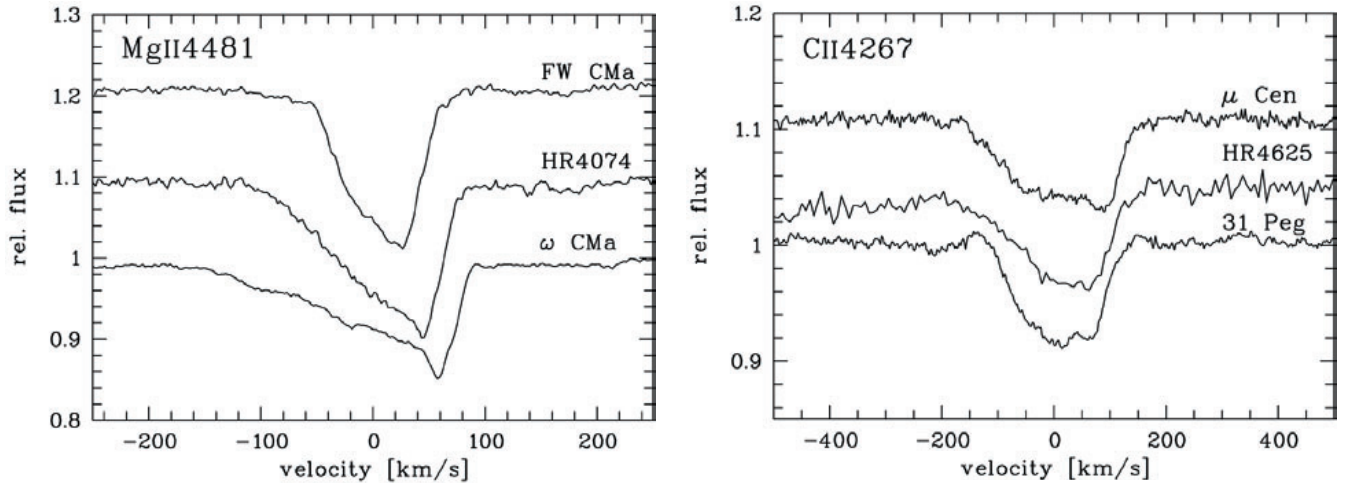


Figure 5: Periodic line profile variability (lpv) of low $v \sin i$ Be stars shown in the extreme asymmetry phase. The lpv of ω CMa is the strongest, but not in principle different from other low $v \sin i$ Be stars. See also Figure 6 for a dynamical view of the lpv of FW CMa, ω CMa, and HR 4625.

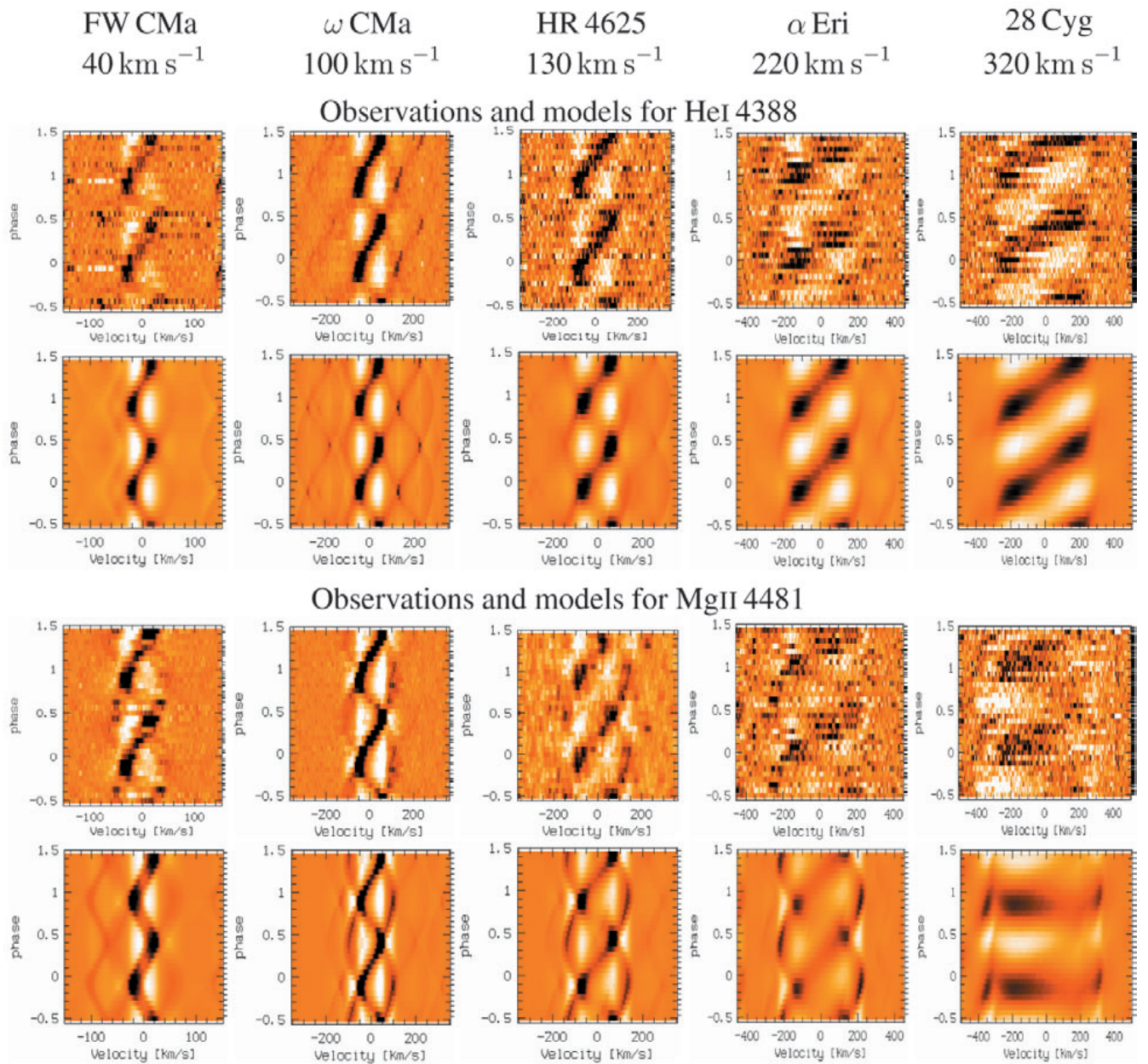


Figure 6: Observed lpv of stars with different $v \sin i$, shown as residuals from the mean line profile for two different lines. It is compared to the ω CMa model being 'viewed' at inclinations between 6° and 70° to match the indicated $v \sin i$ of the observed stars. The apparently asymmetric lpv of Mg II 4481 in 28 Cyg is caused by rotational blending with HeI 4471, visible in both observations and model data.

the resulting reproduction of the l_{pv} of HeI 4471 and MgII 4481. In Fig. 4, results for additional lines of helium and other ions are shown, all computed with the same set of stellar and pulsational parameters.

4. Do all Be stars pulsate?

Since the periodic l_{pv} of ω CMa is among the strongest known, the question needs to be addressed whether it is a typical Be star.

ω CMa is a B2 IV star. Since it is known that Be stars rotate almost critically, its low projected rotational velocity $v \sin i$ points to a pole-on orientation, which is also supported by the derived model parameters. If all (or most) other such Be stars would show this kind of periodic variability (possibly weaker, but in principle the same), the l_{pv} could be explained by n_{rp} in general.

Although most Be stars are of early B spectral type, there are not too many bright ones in the same range of $v \sin i$ as ω CMa. Searching archival data and securing additional observations with FEROS, we found most of them to show spikes like ω CMa, or a similar variability with lower amplitudes, i.e. no fully developed spikes, but global asymmetry variations, as is shown in Figure 5.

A complementary approach focuses on the observed l_{pv} of equator-on (high $v \sin i$) stars. The l_{pv} of these stars looks different from the pole-on ω CMa. But if ω CMa is proto-typical, the differences should be just inclination effects. To address this expectation the model of ω CMa was computed for a set of inclinations, so that the resulting $v \sin i$ would be the same as for some typical Be stars. Then, the modelled variations were compared to the observed ones (Fig. 6). The similarity of model and observations shows that the model of ω CMa represents a typical early-type Be star.

5. Consequences and outlook

The main result of the modelling project is the confirmation that early-type Be stars pulsate nonradially in g -modes. Based on the detailed modelling of ω CMa, it could be shown that this star is proto-typical, and that the periodic l_{pv} of early type Be stars in general is due to nonradial pulsation.

Several stars in the database, including ω CMa, were observed to replenish their disks via outburst events during our campaigns. Although plain n_{rp} cannot account for mass and angular momentum transfer into the disk, there is

observational evidence for a connection between n_{rp} and the disk formation. Among other effects, the l_{pv} pattern of ω CMa changes in several spectral lines during an outburst, which might provide the key to understand the mass transfer mechanism between Be stars and their disks.

Just as the pulsational parameters are determined by the best fit of the variability, the stellar parameters can be determined by the best fit of the mean absolute line profile. The modelling method described above offers the potential to combine these two steps in a single analysis, due to the good reproduction of both residual variability and absolute line profile (see Fig. 6). Since nonradial pulsation breaks the symmetry of the stellar surface w.r.t. rotation, one can even derive the stellar inclination angle from the modelling, while otherwise it is inseparably factored into the projected rotational velocity $v \sin i$. Rotation is becoming increasingly important for understanding stellar structure and evolution. A method to derive v and i separately, utilizing the n_{rp} pattern on the stellar surface, bears great potential not only for Be stars, but for a much wider range of objects, since nonradial pulsation is widespread in the Hertzsprung-Russell-Diagram.

The VLT and the most distant quasars

L. PENTERICCI and H.W. RIX (MPIA, Heidelberg), X. FAN (IAS Princeton), M. STRAUSS (Princeton University)

1. Introduction: optical surveys for high-redshift quasars

Quasars are amongst the most luminous objects in the Universe, allowing us to study them and any intervening material out to very large distances, corresponding to look-back times when the Universe was very young. Finding and studying quasars at high redshifts is one of the best ways to constrain the physical conditions in the early Universe. The mere existence of luminous quasars at such early times, and the implied presence of black holes with $M \geq 10^9 M_{\odot}$ place stringent limits on the epoch at which massive condensed structures formed, thereby constraining structure formation models (e.g. Efsthathiou and Rees 1988).

Most known high redshift quasars have been found as outliers in color space from the stellar locus in multicolor or optical surveys (e.g. Warren et al. 1994, Kennefick et al. 1995). One prominent survey is the Sloan Digital Sky Survey (SDSS, York et al. 2000) which is systematically mapping one-

quarter of the entire sky, producing a detailed multi-color image of it and determining the positions and absolute brightnesses of more than 100 million celestial objects. The SDSS will also measure the distance to a million of the nearest galaxies, producing a three-dimensional picture of the Universe through a volume one hundred times larger than that explored to date.

One of the principal aims of the SDSS is the construction of the largest sample of quasars ever, with more than 100,000 objects spanning a large range of redshift and luminosities, giving us an unprecedented hint at the distribution of matter to the edge of the visible Universe.

Thanks to the accurate 5 band photometry of SDSS, high redshift quasars can be efficiently selected by their distinctive position in color-color diagrams, with characteristic colors due to the main feature of the quasar spectra, viz., the strong Ly α emission line, the Ly α forest and the Lyman limit. During its first year of operation, the SDSS has already found a large number of ex-

tremely distant quasars, including more than 200 new quasars at redshift greater than 4 and the most distant quasar known, SDSS J1030 + 0524 at $z = 6.28$ (Fan et al. 2001). Until a few months ago this was also the most distant object known but it has been surpassed by a galaxy at $z = 6.56$ recently discovered by Hu et al. (2002).

2. VLT observations of the most distant quasars: revealing the conditions of the early Universe

The spectra of very high redshift quasars can tell us a great deal about the conditions in the early Universe. In particular, we can use them as probes of the intergalactic medium (IGM) to determine the state of any intervening material along the line of sight.

One of the fundamental questions of modern cosmology is how and when the Universe became ionized (for a complete review see Loeb & Barkana 2001). When the Universe was very

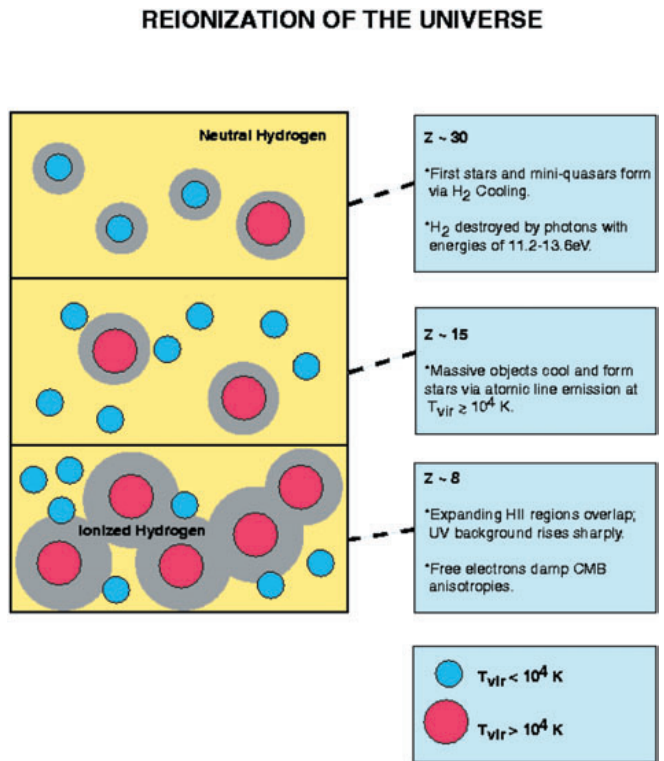
young, after the recombination epoch at $z \sim 1000$, the hydrogen was mostly neutral and homogeneously distributed. As the first luminous sources formed, i.e. quasars and the first generation of stars, they started to ionize the surrounding hydrogen. In the very early stages only small regions around each source became partially or totally ionized, but as time passed and more sources turned on, these “bubbles” of ionized gas expanded until they finally overlapped. The time at which the hydrogen becomes completely ionized throughout most of the space, is called the “reionization epoch” and marks in turn the end of the so-called “dark ages”. The transition from a totally neutral IGM to a completely ionized state that we just described is nicely illustrated in Figure 1 (from Loeb & Barkana 2001).

We can study the process of reionization through the spectra of luminous sources such as quasars: if a quasar is still surrounded by neutral (or partially neutral) hydrogen, its emission shortward of the Ly α line will be completely absorbed. As a consequence we will observe a sudden drop of flux in the spectrum: this is called a Gunn-Peterson trough.

We have recently started several VLT observing programs of follow up observations of SDSS quasars, including the most distant ones, using both ISAAC and FORS. In particular we have obtained optical and near-IR VLT spectroscopy of the most distant quasar SDSS 1030+0524 at $z = 6.28$ and near-IR spectroscopy of the second most distant quasar, SDSS J1306+0356 at $z = 5.99$ (Fan et al. 2001). The data were obtained with ISAAC and FORS2 through a director discretionary time proposal, in service mode. Figure 2 presents the VLT optical spectrum of SDSS 1030+0524: in the upper panel we show the 1-dimensional spectrum and in the lower panel the 2-dimensional spectrum.

The $z = 6.28$ quasar is indeed the first object to show a complete Gunn-Peterson trough: the flux is consistent with zero, within the noise, over a large wavelength region, 8400 Å to 8710 Å; below 8400 Å, there is detected flux. However, we cannot infer from this that *all* of the hydrogen in the IGM was neutral at this epoch: in fact only a small fraction of neutral hydrogen is sufficient to completely absorb the flux from the ionizing source. What is definitely true is that if we observe increasingly distant sources (e.g. Fan et al. 2001) the amount of flux suppression is rising steeply so we can conclude that we are getting closer and closer to the epoch of reionization. What we are probably observing at $z = 6.28$ is the end of the reionization process, i.e. the stage in which the ionized bubbles are overlapping.

Figure 1: A representation of the various stages in the reionization of hydrogen in the intergalactic medium. Initially the IGM is completely neutral. The first stars and quasars (here in blue and red) form at the center of the most massive halos, and start to ionize the surrounding hydrogen. These ionized bubbles grow and then overlap: eventually all the IGM becomes completely ionized (Figure from Loeb & Barkana 2001).



The VLT spectrum of SDSS 1030+0524 also clearly shows the presence of the ionized hydrogen bubble in the immediate surrounding of the quasar, the so-called “proximity effect”. As we mentioned earlier, even if the quasar starts shining in a completely neutral medium it will ionize its surrounding very quickly. From the VLT spectrum we can measure the size of the bubble which is about 1.5 Mpc (physical size at $z = 6.28$). If we assume that all the hydrogen atoms in a sphere of such radius have been ionized by the quasar photons and estimate the ionization rate from the quasar UV continuum, we can then infer a minimum time that the quasar must have been “on”, in order to produce a bubble of the observed size. This time is about 10 to 13 million years depending on the exact shape of the quasar continuum.

There are a number of uncertainties, such as the exact density of the gas in the quasar environment, the fraction of gas that was actually neutral when the quasar switched on and the clumpiness of the gas, i.e. whether it was distributed more or less homogeneously around the quasar. All these factors could mod-

ify the estimate of the quasar age, so the above result must be taken with some caution.

3. Metallicity of high redshift quasar environment: when did the first star form?

Remarkably, the optical and near infrared spectra of these high redshift quasars show strong NV and CIV emission lines. These lines give us the possibility to measure the presence of heavy elements (metals) in the quasars’ broad line region. These metals are synthesized by the local stellar population and their abundance is related to the age of the stars and to the history of star formation. From measure-

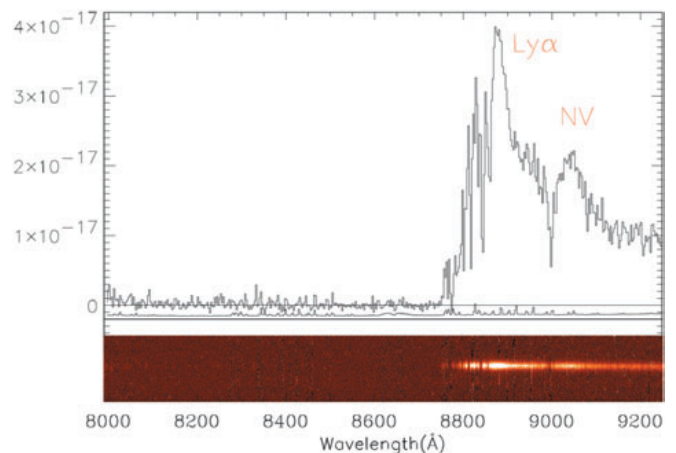


Figure 2: The VLT/ FORS2 one dimensional optical spectrum of the quasar SDSS 1030+0524 showing the lack of flux to the blue of the Ly α emission line. The bottom line shows the error array derived from the sky spectrum and offset by -0.2×10^{-17} . Below is a color representation of the sky-subtracted spectrum on the same wavelength scale. The spatial (vertical) extent of the spectrum shown is 20”.

ment of CIV, Ly α and NV and from limits on HeII derived from the FORS and ISAAC spectra we were able to set constraints on the metallicity in SDSS 1030+0524 and SDSS 1306+0356. The metallicity turns out to be much higher than the solar value. Comparison with models for the formation of metals (e.g. Hamann & Ferland 1999) indicates that stars must have been forming for several hundred million years to produce all the metals observed. Therefore the first stars must have formed around the active nucleus at redshift ~ 8.5 or higher. Note also that the inferred age of the stars is much longer than the age of the quasar derived in the previous section, even considering the uncertainty of both estimates.

The VLT will soon give us more precise and reliable estimates of the age of the quasar environment. Emission lines from other elements, such as Fe and Mg can provide a better constraint to the age of the stars since their abundance depends more strongly on time. Fe is generated by supernovae type Ia on timescales of about 1 Gyr after the initial starburst (Greggio & Renzini 1983), whereas the production of Mg is dominated by supernovae types II, Ib and Ic. So the ratio of Fe to Mg should change dramatically after the first Supernovae Ia explode, i.e. 1 Gyr after the initial starburst.

We are presently carrying out a program to detect such lines in a sample of quasars at redshift between 5 and 6. By measuring the metal abundances we will then be able to set limits on the age of the stars and hence to the age of the Universe at redshifts as high as 6. From this age, constraints can then be put on H_0 , $\Omega_0 = \Lambda = 0$: for $H_0 = 65$, $\Omega_0 = 0.3$ and $\Lambda = 0.7$, the age of the Universe is ~ 1.2 Gyr at $z = 5$, while a model with $\Omega_0 = \Lambda = 0$ has an age exceeding 2 Gyr and a model of $\Omega = 1$ has an age of 0.7 Gyr.

4. Future developments and VLT contribution

The VLT will certainly give further contributions to our understanding of quasar formation and the reionization process. Future targets for VLT observations will be provided by the SDSS in the next few years. From the space density of luminous quasars at $z \sim 6$ we estimate that the SDSS will find a further ~ 10 luminous quasars in the redshift range $6 < z < 6.6$ over the 10,000 deg² of the total survey area (Fan et al. 2001). At even higher redshift ($z > 6.6$) the Ly α emission line moves out of the optical window and into the infrared. Thus the objects become very faint at optical wavelengths due to the absorption by neutral hydrogen gas in the foreground at lower redshifts. SDSS optical

photometry alone is not sufficient to find such objects but needs to be combined with near infrared colors. The next generation near-infrared sky survey, and in particular the UKIRT Infrared Deep Sky Survey (see the article by Stephen Warren in this issue of the Messenger) will provide the ideal complement to SDSS for the search of more distant sources. Indeed UKIDSS has amongst its aims the breaking of the redshift 7 barrier for quasars in order to determine the epoch of reionization.

Follow-up observations with 8-m-class telescopes giving high-resolution, high signal-to-noise ratio spectra of these luminous quasars in the Lyman series absorption regions will provide valuable probes of the reionization epoch (and beyond) and, in particular, measure the spatial inhomogeneity of the reionization process.

References

- Efstathiou, G. & Rees, M.-J. 1988, MNRAS, 230, 5P
 Fan, X. et al. 2001, AJ, 122, 2833
 Greggio, L. & Renzini A. 1983, A&A 118, 217
 Hamann, F. & Ferland, G. 1999, ARA&A, 37, 487
 Hu, E.M. et al. 2002, ApJL, 568, 75
 Kennefick, J.D. et al. 1995, AJ, 110, 78
 Loeb, A. & Barkana, R. 2001, ARA&A, 39, 19L
 Pentericci, L. et al. 2002, AJ, 123, 2151
 York, D.-G. et al. 2000, AJ, 120, 1579
 Warren, S.J. et al. 1994, ApJ, 421, 412

Evidence for external enrichment processes in the globular cluster 47 Tuc?

DANIEL HARBECK, EVA K. GREBEL (Max-Planck-Institut für Astronomie, Heidelberg)
 GRAEME H. SMITH (University of California/Lick Observatory, Santa Cruz, USA)

1. Abundance spreads in globular clusters

Globular clusters (GCs) have long had an appeal to astronomers as laboratories for studying stellar evolution. Part of their attraction arises not only from the vast number of stars that they contain, but also from the common properties that stars within a cluster are often thought to share. For example, in one standard text book (Carroll & Ostlie 1996) we find: "Every member of a given (star) cluster is formed from the same cloud, at the same time, and all with essentially identical compositions." Despite this paradigm, it has been known for 30 years that the element abundances among stars in a given GC can vary significantly. Globular clusters are the oldest star clusters known with ages on the order of the age of the universe. The chemical abundance pat-

tern among their stars is therefore an important clue to the first substantial production of heavy elements by massive stars in the early universe. Understanding the origin of the chemical inhomogeneity of GCs is therefore of interest for cosmology as well as stellar evolution.

The abundance of the elements carbon, nitrogen, and oxygen (C, N, and O) in particular show large variations among the red giants in many GCs (for a review see, e.g., Kraft 1994). These elements are of particular interest since they are the catalysts in the CNO cycle of nuclear fusion, in which hydrogen is converted into helium. The abundances of individual elements such as C and O can be measured directly by high-resolution spectroscopy, but this is very time-consuming even with large telescopes. An efficient alternative to probing the star-to-star scatter in the CNO

elements, especially for larger samples of stars, is to measure absorption band strengths of the CN molecule using low-resolution spectroscopy. The behaviour of this molecule can serve as a useful tracer of inhomogeneities in the individual CNO elements.

Absorption bands of CN occur at a number of places in the visible spectrum. As an example we show an integrated drift-scan spectrum of the moderate metallicity GC 47 Tuc in Figure 1, which was obtained in 2001 at the ESO 1.5m telescope with the B&C spectrograph. The CN absorption band at 3883 Å is clearly visible and is marked in the spectrum. Since the integrated light of 47 Tuc is emitted by a mix of stars, the existence of this strong 3883 Å feature indicates that stars with strong CN bands must be an important component of this cluster. The integrated spectrum, however, cannot tell us

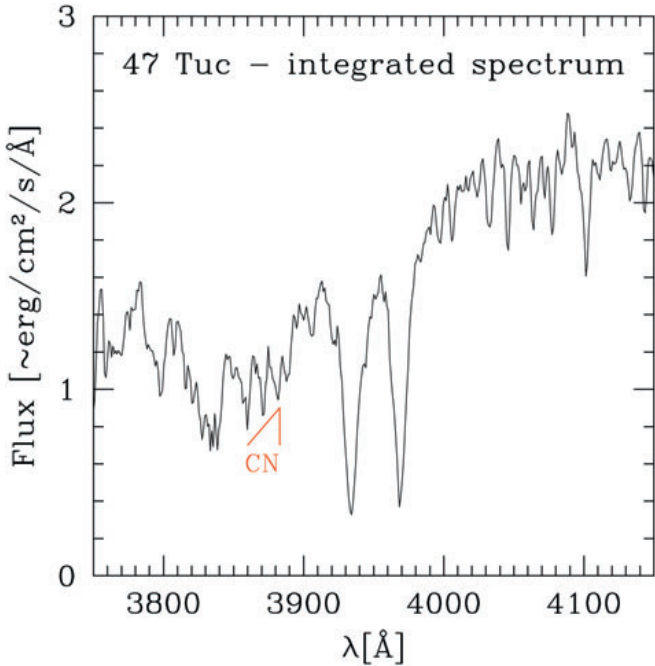


Figure 1: Integrated spectrum of 47 Tuc from the ESO 1.5m B&C spectrograph: The strong absorption band of the CN molecule below 3883 Å is clearly visible.

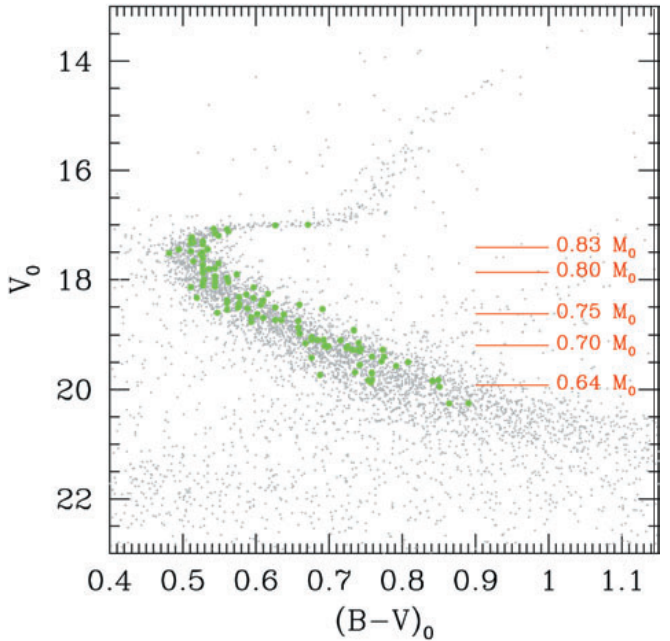


Figure 2: A color-magnitude diagram of 47 Tuc based on ESQ/MPG 2.2m WFI observations. From the main sequence region we selected ~ 115 stars for follow-up spectroscopy at the VLT, which are marked by green dots. Approximate masses for stars at various locations on the main sequence are labelled in red using units of solar masses.

whether all 47 Tuc stars have enhanced CN absorption or whether the CN features vary from star to star. A star-by-star analysis is therefore mandatory.

Studies of CN absorption band strengths have been carried out for many stars in a variety of GCs. The first studies were conducted out with 2-meter-class telescopes and concentrated on bright red giant branch (RGB) stars. Pronounced star-to-star differences in CN content have been found for quite a few globular clusters (see Kraft 1994). In general, CN inhomogeneities in GCs are a common phenomenon and can be seen in moderately metal-poor clusters as well as in more metal-rich ones. With the use of increasingly larger telescopes scatter in the 3883 Å CN band strength has been found along the entire RGB of some clusters, even extending down to the subgiant branch (SGB) and the main sequence turn-off (MSTO) region (Cannon et al. 1998, Cohen 1999a, 1999b).

The origin of the CN abundance spread is still under investigation. A very good introduction to current discussions can be found in Cannon et al (1998), whose arguments we summarize here. Deep interior mixing is a promising candidate for producing surface CN enhancements in GC stars. In the hydrogen-burning region of a star the CNO-cycle alters the abundances of the elements C, N, and O. Although the CNO cycle is a catalytic process, it will increase the nitrogen content of a star, since the relatively slow $N \rightarrow O$ reaction produces a “bottleneck” that causes the build-up of nitrogen at the

expense of C and O. If interior mixing is sufficiently effective and extends deep enough within GC stars, then some CNO-processed material could be dredged up to the surface. The efficiency of deep mixing may vary from star to star; for instance stellar rotation, the rate of which may vary among cluster stars, could induce mixing. Current stellar models do not predict deep convective mixing for stars at the MSTO. Scatter in CN band strengths has nonetheless been detected for stars at the bright end of the main sequence in a few GCs such as 47 Tuc, M71, and NGC 6752. Thus, there are either other forms of mixing or diffusion processes occurring within main sequence GC stars, or else stellar interior processes are not the main instigator of the CN scatter.

Other explanations for the CN variations include primordial variations, self-enrichment and self-pollution. When referring to “primordial variations” we mean that the molecular cloud that formed a GC was not chemically homogeneous. For example, a GC might have formed from two colliding gas clouds having different chemical compositions, leading to a range of abundances in the subsequently formed stars. The time scale for star formation during the birth of a GC may have been long enough to allow for “self-enrichment” by exploding supernovae; stars that formed after such events could be enhanced in supernova ejecta. In these two scenarios the assumption that all stars in a cluster had the same initial chemical composition would not be valid. The problem of these scenarios is

the lack of abundance spreads in heavy elements such as iron in most clusters with CN variations. Finally, intermediate-mass stars undergo significant mass loss while on the asymptotic giant branch. Any CNO-processed material lost via a wind from such stars may be accreted by other stars in the GC and alter the chemical composition of their atmospheres without affecting their iron content.

Stars on the fainter part of the main sequence are the clue to the riddle of the CN variations. These stars experience hydrogen core burning only, which has two major contributing mechanisms: the pp-chain (which converts hydrogen into helium directly) and the CNO cycle. The CNO cycle requires much higher temperatures than the pp-chain to work efficiently. The contribution of the CNO cycle to the total energy production therefore is strongly reduced for lower mass stars due to their lower core temperatures. If CN variations among main sequence stars are caused by CNO-cycle nitrogen enrichment and deep mixing, one expects the scatter in CN to disappear along the MS simply because there is no mechanism left to alter the ratio of these elements. To investigate whether the CN variations do indeed disappear, we have measured CN absorption band strengths for stars in the globular cluster 47 Tuc as faint as 2.5 mag below the MSTO using the VLT.

2. Observations with the VLT

The FORS2 MXU multi-slit spectrograph at the Very Large Telescope

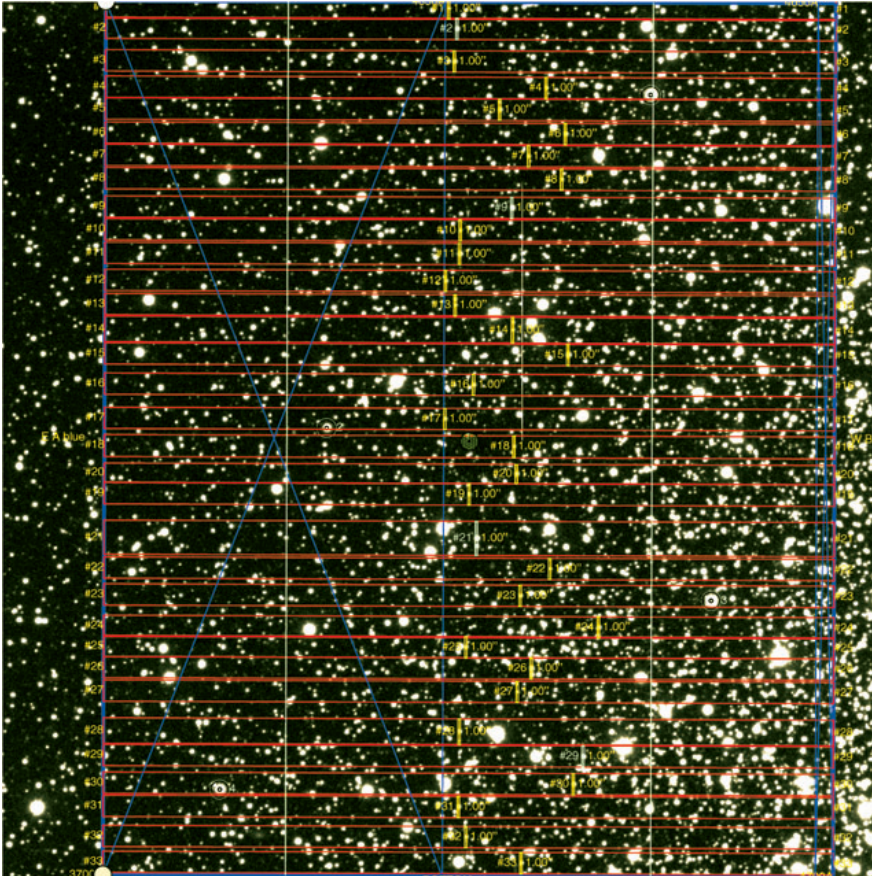


Figure 3: Example of one of the slit masks defined for our FORS/MXU observations. The mask was created using the FIMS software package.

(VLT) was used to obtain spectra for a sample of ~ 115 stars in the GC 47 Tuc. We chose this cluster for several reasons: (i) 47 Tuc stars are known to have inhomogeneities in CN absorption bands from the tip of the RGB down to a magnitude below the MSTO; the distribution of CN-rich and CN-weak stars is bimodal (e.g., Briley 1997 and references therein); (ii) 47 Tuc is relatively metal-rich by GC standards ($[\text{Fe}/\text{H}] = -0.7$ dex). Consequently the stars on the MSTO of 47 Tuc have atmospheres cool enough to form CN, in contrast to the hotter turn-off stars of the most metal-poor GCs.

To select candidate stars for spectroscopy we observed 47 Tuc in September 2000 with the ESO/MPG 2.2m telescope and the Wide Field Imager (WFI). The exposure time was 3×300 s in the filters Johnson B and V. The resulting color magnitude diagram (CMD) for chip #1 of the mosaic camera is shown in Figure 2. The subgiant branch, MSTO and the main sequence are clearly visible. The tip of the RGB is not represented since these stars were saturated on the CCD.

For the creation of the slit mask, three fields that overlap with our WFI observations were preimaged with FORS2 with a seeing better than 1 arc-sec. The definition of slit masks for the FORS2/MXU is supported by a dedi-

cated software package (FIMS) which is distributed by ESO. Thanks to this software the mask creation process is very straightforward to do. Approximately 115 stars were selected for the VLT spectroscopy to be observed in three different slit masks. We show an example of a slit mask definition in Figure 3.

The VLT spectroscopy itself was carried out in service mode during several nights in September 2001. We chose the B600 grating of FORS, which provides a spectral resolution of 5 \AA . The wavelength range for all stars was chosen to cover at least $3700\text{--}5400 \text{ \AA}$. The alignment of the slit masks to the reference stars worked perfectly in service mode, even in the crowded environment of 47 Tuc. The final spectra of the stars have an exposure time of 3.5 hours.

3. CN abundance variations on the main sequence

Figure 4 shows example spectra of pairs of stars in three different luminosity ranges. In all ranges, stars with strong and weak CN absorption features at 3883 \AA can be found. A convenient tool to quantify the CN absorption strength is the $S(3839)$ index (Norris & Smith 1983) that compares

the flux $F(38)$ in the absorption feature with the flux $F(39)$ in a nearby comparison region just to the red of the CN band.

$$S(3839) = -2.5 \times \log_{10} \frac{F(38)}{F(39)}$$

According to Cohen (1999a,b), we used slightly different definitions of the passbands ($F(38)$ from $3861\text{--}3884 \text{ \AA}$ and $F(39)$ from $3884\text{--}3910 \text{ \AA}$) than Norris & Smith (1983) to avoid overlap of hydrogen absorption lines that are important for the hot MSTO stars. We formulated a zero-point-corrected CN index called $\delta S(3839)$, defined such that the stars with the weakest CN bands have an index value close to zero. Larger values of $\delta S(3839)$ indicate a stronger absorption in the CN band. In addition to the calculated index we visually assigned the CN absorption strength for each star to one of five classes ranging from CN-weak to CN-strong. It turned out that for a few stars the observations were too noisy for classification. For some stars, while we could identify the CN absorption, the classification was uncertain. The comparison between our visual classification and the measured absorption strength is shown in Figure 5. There is an excellent correlation between the two.

In Figure 6 we plot the $\delta S(3839)$ index versus the V-band magnitude of the stars along the main sequence of 47 Tuc. The differences in CN band strength that are already apparent in the example spectra in Figure 4 become well documented by the $\delta S(3839)$ index values, especially for the faintest stars. In particular, the bimodality of the distribution stands out: Main sequence stars in 47 Tuc seem to be either CN-strong or CN-weak. A bimodal CN distribution had been reported by other authors previously for stars on the RGB, the SGB, and of the MSTO of 47 Tuc. Our new VLT observations demonstrate that the existence of this CN bimodality is independent of the evolutionary state of the stars.

4. Conclusions

We have found a significant scatter in the CN absorption strength among main sequence 47 Tuc stars at all magnitudes in our survey. In relation to the stars near the main-sequence turn-off, the importance of the CNO cycle among the faintest stars in our sample is reduced by at least a factor of ten due to the decreased core temperature. Since this mechanism for altering the ratio between C and N diminishes substantially for the fainter stars, we conclude that stellar evolution is unlikely to be the only process at work that causes the star-to-star variations in CN band strength. One concern of this in-

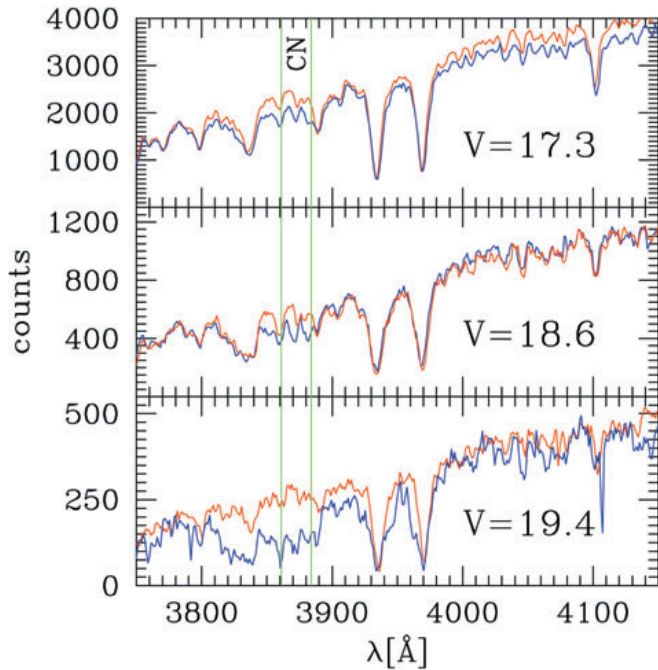


Figure 4: Spectra of main sequence stars in 47 Tuc: we show examples of CN-rich stars (blue) and CN-poor stars (red) at three different magnitudes on the main sequence. Note the clear differences in the $\lambda 3883\text{\AA}$ CN band, in particular for the faintest stars.

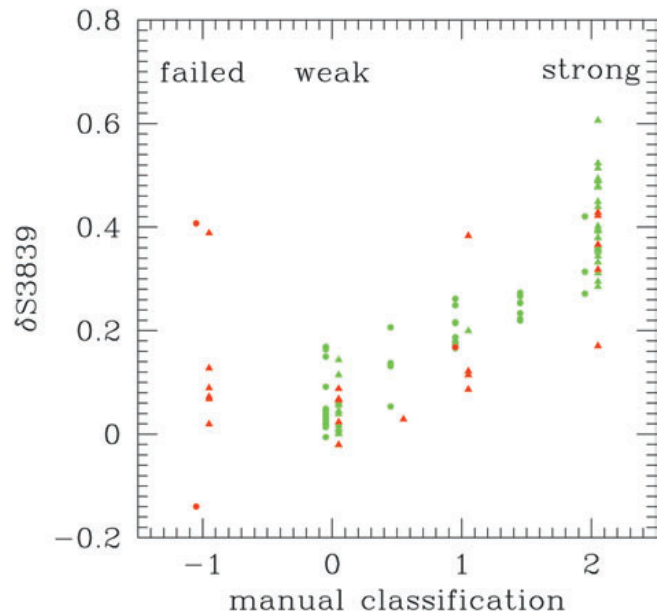


Figure 5: Visual classification vs. calculated CN band strength: Green dots represent secure measurements of the CN absorption lines; red dots indicate that the measurement may be dominated by systematic effects (e.g., strong hydrogen lines). Stars with ≥ 18.5 mag are plotted with triangles, brighter stars are plotted with circles. Note the excellent correlation between the measured absorption band strength and the visual classification.

terpretation is that a decrease in the CN abundance spread among the fainter stars along the main sequence may be hidden by increased CN association in the lower-temperature atmospheres of these stars. Model atmosphere analyses of the observed stars could address this question. It would also be valuable to observe the CN band strengths of stars one magnitude fainter than the current sample. For example, our simple calculations predict a decrease of the CNO-cycle efficiency for such stars by a factor of 100 compared to the MSTO. If such deep observations also find CN variations, then they would verify our results.

While internal stellar evolution seems unlikely as the origin of the CN variations in 47 Tuc, external processes may have played an important role. Unfortunately, from the low resolution spectroscopy alone, the true origin of the enhanced abundances of the CN-strong stars cannot be determined. The next step is to search for the fingerprint of different enrichment processes: cluster self-enrichment by massive stars versus accretion of material ejected in winds from intermediate-mass stars. High resolution spectroscopy with UVES at the VLT might provide answers to these questions.

References

Briley, M. M. 1997, AJ, 114, 1051
 Cannon, R. D., Croke, B. F. W., Bell, R. A., Hesser, J. E., & Stathakis, R. A. 1998, MNRAS, 298, 601

Carroll, B. W. & Ostlie, D. A. 1996, An Introduction to Modern Astrophysics, Addison-Wesley.
 Cohen, J. G. 1999a, AJ, 117, 2428

Cohen, J. G. 1999b, AJ, 117, 2434
 Kraft, R. P. 1994, PASP, 106, 553
 Smith, G. H. & Norris, J. 1983, ApJ, 264, 215

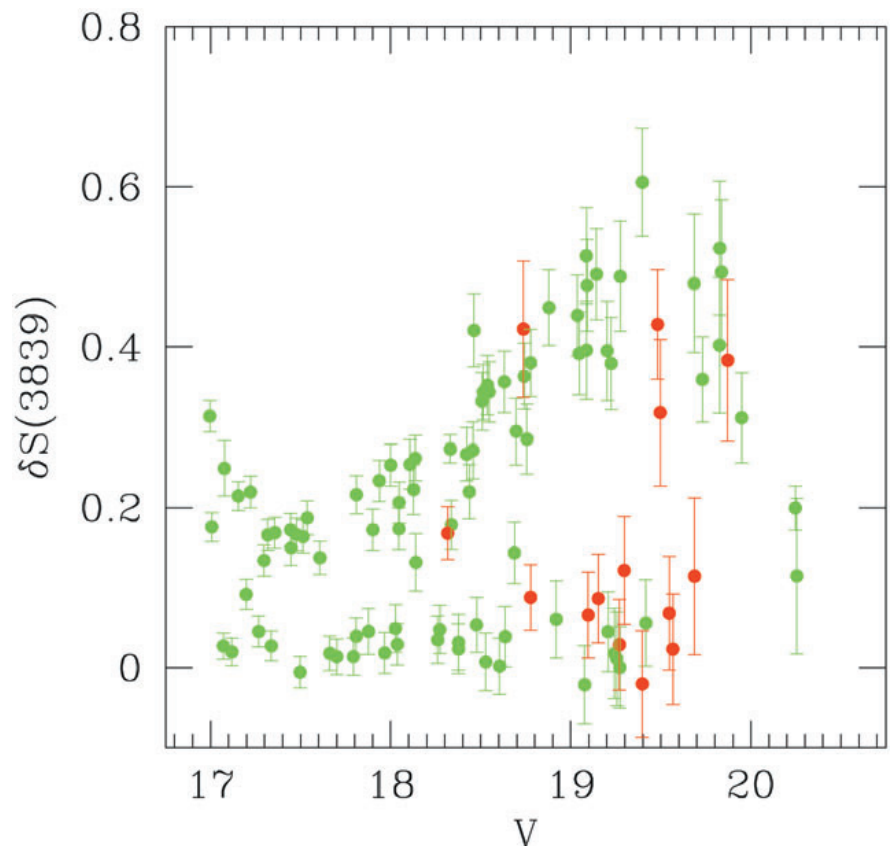


Figure 6: The $\delta S(3839)$ CN index is shown plotted against V magnitude for stars on the main sequence of 47 Tuc. Secure measurements are plotted with green dots; red dots represent uncertain measurements. Note the bimodal distribution of the CN absorption strengths, with stars falling into two relatively distinct groups on the basis of the CN index.



Aerial view of Paranal, with the Lulllaillaco volcano (6730 m) in the background, 190 km distant. (Photo: G. Hudepohl.)

The UKIRT Infrared Deep Sky Survey becomes an ESO public survey

STEVE WARREN, UKIDSS Survey Scientist,
Imperial College, London



1. Overview

UKIDSS is the next generation near-infrared JHK sky survey, the successor to 2MASS. UKIDSS will use the UKIRT wide field camera WFCAM, currently under construction in Edinburgh and scheduled for commissioning at the end of 2003. The camera uses four Rockwell Hawaii II 2048×2048 HgCdTe arrays (Figs 1 and 5). When commissioned WFCAM will have the widest field of view of any near-infrared camera in the world, capturing a solid angle of 0.21 square degrees in a single ex-

posure. In addition to the wide field, the survey will provide a wealth of information revealed in the near-infrared because of the lower extinction.

UKIDSS is a UK initiative and was the idea of Andy Lawrence (IfA, Edinburgh) who is the UKIDSS Principal Investigator. As part of the in-kind contribution of the UK to the ESO membership joining fee the UKIDSS data (raw, processed, and image catalogues) will be available to the entire ESO community immediately the data enter the archive. UKIDSS is therefore an ESO public survey, and the purpose of this article is to inform the ESO community about UKIDSS, describing the plans, and highlighting the opportunities for VLT science. For more details visit the website www.ukidss.org (Fig. 1). The UKIDSS Consortium is a collection of some 60 UK astronomers who are responsible for the design and execution of the survey. We welcome the input of ESO astronomers to this effort (contact details are provided at the end of this article).

UKIDSS in fact consists of five surveys exploring both high and low

Galactic latitudes to a variety of depths. The surveys will take some seven years to complete, finishing in 2010, and will require a total of 1000 nights on UKIRT. Details of the five surveys are summarised in Table 1. The Large Area Survey (LAS) covers 4000 square degrees at high Galactic latitudes, to $K=18.4$. This depth is three magnitudes deeper than 2MASS. The LAS will be the true near-infrared counterpart to the Sloan survey. The Galactic Plane Survey (GPS) will provide a panoramic clear atlas of the Milky Way disk, reaching $K=19.0$, surveying the strip to 5 degrees above and below the plane along a length 180 degrees. The Galactic Clusters Survey (GCS) will undertake a fundamental study of the faint end of the stellar initial mass function, imaging the nearest stellar clusters to a depth $K=18.7$. Finally two deep surveys, the Deep Extragalactic Survey (DXS) reaching $K=21$ over 35 square degrees, and the Ultra Deep Survey (UDS) reaching $K=23$ over 0.77 square degrees, will study galaxies at high redshifts. Fig. 2 plots the combinations of depth and area of the five elements of

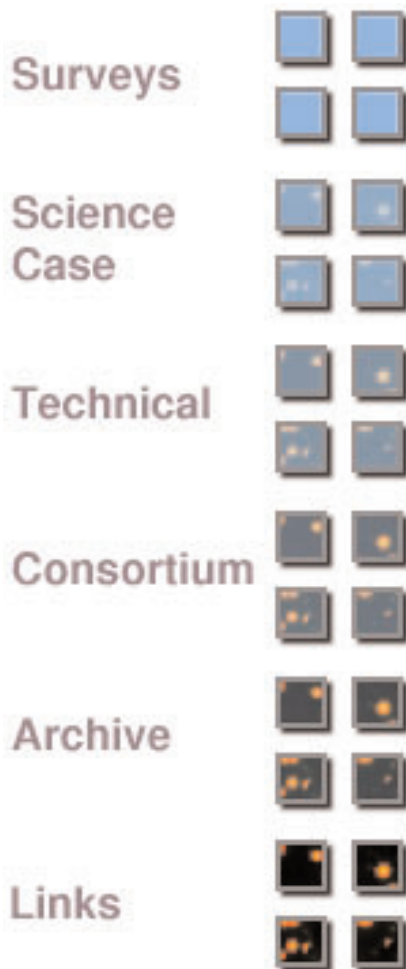
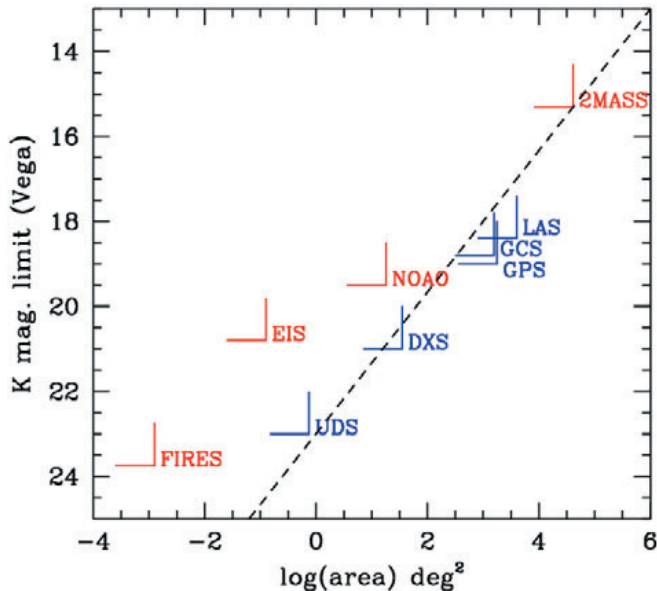


Figure 1: This figure shows the UKIDSS website navigation menu (www.ukidss.org), and pictures WFCAM as night falls.

Table 1: Details of the five elements of UKIDSS. The quoted depths are total magnitude 5 sigma for a point source. The estimated number of nights for each survey includes an allowance for poor weather. The Y band covers the wavelength range 0.97–1.07 μm .

	Filter	Area sq. degs	Mag. Limit (Vega)	Nights
Large Area Survey LAS	Y J H K	4000	20.5 20.0 18.8 18.4	262
Galactic Plane Survey GPS	J H K H ₂	1800 300	20.0 19.1 19.0 —	186
Galactic Clusters Survey GCS	J H K	1600	19.7 18.8 18.7	84
Deep Extragalactic Survey DXS	J H K	35 5 35	22.5 22.0 21.0	118
Ultra Deep Survey UDS	J H K	0.77	25.0 24.0 23.0	296

Figure 2: Comparison of survey area and depth in K of UKIDSS against existing or planned near-ir surveys. Note the enormous range of the X axis, 10 orders of magnitude. The five UKIDSS elements are plotted in blue. The surveys for comparison, plotted in red, are: 2MASS, the NOAO deep survey, the ESO Imaging Survey EIS, and the very deep FIRES VLT image of HDF-S (see Fig. 3). The dashed line shows the Euclidian relation between number counts and depth, normalised to 2MASS. The position of a survey relative to this line is a measure of the volume of space surveyed. This illustrates, for example, that for surveys for brown dwarfs 2MASS will detect many more than the KPNO survey, and that the LAS is an order of magnitude bigger than 2MASS.



UKIDSS, compared against some other near-ir surveys. The basic point illustrated in this plot is that at any depth

UKIDSS will cover at least an order of magnitude more area than any existing or planned survey.

WFCAM will start UKIDSS early in 2004, just at the same time when VST/OmegaCam will enter operation on Paranal, thus offering the opportunity to combine optical and near-infrared data as appropriate for the various surveys.

2. Science headlines

Fig. 3 illustrates four of the principal generic targets of UKIDSS. The headline scientific goals are the following:

- to find the nearest and faintest sub-stellar objects
- to break the $z = 7$ quasar barrier
- to determine the epoch of re-ionisation
- to determine the substellar mass function
- to discover Population II brown dwarfs
- to measure the abundance of galaxy clusters at $1 < z < 1.5$
- to measure the growth of structure and bias from $z = 3$ to the present day
- to determine the epoch of spheroid formation
- to clarify the relationship between EROs, ULIRGs, AGN and protogalaxies
- to map the Milky Way through the dust, to several kpc
- to increase the number of known Young Stellar Objects by an order of magnitude, including rare types such as FU Orionis stars

3. The five surveys: LAS, GPS, GCS, DXS, UDS

Fig. 4 is a map showing the provisional locations of the different fields that will be covered by the five surveys. Since the announcement that the UK will join ESO the field selection has been adjusted to a more southerly configuration, to improve access from the VLT. The selection of fields for the first two years of observations is almost complete, and the choices will be posted on the UKIDSS web page in July this year. A brief description of each survey follows.

Large Area Survey (LAS)

The LAS was conceived as the infrared counterpart to the Sloan Digital Sky Survey (SDSS), as well as an atlas for identification of sources detected in surveys at other wavelengths. SDSS fields covering 4000 square degrees will be observed in the four passbands YJHK, with a second pass in J a few years later, for proper motions. Opening the near-ir window will greatly clarify the make-up of low-redshift galaxies in terms of mix of stellar populations and dust content. The long-wavelength data will also enhance the detectability of distant galaxy clusters, as well as reddened X-ray/far-IR/radio survey

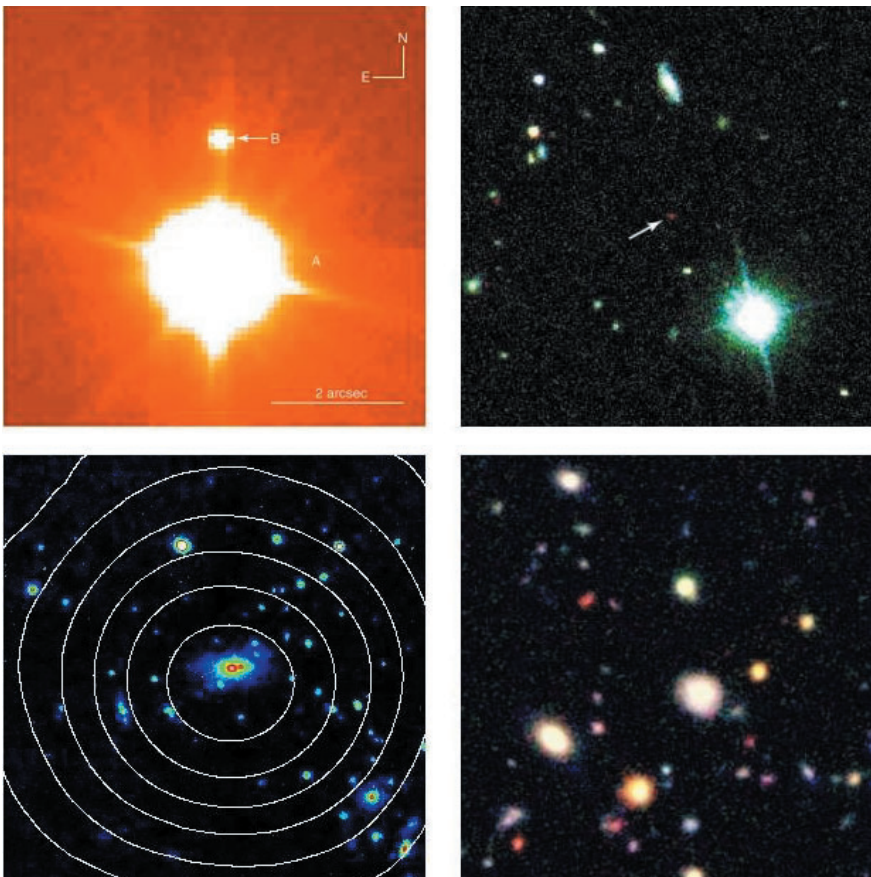


Figure 3: Four of the principal generic targets of UKIDSS. Upper left: brown dwarfs - VLT/KUEYEN I-band image of the young brown dwarf TWA-5B, Neuhäuser et al., A&A, 360 (ESO PR 17a/00). Upper right: the highest-redshift quasars - optical colour composite of SDSS J1030+0524, $z = 6.3$, currently the most distant quasar known (courtesy Laura Pentericci; see article on p. 24 of this issue). Lower left: distant galaxy clusters - K-band image of the cluster J1226.9 + 3322, $z = 0.89$, with X-ray contours overplotted (courtesy Laurence Jones and Simon Ellis). Lower right: galaxies at very high redshifts - near-ir JHK colour composite of a small 36×36 arcsec subsection of the deepest near-ir ground-based image yet taken, the FIRES observations of the HDF-S, Labbe et al. 2002, submitted (courtesy Marijn Franx).

sources. However it is the opportunity for finding new classes of rare objects, because of the great volume surveyed (Fig. 2), which is the most exciting prospect of the LAS. In the search for brown dwarfs the LAS will explore an order of magnitude more volume than 2MASS, and therefore will be the most powerful survey for both the coolest and the least luminous dwarfs. We hope to uncover the cool sequence extending beyond type T, also to detect Population II brown dwarfs using proper motion, and to discover the lowest mass dwarfs, possibly free-floating planets at sub-parsec distances.

We anticipate similar success in the search for the highest redshift quasars. Building on the success of the SDSS in finding $z > 6$ quasars (see the article by Pentericci et al. on p. 24 of this issue) we hope to extend this frontier to redshift $z = 7$ and beyond. This work employs the Y band, which covers the wavelength range 0.97–1.07 μm . This filter is distinct in wavelength from the SDSS z' band, and the z' -Y colour is crucial for the highest redshift quasars, so we preferred to give the filter a new name rather than call it z (infrared).

In summary, the LAS aims to discover both the nearest (outside the solar system) and the farthest known objects in the Universe! In between these two extremes the LAS will also pick up the intrinsically brightest Extremely Red Objects (ERO galaxies) over a volume thousands of times bigger than so far explored.

Galactic Plane Survey (GPS)

The GPS will map in JHK half the Milky Way within latitude ± 5 degrees, covering arcs of longitude $15^\circ < \ell < 107^\circ$, and $142^\circ < \ell < 230^\circ$ (Fig. 4). Currently under discussion is the possibility of extending the survey by including fields in the Galactic bulge, as well as a thin strip extending into the Galactic centre. The GPS will be scanned three times in K, improving the depth to $K = 19.0$ and providing variability information. This is deep enough to see all the way down the IMF in distant star formation regions, to detect luminous objects such as OB stars and post-AGB stars across the whole Galaxy, and to detect G-M stars to several kpc. Additionally a narrow-band molecular hydrogen survey over a smaller area (300 square degrees) will be conducted in the Taurus-Auriga-Perseus dark cloud region.

The principal science drivers of the GPS are: (1) creation of a legacy database and 3-D Atlas; (2) study of star formation and the IMF with emphasis on environmental dependence; (3) detection of counterparts to X-ray and gamma-ray sources; (4) AGB stars, PPN and Planetary Nebulae, including detection of brief phases of stellar evolution; and (5) brown dwarfs: the GPS is

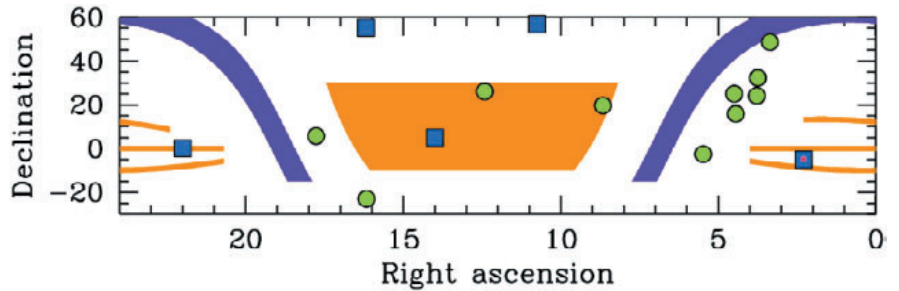


Figure 4: This plot marks the provisional locations of the survey fields, which are currently being finalised. The LAS is shown in orange, and will cover the most southerly of the northern Galactic hemisphere SDSS stripes, as well as the three southern Galactic hemisphere SDSS Stripes. The GPS is shown in purple. The gaps in Galactic longitude coverage of the GPS are imposed by declination constraints $60^\circ > \delta > -15^\circ$. The GCS fields are marked by green circles. The DXS will choose four fields from the 5 fields marked by blue squares. The UDS field selected is the Subaru-XMM field, located at J0218-05, and is marked by a small red square inside the DXS field at that location.

similar in scope to the LAS in this regard.

Galactic Clusters Survey (GCS)

The GCS is aimed at the crucial question of the sub-stellar mass function. The stellar mass function is well determined down to the brown-dwarf boundary but more or less unknown below, and the question of whether the IMF as a whole is universal is unanswered. The GCS will survey eleven large open star clusters and star formation associations in JHK, with a second pass in K for proper motions. These clusters are all relatively nearby and are several degrees across. The GCS improves on current studies, not primarily by going deeper, but by collecting much larger numbers, and examining clusters with a range of ages and metallicities in order to address the issue of universality. The mass limit reached varies somewhat from cluster to cluster, but is typically near 30 Jupiter masses.

Deep Extragalactic Survey (DXS)

The DXS will map 35 square degrees of sky to depths of $K = 21$, and $J = 22.5$, in three separate regions. The theme of the DXS is a comparison of the properties of the Universe at $1 < z < 2$ against the properties of the Universe today. The DXS will survey a similar volume at these redshifts to the 2dF and SDSS volumes, and the near-infrared gives coverage of the same rest-frame wavelengths as SDSS. Much of the DXS science relies on multi-wavelength coverage. As the final fields are selected over the next year, at the same time as *XMM-Newton*, *GALEX*, *CFHLS*, *VIRMOS*, *VST*, and *SIRTF* plans are finalised, international multi-wavelength key areas will emerge.

The principal goal of the DXS, which sets the scope of the survey, is the measurement of the abundance of rich

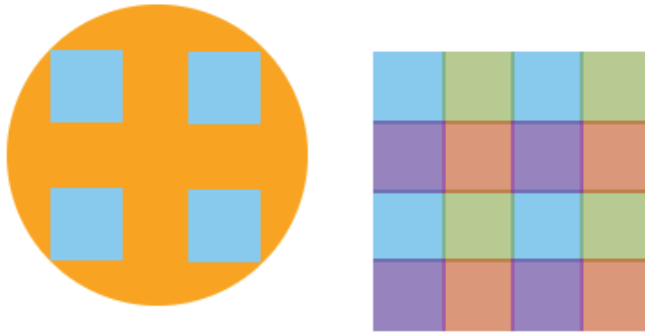
galaxy clusters at $z > 1$. The purpose is to obtain constraints on cosmological parameters. Ultimately we hope to make an important contribution to reaching beyond the three-parameter H_0, Ω_m, Λ cosmology that describes the geometry and dynamics of the Universe, to obtain useful constraints on the dark energy equation of state parameter $w = P/\rho$, and thereby to gain insight into the nature of the dark energy: cosmological constant or quintessence. Two other important goals of the DXS are (i) to provide the photometric catalogues for surveys at $z > 1$, including a redshift survey similar in scope to the 2dF galaxy redshift survey, to measure the evolution of large scale structure, and (ii) to quantify the contribution from both star formation and AGN to the cosmic energy budget, as a function of wavelength over the X-ray to far-infrared region, and to measure clustering for the different classes of object; normal galaxies (by type), starbursts, EROs, AGN.

Ultra Deep Survey (UDS)

The UDS aims to produce the first large-volume map of the Universe at high redshift, surveying a region 100 Mpc comoving across and 2 Gpc deep ($2 < z < 4$). Essentially the aim is to go as deep as is feasible over an area of one WFCAM tile (four pointings, Fig. 5). The depth has been chosen by reference to the detectability of a $z = 3 L_*$ elliptical that formed at $z = 5$. Accounting for the surface-brightness profile of such a galaxy, the required equivalent point-source depth is $K = 23$.

The prime aim of the UDS is the measurement of the abundance of high-redshift elliptical galaxies. Supplementary goals are the measurement of the clustering of galaxies at $z = 3$, and clarification of the relationship between EROs, ULIRGs, AGN and protogalaxies. The abundance of ellipticals at high redshift is a key test of hierarchical the-

Figure 5: Left: Focal plane arrangement of WFCAM. Each array (blue) is 2048×2048 pixels, with pixel size 0.4 arcsec. The 2×2 arrangement of arrays is contained within a circular field of diameter 0.97° . Right: Filled-in tile after 2×2 macro-steps. Allowing for the overlaps, the solid angle of a tile is 0.77 square degree. The deepest survey, the UDS, will cover a single tile.



ories of structure formation, and the scope of the UDS is sufficient to distinguish between current competing models. The inspiration for the UDS came from the success of the HDF as a public legacy database. In the same way we expect that the UDS will be used for many important science projects that have not yet been thought of.

4. WFCAM: The UKIRT Wide-Field Camera

WFCAM is a cryogenic Schmidt-type near-ir camera under construction at the UK ATC in Edinburgh. The focal

plane will hold four 2048×2048 PACE HgCdTe arrays. The spacing between detectors is 90% of the array width. The array configuration is illustrated in Fig. 5 (left). The pixel size is 0.4 arcsec, so the instantaneous exposed field of view of WFCAM is 0.21 square degree. With this configuration a single complete seamless 4×4 tile is achieved in four pointings, as illustrated in Fig. 5 (right). Accounting for overlaps the solid angle of a single tile is 0.77 square degree.

The WFCAM focal plane has a diameter 1.0° . The wide field of view has been achieved by a novel forward-

Cassegrain design which achieves a high degree of off-axis correction and includes a cold pupil stop. Further information can be found at www.roe.ac.uk/atc/projects. Tip-tilt image stabilisation will be achieved using the existing tip-tilt hexapod stage with a new #9 secondary mirror. The large pixel size was chosen to maximise survey speed. With the good image quality enjoyed by UKIRT the median seeing psf will be undersampled. We propose to microstep with a 2×2 $N+0.5$ pixel step to improve the sampling, interleaving the data to create the final image.

5. Consortium membership

Membership of the consortium implies a commitment from the individual to participate fully in the work of the consortium, which includes undertaking technical studies, preparing proposals and reports to the UKIRT Board, and contributing to the observing effort at the level of up to 7 nights per year, or equivalent contribution of effort in some other form. Interested astronomers should contact either Steve Warren (sjw4@ic.ac.uk), or Andy Lawrence (al@roe.ac.uk).



The Horsehead Nebula – ESO/MPG 2.2-m telescope. (ESO PR Photo 02a/02.)

Summary of the ESO-CERN-ESA Symposium on Astronomy, Cosmology and Fundamental Physics

Held at Garching bei München, Germany, 4-7 March 2002

M. JACOB¹, P. SHAVER², L. DILELLA³, A. GIMENEZ⁴

¹Chairman, Joint Astrophysics Division of the EPS and EAS

²ESO

³CERN (European Centre for Nuclear Research, Geneva, Switzerland)

⁴ESA (European Space Agency, ESTEC, Noordwijk, Netherlands)

Astronomy, cosmology and fundamental physics have thriving interfaces and modern research topics that bring together scientists from these different domains. New results and open questions call for meetings covering all of these fields. This year saw the first such meeting jointly organized by the three organizations ESO, CERN and ESA. The symposium took place in Garching on 4-7 March with about 200 participants. It gave a broad overview and so consisted largely of invited talks, with some contributed talks and over 50 posters on display.

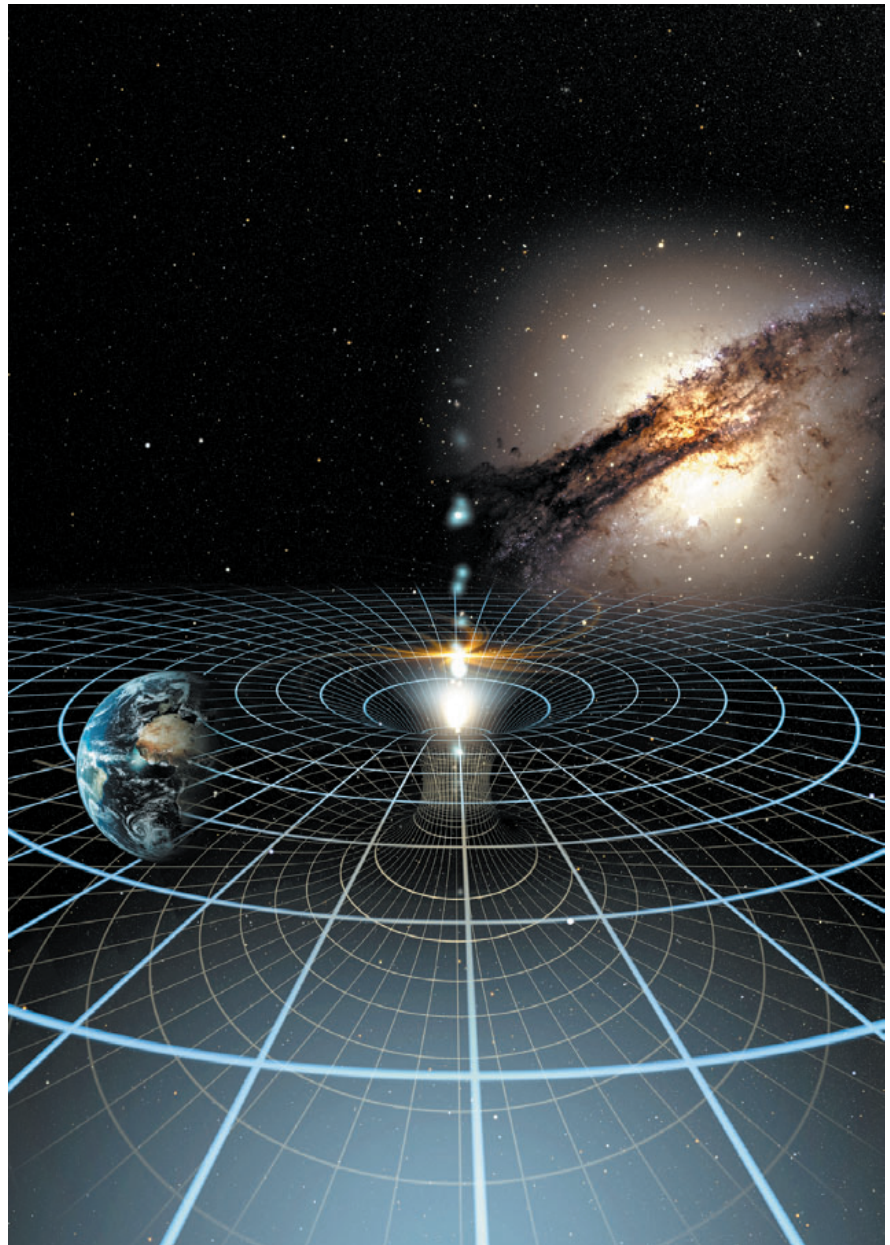
The Director General of ESO, Dr. Catherine Cesarsky, opened the Symposium with an overview of the current state of many of the fields to be discussed at the Symposium. She stressed the rapid pace of development in all of these areas, ranging from the spectacular convergence of the major cosmological parameters to the discovery of over 80 extrasolar planets.

N. Turok introduced the cosmology part of the Symposium with a stimulating talk provocatively entitled "The Early Universe – Past and Future". He challenged the relation of the remarkable cosmic concordance picture with standard inflationary models of the Universe, and described a possible alternative involving an infinite recycling of the Universe through colliding branes, in which time is eternal. Possible tests could be provided by a correlation of an all-sky CBR map with X-ray surveys or by CBR polarization measurements.

A series of talks dealt with the evidence for and remarkable convergence of the cosmological parameters. P. de Bernardis described the amazing new results from the current microwave background observations. With the improved data three acoustic peaks in the structure of the microwave background are seen. Results will soon be coming from the MAP satellite, which has already surveyed 85% of the sky. Polarization measurements will be critical in testing the adiabatic inflationary scenario. B. Leibundgut gave the evidence from high-redshift supernova studies for an accelerating Universe. He gave a critical assessment of the

steps in this analysis, and stressed the importance of the local calibrators. In the future thousands of distant supernovae will be accessible with the large telescopes. Y. Mellier spoke on the observations of cosmic shear from weak gravitational lensing, stressing the excellent agreement between six different teams working with six different tele-

scopes. He mentioned the problem of biasing, and showed that future large-scale surveys such as that being planned on the CFHT will provide easy discrimination. H. Böhringer provided the evidence from clusters of galaxies, showing that three independent approaches all give a good fit with the concordance model.





A press conference was held during the Symposium. From left to right are Prof. Sir Martin Rees (Cambridge University), Dr. David Southwood (ESA), Dr. Catherine Cesarsky (ESO Director General), Dr. John Ellis (CERN), and Dr. Michel Mayor (Observatoire de Genève).

A comprehensive overview of the current state of our knowledge of the cosmological parameters was provided by L. Krauss. He started with the Hubble constant, showing the excellent agreement between different groups. He summarized results from the CMB fluctuations, the ages of the oldest stars, the baryon density from deuterium and ^3He measurements, the dark matter density from X-ray clusters, the large scale structure results from the Sloan and 2DF surveys, and concluded that everything fits (the “concordance model”), but that the theoretical basis remains unclear.

A. Vilenkin addressed the Cosmological Constant Problems (CCPs) and their Solutions. The two major problems cited were the value of the vacuum energy density, and the “time coincidence problem” (i.e. why we happen to live just at the time when the vacuum energy dominates). He considered possible particle physics solutions, Brane World solutions, Quintessence models, and the Cosmological Anthropic Principle. He concluded that the anthropic approach naturally resolves both CCPs and opens windows to the super-large scales beyond the visible Universe.

One of the major transition phases of the observable Universe, the “Reionization Epoch” when the first stars formed and ended the “Dark Ages” that followed recombination, was discussed by P. Madau. He described theories for the development of the early massive structures, and reviewed evidence that the helium reionization epoch may already have been detected.

Direct searches for dark matter candidates were reviewed by C. Tao. Gravitational microlensing searches for massive baryonic objects explain at most 20% of the dark matter in our Galaxy. Other searches focus on the possible existence of hypothetical massive, neutral particles which interact

only very weakly with matter, such as neutralinos. A claimed signal from the DAMA experiment at Gran Sasso has not been confirmed by other experiments. Several experiments are presently taking data and more sensitive experiments are in preparation.

P. Hernandez summarized the evidence for neutrino oscillations. Recent results using solar and atmospheric neutrinos provide convincing evidence for neutrino oscillations, requiring that neutrinos have a non-zero mass. Neutrino oscillations are probably the most important new phenomenon discovered in particle physics in the last decade (although their masses are not sufficient to provide an appreciable contribution to dark matter). Intense experimental activity is presently in progress. In the longer term, neutrino beams with much higher fluxes will be required to study this phenomenon in detail, including the possible observation of CP violation.

The Standard Model of Particle Physics and the tests performed at low energies were described by A. Pich, highlighting the very impressive precision achieved in comparing measurements with theoretical predictions in particular cases. He also reviewed recent results on CP violation. During the last year large CP violating effects have been reported, and future experiments should clarify the mechanisms responsible for this phenomenon.

High energy tests of the Standard Model were reviewed by F. Gianotti. These include the studies of the W and Z bosons at the e^+e^- collider LEP and the discovery of the top quark at the Fermilab proton-antiproton collider. The W and Z masses are presently known with a precision of 0.05% and 0.0024%, respectively, and other parameters of the Standard Model measured at LEP are measured with typical precisions of the order of 0.1%. In addition, the LEP

experiments have provided for the first time a clear demonstration of the existence of the three-boson interaction predicted by the electroweak theory. In the framework of the Standard Model, the LEP measurements have been used to constrain the mass of the Higgs boson, which is the only missing piece of the theory. The prediction is $m_H = 85^{+54}_{-34}$ GeV, giving good hopes for the discovery of this particle at one of the future high-energy colliders (the improved proton-antiproton collider at Fermilab, which is presently in the commissioning phase, or, more likely, the CERN LHC). Gianotti also reviewed the hint for the production of the Higgs boson with a mass of 114 GeV, obtained by the LEP experiments during the last year of LEP operation. Gianotti concluded that the prospects to discover the Higgs boson at the LHC are excellent, as are the prospects to discover the supersymmetric partners of known particles, if they exist.

Pierre Le Coultre showed how one of the LEP detector (L3) can be used as a detector for cosmic ray muons. The results will constrain cosmic ray models which are used to predict the fluxes of atmospheric neutrinos.

Despite its successes, the Standard Model of particle physics contains too many parameters and theorists do not see it as the final theory. In addition, it does not include gravitational interaction, and the mass of the standard Higgs boson becomes unstable when quantum corrections are taken into account. J. Ellis discussed new physics which could solve these problems. The most popular model is Supersymmetry, which adds a new scalar boson to each known fermion, and a new fermion to each known boson. These hypothetical particles have not yet been discovered, but theorists are confident that their masses are lower than 1 TeV, if they exist. The

hunt for supersymmetric particles will be one of the main activities at the LHC. Ellis discussed additional theoretical ideas which could give rise to unexpected and spectacular events at the LHC.

Stimulated by a recent claim on the basis of high redshift QSO spectra that the fine structure constant Alpha may be varying with cosmic time, G. Fiorentini reviewed other possible evidence for its variation. So far the only positive claim is that from the QSO spectra, conflicting with the other evidence, and more dedicated experiments will be required to solve this puzzle.

The first of a series of talks on high energy astrophysics was given by E. van den Heuvel. He spoke about Gamma Ray Bursts, the most powerful known cosmic explosions. The models involve relativistic fireballs from either super/hypernovae ("collapsars"), or the mergers of neutron stars with other neutron stars or black holes. A few thousand such bursts have now been observed; the most distant so far known is at $z = 4.5$. The Swift satellite, to be launched next year, will provide rapid response and accurate positions for follow-up by telescopes such as the VLT.

H. Völk reviewed the subject of high-energy γ -rays. In the region up to a few GeV, these γ -rays are detected by measuring their conversion to e^+e^- pairs in satellites, while at higher energies (up to 100 TeV) ground-based Čerenkov detectors are used to detect the electromagnetic showers produced in the Earth's atmosphere. Progress in this field is expected from the future Gamma Ray Large Area Telescope (GLAST) satellite mission which will study γ -rays up to energies of 100 GeV by means of a detector combining large acceptance and excellent angular and energy resolution.

Studies of cosmic rays at extremely high energies (up to 10^{20} eV) were reviewed by A. Watson. The interaction of these particles with the Earth's atmosphere produces extended air showers which are studied by counting the muon multiplicity in a large number of detectors scattered over a large area. The large Pierre Auger Laboratory in Argentina will start data taking soon. Another experiment, EUSO, will measure the nitrogen fluorescence from very high-energy cosmic rays using detectors mounted on the International Space Station, with the advantage of covering a much larger area than ground-based experiments.

The presence of some reported events of extreme energy (above 10^{11} GeV), such that proton primaries should have been stopped by the cosmic microwave radiation, raises an important puzzle. With respect to primary charged particles, high energy neutrinos and γ -rays have the advantage of pointing to the source. Neu-

trinos interact weakly, so they are the only particles that can provide information from the edge of the Universe and from sources deep inside active regions. However, detectors with very large masses are needed. F. Halzen reviewed the status of AMANDA, a large detector consisting of strings of photomultiplier tubes buried deep in the Antarctic ice cap and looking down to measure Čerenkov radiation in ice from charged particles. Other underwater experiments built on the same principle are operating and in preparation.

The X-ray background has now been almost completely resolved into discrete sources by the latest satellites, Chandra and XMM. As described by G. Hasinger, many of these sources involve optically obscured active galactic nuclei (AGN), with accretion onto central black holes. The redshift distribution peaks at a surprisingly low redshift, $z \sim 0.6$, and there is a clear deficit at $z > 4$, indicating a decrease in the space density at high redshift, in agreement with earlier results on QSOs. Future missions such as Rosita, Duet and Xeus may find some of the very rare high-redshift X-ray QSOs.

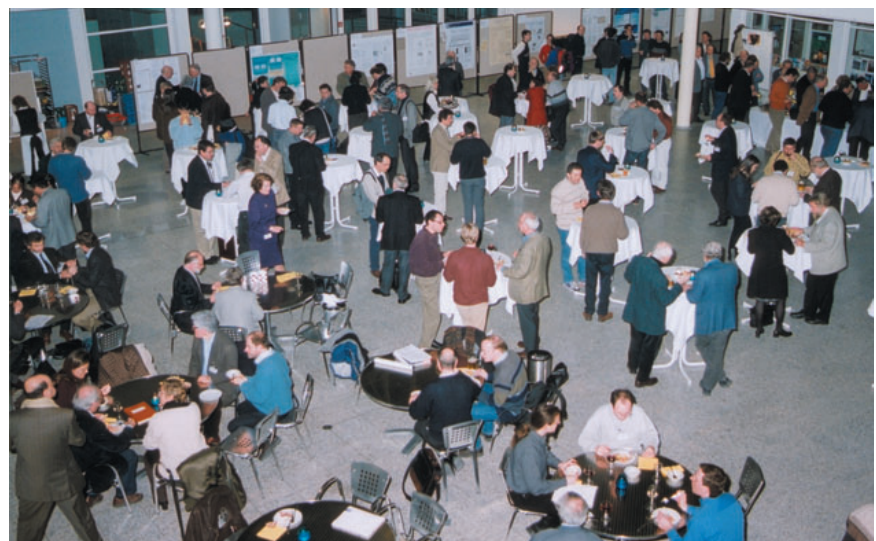
L. Woltjer gave an assessment of our current knowledge of neutron stars. The masses and temperature fit the "standard solution", and there have been many models that agree. Pulsars have provided new constraints and problems, one of which was the relatively few radio pulsars located in supernova remnants. Now it is known that there are objects in about 80% of supernova remnants. There has been a continuing debate over the velocities of neutron stars, and its resolution will be important in the understanding of their origins.

The ubiquity of black holes in the centres of galaxies is now widely believed. R. Bender outlined the evidence for several cases. Spectacular new evidence has come from X-ray spectra,

which indicate strong gravitational effects. Only supermassive black holes provide a plausible explanation for all such phenomena, although direct evidence is still hard to obtain. Supermassive black holes appear to be present in most galaxies, and there are certainly enough to explain the QSO phenomenon. A. Eckart showed striking evidence for the black hole in the centre of our own Galaxy. The proper motions of stars in the inner region imply an enclosed mass which is almost certainly a black hole.

Gravitational waves were the subject of the next two talks. B. Schutz reviewed the possible sources of gravitational waves. The merging of two black holes of a million solar masses at $z = 1$ would give an amplitude 5 orders of magnitude higher than the detection threshold of LISA. The merger would take only minutes but the spiral down, with a varying frequency of 0.1 to 10 mHz, would take months. For stable binaries, observing the signal over many periods greatly helps in reaching lower amplitudes. There is complementarity between detectors on the ground (frequencies above 10 Hz) and detectors in space (set at frequencies below 0.1 Hz). The amplitude sensitivity should in both cases reach below 10^{-22} K. Danzmann then outlined the prospects for detecting gravitational waves. He showed that resonating ground detectors were limited to the detection of a supernova in the galaxy but that more promising prospects were offered by interferometers. LIGO should reach to 20 Mpc soon for such a signal, and to 200 Mpc in 2006. For LISA, prospects are great for the observation of massive black holes merging anywhere in the universe.

S. Vitale described other space missions on fundamental physics under study at ESA. STEP should test the equivalence principle at the level of 10^{-18} , 6 orders of magnitude better than



Participants enjoying the Symposium buffet dinner.

the present limit. The ACES mission, on the ISS, should produce a very high precision clock and the HYPER one (free flyer) should study cold atom interferometry in space with the prospect of making very high sensitivity gyroscopes. R. Battiston discussed astroparticle physics from space, pointing out that cosmic ray studies were the beginning of particle physics. He reviewed the studies of cosmic rays made with balloons and satellites, and the prospects for searches for new particles: antimatter, dark matter, and ultraheavy particles. A new detector with a sensitivity to anti-nuclei improved by a factor of 1000 will be installed on the International Space Station.

G. Raffelt discussed how stars can be intense sources of weakly interacting particles. One such particle is the axion, which was conceived to explain the absence of CP violation in the strong interaction. A CERN experiment (CAST) will search for axions using an LHC magnet pointed at the Sun and detecting the axion \rightarrow X-ray conversion in the magnetic field.

F. Paresce described the first science results from the VLT interferometer. A large number of stellar sources with correlated magnitudes brighter than $K \sim 6$ and $K \sim 3$ have been observed with the 8m and 40cm telescopes respectively, allowing the establishment of tighter constraints on theoretical stellar models. The great scientific potential of the full VLTI system was outlined.

A group of three talks dealt with the exciting new field of extrasolar planets. E. van Dishoeck described observations and theories of forming planetary systems. Infrared and millimetre emission comes from dusty disks surrounding many young stars. The chemistry of these circumstellar disks, deduced from observations of the many molecular lines, provides essential clues to their evolution and planet formation. For future observations high angular resolution will be essential, and ALMA will play a dominant role. Other important facilities will include the VLT/VLTI, SIRTF, NGST and Herschel.

The spectacular advances in the discovery of extrasolar planets (from none in 1995 to over 80 today) were described by M. Mayor. There is a huge diversity, which was unexpected. Many are at 0.03–0.05 AU, many have eccentric orbits, and typical masses are in the range $0.15\text{--}10 M_J/\sin i$. Most have been discovered from radial velocity measurements. Photometric transits have also now been observed – 46 of them from one recent survey alone. And there are now 7 or 8 published systems with multiple planets. Many aspects are now being actively studied – the origins of the “hot Jupiters”, the mass functions of substellar companions, the orbital eccentricities, the relation to the metallicity of the star. For the

future, M. Mayor mentioned the new HARPS instrument for the ESO 3.6m telescope, the possibility of astrometry with Prima on the VLT, and prospects in space.

M. Perryman followed on from M. Mayor’s talk by considering the prospects for the detection of earth-like extrasolar planets – lower mass systems, in particular ones where life might form. He described prospects with the astrometric mission GAIA, due for launch in 2010–2012. With its 1 micro-arcsec accuracy, it will detect 20,000–30,000 planetary systems, and will find $\sim 10,000$ planetary systems by photometry alone. The later Eddington mission will detect photometric transits of 500,000 stars, including some 2,000 due to earth-mass planets. The photometric accuracy will suffice to detect planetary rings and moons. Finally, he considered the conditions thought necessary for life. The DARWIN mission, with a launch date sometime after 2015, would be a 50–250m baseline interferometer employing six 1.5m telescopes. It would make possible direct imaging of solar systems like ours, and seek spectral signatures of possible biomarkers. Surface imaging of earth-like extrasolar planets may be possible with the next generation of extremely large telescopes (OWL, CELT), and very large space arrays.

During the last afternoon there were talks on the future perspectives at ESA, CERN and ESO. Many exciting projects are under construction or at the planning stage in all three organisations. D. Southwood gave a long and impressive list of ESA space missions, present and future, with five launches in just the next year and plans extending well over a decade into the future. He concluded with comments on the role of science in Europe, highlighting the declaration of the EU Council of Ministers that “Europe should become the most competitive and dynamic knowledge based economy in the world”.

The future of CERN was reviewed by J. Ellis. In the short term most of the CERN effort is devoted to the construction of the Large Hadron Collider (LHC), a machine where two proton beams, each with an energy of 7 TeV, collide head-on with an interaction rate of $5 \times 10^8 \text{ s}^{-1}$ in each of two general-purpose detectors. The LHC and detectors are now in the construction phase and physics should start in 2007. The LHC will also accelerate heavy ions to study the so-called “quark-gluon plasma”, which is the state of matter of the early Universe before baryogenesis. Ellis also reviewed the R&D activity on accelerator technology which goes on in parallel with LHC construction, to prepare for the post-LHC era.

ESO’s current and future programmes were outlined by the Director General, C. Cesarsky. All four 8-meter

unit telescopes of the VLT are operating with high efficiency, and the suite of VLT instruments is rapidly increasing. Two survey telescopes are also being added. Adaptive optics systems have given the VLT images added sharpness, and the VLT Interferometer has already started producing science, as outlined earlier by F. Paresce. A major new ESO project is the Atacama Large Millimeter Array (ALMA), which, with its 64 12-meter antennas operating at 5000m altitude, will become a millimeter/submillimeter equivalent of the VLT/VLTI and NGST. It will be an equal partnership with the U.S. and possibly Japan, with completion foreseen for 2011. Further into the future will be OWL, a giant 100-meter diameter optical-infrared telescope, and scientific and technical investigations for this facility are already well underway.

The concluding lecture was given by M. Rees. He saw the Symposium as linking the very small with the very large, and mentioned three major developments discussed at the meeting: the discovery of extrasolar planets, the evidence on neutrino masses, and the determination of important key numbers of the Universe in just the last few years. He remarked on how conclusions regarding the flat Universe and its contents (5% baryons, 25% dark matter, and 70% dark energy) have come from independent sources, with amazing agreement, and the challenges they pose to particle physics. In ten years hence he expects the basic parameters to be well known, and he reflected on the two major challenges that may face us in the post-2010 era: an understanding from the very early ($<10^{-12}$ sec) Universe as to why these numbers have these particular values, and an understanding of cosmic evolution at $>10^8$ yrs. In the latter context he considered the possible detection of the earliest luminous objects, the formation and evolution of galactic nuclei and black holes, the mysteries and potential of Gamma Ray Bursts, and the probable detection of gravitational waves from such objects. Finally, he speculated on the mysteries of the very early Universe. In particular, why do the laws of our Universe have latent in them all the complexity of our Universe? There are now many models, and he wondered how many Big Bangs? According to the Cosmological Anthropic Principle, the laws of our Universe just happen to be “the by-laws governing our patch”. With the rapidly increasing data rates he anticipated the development of huge databases making possible a wider participation in science, and he felt that the crescendo of the last few years will continue with the great new scientific facilities becoming available.

Finally, over 50 poster papers were presented, covering a wide range of exciting topics including cosmological

models, Quintessence, the CMB, cosmic shear, the cosmological constants, Gamma Ray Bursts, galaxy formation, galaxy clusters, gravitational lensing, new space missions, probes for supermassive black holes, quasar absorption line studies, experiments in fundamental physics, extrasolar planets and others. The programme included a fascinating special evening lecture by Jean-Claude Carrière, well-known author, on the subject of "Time".

The full proceedings of this Symposium will be published in the Springer-Verlag series "ESO Astrophysics Symposia".

The Scientific Organizing Committee was comprised of: R. Battiston (Univ. of Perugia), R. Bender (Univ. of Munich), A. de Rujula (CERN), L. DiLella (CERN), C. Fabjan (CERN), A. Gimenez (ESA), M. Jacob (JAD), F. Pacini (Arcetri), A. Renzini (ESO), P. Shaver (ESO; chair), M. Spiro (Saclay), B. Taylor (ESA), P. van

der Kruit (Univ. of Groningen), S. Vitale (Univ. of Trento), S. Volonte (ESA), and M. Ward (Univ. of Leicester).

We are most grateful to the Symposium Secretaries Britt Sjöberg of the ESO/ESA ST-ECF and Christina Stoffer of ESO for the organizational work before and during the Symposium, and to the ESO students and fellows, led by Harald Kuntschner, who looked after the facilities during the meeting.



The Tarantula Nebula in the Large Magellanic Cloud – ESO/MPG 2.2-m telescope (ESO PR Photo 14a/02.)

IAOC Workshop in La Serena: Galactic Star Formation across the Stellar Mass Spectrum

The growing number of first-class astronomical research facilities make Chile also a more and more attractive place for hosting scientific conferences with broad international profile and participation. Originally started as an informal, biannual workshop intended to foster the scientific interaction among the observatories in Chile, the “ESO/Tololo/Las Campanas” workshop has broadened its basis (and sponsoring institutions!), and now includes the National Radio Astronomy Observatory NRAO (as one of the main participants in the ALMA project), and the Gemini Observatory. This collection of observatories has been dubbed IAOC, International Astronomical Observatories in Chile. As its first conference, the IAOC organized a workshop on “Galactic Star

Formation across the Stellar Mass Spectrum”, held in La Serena from March 11 to 15. The aim of the workshop was to join together the most recent observational and theoretical results of Galactic star formation into a coherent picture of how stars form as a function of mass, with special focus on recent progress made in the areas of intermediate- and high-mass star formation. The high interest in the topic is documented by more than 180 conference participants, 80 from abroad. Ten invited review speakers explored the similarities and differences between low-, intermediate-, and high-mass star formation in the context of:

- Structure and Initial Conditions of the ISM and Molecular Clouds

- Initial Mass Function, Star Formation Rate, and Star Formation Efficiency
- Star Formation Theory and Supporting Observations
- Disk and Planet Formation around Stars of Increasing Mass
- Energetics (Jets, Winds, Outflows, Infall, Ionizing Radiation)
- Multiplicity of Formation
- Future Star Formation Studies at the International Observatories in Chile

Latest research results were shared in 40 contributed talks and 35 poster presentations, and an ASP conference proceedings book is already in press. Excursions to the Gemini Observatory site, and the nearby “pisco” vineyards complemented this vivid and successful workshop.
M. STERZIK

Astronomical Virtual Observatories discussed in Chile

After the meeting organized in Santiago by Conicyt in July 2001, “Large Databases for Astronomy”, the next step to be discussed was the concept of Virtual Observatory: given a set of databases, how can they be pooled into one large data resource to be searched with appropriate data mining tools? Such concepts are currently being developed both in Europe and in the US and it was felt very important that the astronomical community working in Chile be aware of and get a chance to contribute to these new visions about the astronomy of tomorrow.

Therefore, a one day Topical Meeting “Astronomical Virtual Observatories” was organized by ESO in Santiago, with the sponsorship of Conicyt, AURA, NOAO/CTIO and Gemini, on April 22nd 2002.

Attendees were from CTIO, ESO, PUC, Universidad de Chile, Universidad de Concepción, Universidad de Valparaíso and from the REUNA net-

work consortium. After the opening words by D. Alloin (Office for Science, ESO) and a brief address by C. Lazo (Executive Director Conicyt), the participants enjoyed a series of enlightening talks. The European AVO project was presented by P. Quinn (DMD, ESO), while the NVO project developed in the USA was introduced by T. Boroson (NOAO). Then we had a report by L. Campusano (U. Chile/Conicyt) about the initiatives of Conicyt on large astronomical databases in 2001. In the afternoon, the ASTROVIRTEL experiment was reported on by P. Benvenuti (ST/ECF).

Finally, three talks were devoted to archive and pipeline setup: the NOAO survey archive by D. Shaw (NOAO), the pipeline and real-time archiving at NOAO by C. Smith (CTIO) and the ESO astronomical archive by B. Pirenne (DMD, ESO). Lively discussions took place on various points including: new types of astronomical research to be

expected from VOs, data quality assessments, bandwidth accessibility in Chile, ways of involving the Chilean community in this effort/challenge, etc.

We ended the Topical Meeting with some Chilean wine tasting in order to thank the lecturers who had travelled such a long way to share with us their vision and enthusiasm about the Virtual Observatory.

Thanks also go to the secretary of the Office for Science and to the members of the IT/computing team in Vitacura who took care of the practical organization of this Topical Meeting and of the accompanying tutorial on ESO archive practice which had been organized for students at ESO on Friday April 19.

The speakers’ contributions can be found on the ESO/Santiago webpage at: <http://www.sc.eso.org/santiago/science/VO2002.html>

*DANIELLE ALLOIN and
LUIS CAMPUSANO*

Hunting for Planets – GENIE Workshop at Leiden University

The search for exo-planets has had extra-ordinary success in the last 7 years. About 80 objects classified as planets have been unambiguously detected, orbiting around nearby (10–20 pc) sun-like stars. However, finding earth-like planets requires observations

from space. Therefore, both ESA and NASA have started the technological development for space interferometers looking for a sister Earth. For ESA’s DARWIN project, European industry is working on laboratory experiments to verify the concept of Nulling interferom-

etry which is well suited for directly detecting planets.

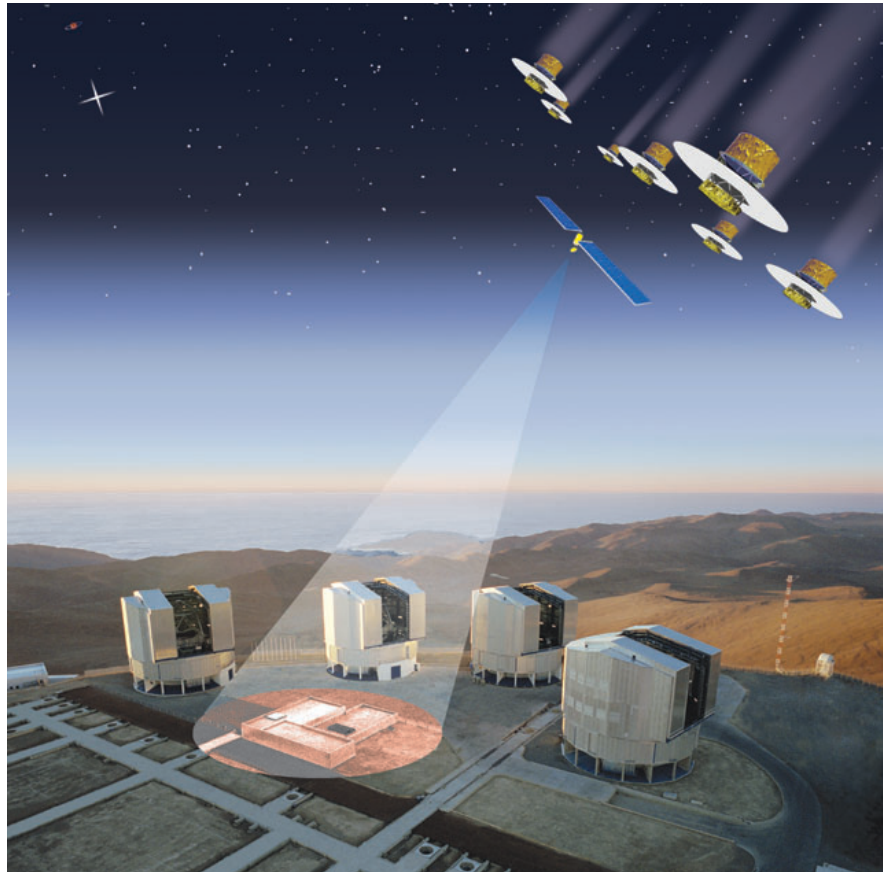
In preparation for DARWIN, ESA and ESO have decided to collaborate on GENIE, the Ground Based European Nulling Interferometer Experiment for the VLTI. The goal is both to test the

necessary technology in a real interferometer environment and to become a full facility science instrument for the VLTI.

From June 3–6 a workshop took place at Leiden University, jointly organised by NEVEC, ESA and ESO, to discuss the Nulling technology and the science that is expected with GENIE. The number of participants, 83 in total, exceeded the expectations by far and demonstrated the large interest of the community in this subject.

The GENIE concepts discussed during the workshop concentrate on a two/four-way beam combiner operating in the infrared (L, M or N band). Although the N band is better suited for detecting planets from space, on the ground the calibration of the enormous thermal background poses a severe problem. Therefore the question remains open as to whether the L/M bands are better suited for DARWIN system tests. The science objective of GENIE is to observe a couple of hundred candidate stars for DARWIN in order to measure the zodiacal light and bright extra-solar planets. Many other science programmes (AGN, binary stars, T Tauri disks around young stars, or debris disks around main sequence stars) with faint matter close to a bright source could also take advantage of GENIE. Kick-off for GENIE is in summer 2002, and the instrument is scheduled for commissioning in 2006.

Andreas Glindemann

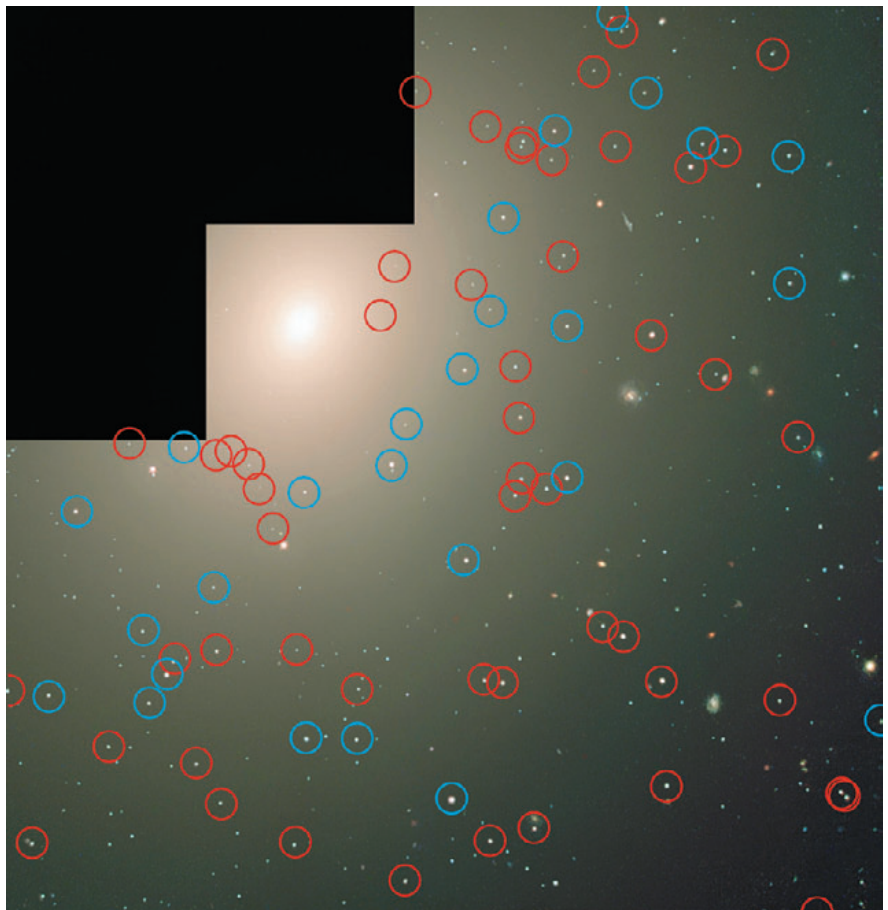


The poster image for the GENIE workshop held recently in Leiden. It shows an artist's impression of a possible DARWIN space interferometer superimposed on a photograph of the VLT/VLTI, with the central beam combining satellite highlighting the VLTI beam combination laboratory. Figure courtesy of NEVEC.

Young Stars in Old Galaxies – a Cosmic Hide and Seek Game

A group of researchers around M. Kissler-Patig (ESO) studies the formation and evolution history of galaxies through the study of their globular clusters. Recently, the combination of optical and near-infrared images allowed them to detect a “young” population in a galaxy that was believed to be old. Are some old ellipticals hiding their true story? (See ESO Press Release 11/02.)

The figure shows a colour composite of the elliptical galaxy NGC 4365, prepared from two exposures with the HST and one from the VLT. Many of the objects seen are stellar clusters in this galaxy. There are also a large number of background galaxies in the field. The distribution of “old” (red circles) and “young” (blue circles) stellar clusters in NGC 4365 are shown.



Information from the ESO Educational Office

A. BACHER AND R.M. WEST (ESO EPR DEPT.)

The ESO Educational Office is involved in several on-going projects, some of which take place within ESO and others which are carried out in collaboration with some of the other European Intergovernmental Research Organisations (EIRO). In this connection, the co-ordination that is now taking place via the EIROforum Working Group on Outreach and Education is playing an increasingly important role. The close and efficient collaboration with the European Association for Astronomy Education (EAAE) continues.

Physics on Stage

Following the extremely successful "Physics on Stage" that took place during the year 2000, a second event in this series was organised in April 2002, mainly through the initiative of ESA, but again in full collaboration with CERN, ESO and some of the other EIROs. More than 300 participants met at ESTEC in Noordwijk (The Netherlands) during a one-week conference, also this time with active participation of high-level officials, among others the Dutch Minister for Research and also the European Commissioner for Research, Philippe Busquin (see photo). On this occasion, the European Science Teaching Award for outstanding education efforts was given for the first time.

There is an obvious and urgent need for continuation of this type of programme which has proven exceptional-

ly stimulating for physics teachers from all over Europe. The EIROFORUM Working Group has therefore made a joint application to the European Commission (EC) for "Physics on Stage 3" in 2003, again under the auspices of the European Science and Technology Week. On this occasion, it is the intention to widen the programme towards other research disciplines, e.g. biochemistry and to increase the number of participating countries to approximately 30. A new element will be a thorough evaluation of the project impact.

For the future, plans are being developed by the EIRO Working Group for a longer-term collaborative project within the 6th Framework Programme of the European Union.

Catch a star!

Within this year's European Science Week, a joint project between ESO and the EAAE, known as "Catch a Star!", has been set up at short notice, following an idea by EAAE Vice-President Rosa Maria Ros (Spain). The central idea is that groups of up to three students and one teacher at a primary and secondary schools in Europe will "catch" a celestial object of their choice, which they must then describe in some detail in a corresponding report. Full details are available at the project website at: <http://www.eso.org/outreach/eduoff/catchastar/>



"Catch a Star!" logo.

By mid-June, about 130 projects with more than 500 participants had been registered. To participate in the final round, the groups must send their reports to the organisers who will evaluate them; those which are accepted will be placed on the project website, ultimately representing a tremendous source of useful information, especially for educators. The winners will be drawn by lottery with the first prize being a trip to the Paranal Observatory. However, there will also be many other prizes and the first 1000 participants will also receive a "Catch a Star!" T-shirt.

Couldn't be without it

Parallel to that ESO/EAAE educational project, the seven EIROs are organising another Europe-wide programme, known as "Couldn't Be Without It" (cf. <http://info.web.cern.ch/info/scitech/>). It aims at explaining to the wide public how basic science is behind virtually all of the technology on which our daily lives depend. We are only able to enjoy mobile phones, fast and safe means of transport, effective household machines etc., because many generations of industrious scientists have worked hard to unravel nature's secrets. This programme involves the production of numerous teaching kits for schools and there will be a wide range of prizes to win for the participating public. It terminates with a final, spectacular webcast from CERN in November this year.



At the Final Event of "Physics on Stage 2" (ESTEC, Noordwijk, The Netherlands): European Commissioner Philippe Busquin (front row) listens to Danish physics teacher Mogens Winther.

FAST 2002

15 European high-school teachers with a special affinity to astronomy will participate in the first teachers' training course organised by ESO (FAST 2002, cf. <http://www.eso.org/outreach/eduoff/fast2002/>). During one week in August 2002 they will listen to lectures by ESO scientists and participate in workshops mainly oriented towards new means and methods for astronomy courses at high-school level. Both the teachers and the ESO Educational Office will gain a lot of experience from this first event - and it is the intention to organise more such courses during the coming years. These courses supplement the more general EAAE Summer Schools that are also supported by ESO.

Also in this context, the ESO/ESA Astronomy Exercise Series (see Messenger 107, page 44) has been greatly

appreciated by the teaching community. More than 500 requests have been received during the past months from teachers all over the world and many others have taken over these exercises from the dedicated website (<http://www.astroex.org/>). In view of this very encouraging development, it has been decided to translate these exercises into other languages; Dutch, French and Italian versions will soon become available.

Venus Transit 2004

Finally, and again in a close collaboration between ESO and the EAAE (and most likely with other future partners), another educational programme ("Venus Transit 2004") that also has the potential to develop into an exceptional public and media event is now in the process of being defined. It concerns

the rare astronomical event that takes place on June 8, 2004, when the planet Venus will move in front of ("transit") the solar disk - the most recent such event was in 1882; the next will be in 2012 and 2117. It is the intention to involve the general public directly by providing easy-to-understand information about how this phenomenon can be observed with simple means. By means of numerous timing observations from different geographical locations, it is possible to deduce the solar parallax (with some uncertainty), in other words the distance to the Sun, and hence to climb the first step on the cosmic distance ladder. Look at <http://www.eso.org/outreach/eduoff/vt-2004/> for more information, as this ambitious programme is being developed during the coming months, in consultation with collaborators at Europe's schools and planetaria.

ESO in the European Parliament

Astronomy and Astrophysics is not normally at the centre of attention at the highest political circles in Europe. However, the renaissance that our science is currently experiencing, not least based on the spectacular success of the VLT, has not gone unnoticed among the decision makers in Europe.

For ESO, both the entry of additional member-states and the new and future projects that aim at providing a solid base for the further development of European Astronomy and Astrophysics, have had considerable effects. At the same time, ESO's technological and scientific successes demonstrate the advantages and great capabilities of a focussed and concerted European effort within an important field of fundamental science.

Taking account of this, the Committee for Industry, Trade, Research and Energy (ITRE) of the European Parliament decided to organise a 90-min Mini-hearing under the title 'Cutting Edge Science - A New Epoch for European Astrophysics'. This important event took place on 27 May in the Paul-Henri Spaak building of the European Parliament in Brussels. It was chaired by Mr Carlos Westendorp y Cabeza, former Minister of Foreign Affairs for Spain and now chairman of the ITRE Committee. The prime goal of the meeting was to give information about the many aspects of contemporary astronomical research, from the current state of the science itself through the advanced technologies employed and on to the related, societal aspects. As could be expected, the plans for future infrastructures and large facilities played a significant role in the discussion.

Addressing the committee members for ESO were Dr Catherine Cesarsky, Dr Roberto Gilmozzi and Dr Richard West, while Prof. Francisco Sanchez spoke on behalf of the Instituto de Astrofísica de Canarias (IAC). The deputies expressed strong interest in the comprehensive information pre-

sented and they followed up with their own views in a subsequent, lively debate. It was evident that both the aspect of European competitiveness in science and technology and the model function of Astronomy was fully registered by the parliamentarians.

C. MADSEN, ESO

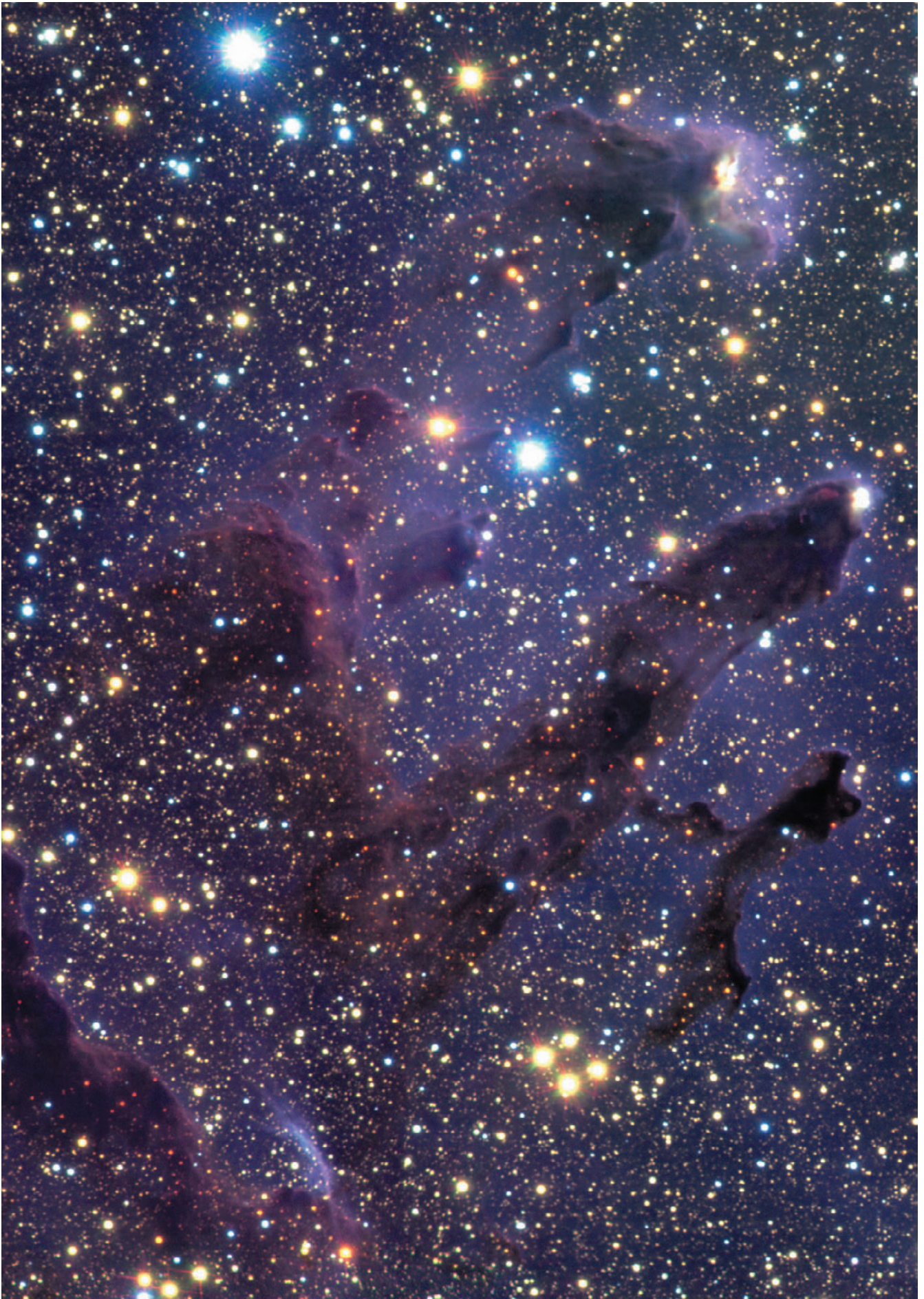
Obituary KURT HUNGER

On May 27, 2002 Prof. Kurt Hunger passed away at an age of 80. Kurt Hunger was a true European and a passionate and active supporter of the European Southern Observatory. He served on many ESO committees such as the OPC, which he chaired for several years, and the Council. He was President of the ESO Council from 1985 to 1987, a period extremely important for the organization. During this time Kurt Hunger together with Lo Woltjer as Director General became the driving forces in the promotion of the VLT project in the member countries. Their success provided the basis for the development of ESO into the next century as one of the most powerful observatories in the world and a focal point of astronomical research in Europe.

Kurt Hunger studied physics and astronomy as a student of Albrecht Unsöld at Kiel University. His research focussed on quantitative stellar spectroscopy and the physics of stellar atmospheres. After several years of research in the USA he returned to Germany in 1968 to take on a professorship at the Technical University of Berlin, where he started to build up the Institute for Astrophysics. His work was extremely fruitful. He was very quickly able to form a group of active researchers and students and to establish astrophysics in Berlin in a very complicated period at the universities. In 1976 he accepted a chair of astrophysics at the University of Kiel. This was the beginning of the development of a new school of model atmospheres, radiative transfer and quantitative spectroscopy, which became one of the most successful groups in European astronomy. Many of his students pursued successful careers in astronomy and became professors or lecturers at German universities. They all met in September 2001 in Kiel to celebrate Kurt Hunger's 80th birthday in a two day science workshop dedicated to stellar spectroscopy. It was a deeply moving moment, when Kurt presented a science paper on the chemical composition of helium stars.

Those of us, who had the privilege to learn from him and to work with him, will remember Kurt Hunger as a teacher and as a colleague, who was always on our side, helpful and supportive. He was a man of great vision and of a great heart.

ROLF-PETER KUDRITZKI
Institute for Astronomy, University of Hawaii



The "Pillars of Creation" in the Eagle Nebula, in infrared light – VLT Antu+ISAAC. Image by Mark McCaughrean and Morton Andersen, Astrophysical Institute Potsdam. (ESO PR Photo 37b/01.)

German Foreign Minister Visits Paranal Observatory

Replicated from ESO Press Release 02/02 (7 March 2002)



Figure 1: Minister Fischer (left) is received at the entrance to the Observatory by the ESO Representative in Chile, Daniel Hofstadt.

During his tour of countries in South America, the Honourable Foreign Minister of Germany, Mr. Joschka Fischer, stopped over at the ESO Paranal Observatory on the night of Wednesday, March 6–7, 2002.

Arriving in Antofagasta, capital of the II Chilean region, the Foreign Minister and his suite was met by local Chilean officials, headed by Mr. Jorge Molina, Intendente of the Region, as well as His Excellency, the German Ambassador to Chile, Mr. Georg CS Dick and others. In the afternoon of March 6, the Foreign

Minister, accompanied by a distinguished delegation from the German Federal Parliament as well as by businessmen from Germany, travelled to Paranal, site of the world's largest optical/infrared astronomical facility, the ESO Very Large Telescope (VLT).

The delegation was welcomed by the Observatory Director, Dr. Roberto Gilmozzi, the VLT Programme Manager, Professor Massimo Tarenghi, the ESO Representative in Chile, Mr. Daniel Hofstadt and ESO staff members, and also by Mr. Reinhard Junker, Deputy Direc-

tor General (European Co-operation) at the German Ministry for Education and Research.

The visitors were shown the various high-tech installations at this remote desert site, some of which have been constructed by German firms. Moreover, most of the large, front-line VLT astronomical instruments have been built in collaboration between ESO and European research institutes, several of these in Germany.

One of the latest arrivals to Paranal, the CONICA camera, was built under an ESO contract by the Max-Planck Institutes for Astronomy (MPIA, in Heidelberg) and Extraterrestrial Physics (MPE, in Garching).

The guests had the opportunity to enjoy the spectacular sunset over the Pacific Ocean from the terrace of the new Residencia building. At the beginning of the night, the Minister was invited to the Control Room for the VLT Interferometer (VLTI) from where this unique new facility is now being thoroughly tested before it is put into service later this year.

In his expression of thanks, Minister Fischer enthusiastically referred to his visit at Paranal. He said he was truly impressed by the technology of the telescopes and considered the VLT project a model of European technological and scientific cooperation.

Later in the evening, the Minister was invited to perform an observing sequence at the console of the MELIPAL telescope.



Figure 2: During the visit to the observing platform at the top of Paranal: from left to right, the Minister, VLT-Program-Manager Massimo Tarenghi and Observatory Director Roberto Gilmozzi.

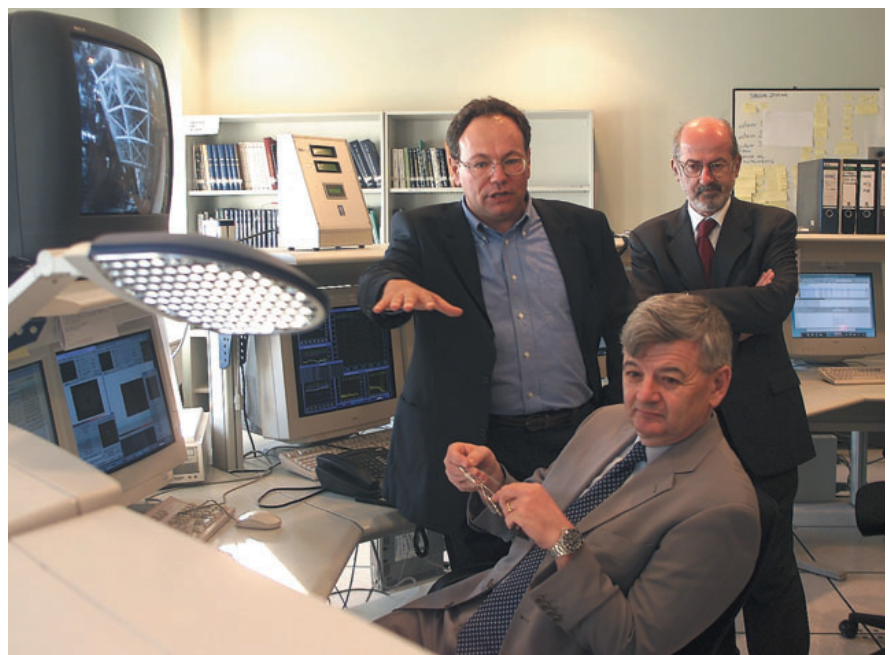


Figure 3: The Minister, seated at the control console for the VLT ANTU telescope (Roberto Gilmozzi and Massimo Tarenghi in the background).

ANNOUNCEMENTS

The Very Large Telescope Interferometer: Challenges for the Future

A JENAM 2002 Workshop to be held at Porto, Portugal on September 4-7

Sponsored by the European Southern Observatory

The last quarter of a century witnessed the maturing of optical interferometry and associated technologies. The third millennium started with common user facilities achieving first light: the Keck Interferometer, the Very Large Telescope Interferometer (VLTI), and the CHARA array.

The VLTI provides a unique combination of sensitivity and number of baselines therefore opening to the ESO community a mostly unexplored astrophysical territory. The challenge to the community is to make the VLTI a productive science machine.

This workshop will address optical interferometry science. It will start with a presentation of interferometry basics and of the VLTI instrumentation (AMBER/MIDI). Most of the workshop is devoted to the presentation of the current status and future prospects of interferometry science in the fields of exoplanets, stellar parameters and binary stars, young stellar object accretion disks and outflows, imaging stars and their environments, stellar shells, pulsations and mass loss, nuclear regions of AGNs - torus and broad line regions and radio jets, etc. The workshop will end with a look at competing/complementary facilities and a round table discussion on future directions in optical interferometry science and instrumentation.

More details are available at:

<http://www.sp-astronomia.pt/jenam2002/ws-vlti> or contact ws-vlti@sp-astronomia.pt

Workshop Scientific Organizing Committee:

M. Fridlund (ESA), A. Glindeman (ESO), C. Haniff (UK), T. Henning (Germany), F. Malbet (France), D. Queloz (Switzerland), A. Quirrenbach (Netherlands/USA), L. Testi (Italy) and P. Garcia (Portugal).

PERSONNEL MOVEMENTS

International Staff

(1 April – 30 June 2002)

ARRIVALS

EUROPE

BERGOND, Gilles (F), Associate
BÖCKER, Michael (D), Safety Engineer
DIETRICH, Jörg (D), Associate
HAASE, Jonas (DK), Astronomical Data Archive and
Pipeline Software Specialist
HARTUNG, Markus (A), Student
SCHEDL, Iris (A), Secretary

CHILE

DE FIGUEIREDO MELO, Claudio (BR), Fellow
FOELLM, Cédric (CH), Operations Astronomer
SANGASSET, Pierre (F), Mechanical Engineer
SMOKER, Jonathan (GB), Operations Staff Astronomer
WILLIS, Jon (GB), Fellow
ZALTRON, Paolo (I), Associate

DEPARTURES

EUROPE

CABANERO RODRIGUEZ, Susana (E), Student

CRISTIANI, Stefano (I), Instrument Scientist
DARBON GONCALVES, Anabela (P), Fellow
HESS, Joachim (D), Associate
QUEBATTE, Jean (CH), Manager ESO Photolab
TÜLLMANN, Ralph (D), Student

CHILE

KÜRSTER, Martin (D), Astronomer
LAGER, Michael (S), Associate SEST
MADEJSKY, Rainer (D), Associate
PINTE, Christophe (F), Associate

Local Staff

(1 March 2002 – 30 May 2002)

ARRIVALS

ROZAS PAYCHO, Felix Alberto, Maintenance Technician

DEPARTURES

DELGADO BORQUEZ, Francisco, Software Engineer
ROJAS BARRA, Manuel, Telescope Instruments Operator

ESO Fellowship Programme 2002/2003

The European Southern Observatory (ESO) awards several postdoctoral fellowships tenable at the ESO Headquarters, located in Garching near Munich, and at ESO's Astronomy Centre in Santiago, Chile. The ESO fellowship programme offers a unique opportunity for young scientists to pursue their research programmes while learning and participating in the process of observational astronomy with state-of-the-art facilities. ESO facilities include the Very Large Telescope (VLT) Observatory on Cerro Paranal, the La Silla Observatory and the astronomical centres in Garching and Santiago. ESO operates optical telescopes with apertures in the range from 2 m to 8 m, and the 15-m SEST millimetre radio telescope.

The main areas of activity are:

- research in observational and theoretical astrophysics;
- developing the interferometer and adaptive optics for the VLT;
- operating the Paranal and La Silla Observatories;
- development of instruments for current ESO telescopes;
- calibration, analysis, management and archiving of data from the current ESO telescopes;
- developing the Atacama Large Millimeter Array (ALMA);
- fostering co-operation in astronomy and astrophysics within Europe and Chile.

The main scientific interest of ESO Faculty astronomers in Garching and in Chile are given in the ESO web site (<http://www.eso.org/science/facultymembers.html>).

Both the ESO Headquarters and the Astronomy Centre in Santiago offer extensive computing facilities, libraries and other infrastructure for research support.

There are ample opportunities for scientific collaborations. The ESO Headquarters host the Space Telescope European Coordinating Facility (ST-ECF) and are situated in the immediate neighbourhood of the Max-Planck Institutes for Astrophysics and for Extraterrestrial Physics and are only a few kilometers away from the Observatory of the Ludwig-Maximilian University. In Chile, ESO fellows have the opportunity to collaborate with the rapidly expanding Chilean astronomical community in a growing partnership between ESO and the host country's academic community.

Fellows in Garching spend up to 25% of their time on the support or development activities mentioned above, in addition to personal research. They can select functional activities in one of the following areas: instrumentation, user support, archive, VLTI, ALMA or science operations at the Paranal Observatory. Fellowships in Garching start with an initial contract for one year normally followed by a two-year extension.

In Chile, the fellowships are granted for one year initially with an extension of three additional years. During the first three years, the fellows are assigned to either the Paranal or La Silla operations groups. They support the astronomers in charge of operational tasks at a level of 50% of their time, with 80 nights per year at either the Paranal or La Silla Observatory and 35 days per year at the Santiago Office. During the fourth year there is no functional work and several options are provided. The fellow may be hosted by a Chilean institution and will thus be eligible to propose for Chilean observing time on all telescopes in Chile. The other options are to spend the fourth year either at ESO's Astronomy Centre at Santiago, Chile, or the ESO Headquarters in Garching, or an institute of astronomy/astrophysics in an ESO member state.

We offer an attractive remuneration package including a competitive salary (tax-free), comprehensive social benefits, and provide financial support in relocating families. Furthermore, an expatriation allowance as well as some other allowances may be added. The Outline of the Terms of Service for Fellows (<http://www.eso.org/gen-fac/adm/pers/fellows.html>) provides some more details on employment conditions/benefits.

Candidates will be notified of the results of the selection process in February 2003. Fellowships begin between April and October of the year in which they are awarded. Selected fellows can join ESO only after having completed their doctorate.

Applications must be made on the ESO Fellowship Application Form at <http://www.eso.org/gen-fac/adm/pers/forms/index.html>. The applicant should arrange for three letters of recommendation from persons familiar with his/her scientific work to be sent directly to ESO. Applications and the three letters must reach ESO by October 15, 2002.

Completed applications should be addressed to:

European Southern Observatory

Fellowship Programme

Karl-Schwarzschild-Str. 2, 85748 Garching bei München, Germany

vacancy@eso.org

Contact person: Angelika Beller, Tel. +49 89 320 06-553, Fax +49 89 320 06-490, e-mail: abeller@eso.org

LIST OF SCIENTIFIC PREPRINTS

March–June 2001

1460. J.P.U. Fynbo, P. Møller, B. Thomsen, J. Hjorth, J. Gorosabel, M.I. Andersen, M.P. Egholm, S. Holland, B.L. Jensen, H. Pedersen and M. Weidinger: Deep Ly α imaging of two $z=2.04$ GRB host galaxy fields. *A&A*.
1461. L. Vanzì, S. Bagnulo, E. Le Floc'h, R. Maiolino, E. Pompei, W. Walsh: Multi-wavelength Study of IRAS 19254-7245 – The Superantennae. *A&A*.
1462. J. Reunanen, J.K. Kotilainen, M.A. Prieto: Near-infrared spectroscopy of nearby Seyfert galaxies. I. First results. *MNRAS*.
1463. M. Contini, S.M. Viegas, M.A. Prieto: The signature of high velocity gas in the spectra of NGC 4151. *A&A*.
1464. G. Li Causi, G. De Marchi, F. Paresce: On the accuracy of the S/N estimates obtained with the exposure time calculator of the Wide Field Planetary Camera 2 on board the Hubble Space Telescope. *PASP*.
1465. F. Comerón, A. Pasquali, G. Rodighiero, V. Stanishev, E. De Filippis, B. López Martí, M.C. Gálvez Ortiz, A. Stankov, R. Gredel: On the massive star contents of Cygnus OB2. *A&A*.

ESO, the European Southern Observatory, was created in 1962 to "... establish and operate an astronomical observatory in the southern hemisphere, equipped with powerful instruments, with the aim of furthering and organising collaboration in astronomy..." It is supported by nine countries: Belgium, Denmark, France, Germany, Italy, the Netherlands, Portugal, Sweden and Switzerland, soon to be joined by the United Kingdom. ESO operates at two sites in the Atacama desert region of Chile. The new Very Large Telescope (VLT), the largest in the world, is located on Paranal, a 2,600 m high mountain approximately 130 km south of Antofagasta, in the driest part of the Atacama desert where the conditions are excellent for astronomical observations. The VLT consists of four 8.2-metre diameter telescopes. These telescopes can be used separately, or in combination as a giant interferometer (VLTI). At La Silla, 600 km north of Santiago de Chile at 2,400 m altitude, ESO operates several optical telescopes with diameters up to 3.6 m and a submillimetre radio telescope (SEST). Over 1300 proposals are made each year for the use of the ESO telescopes. The ESO headquarters are located in Garching, near Munich, Germany. This is the scientific, technical and administrative centre of ESO where technical development programmes are carried out to provide the Paranal and La Silla observatories with the most advanced instruments. There are also extensive astronomical data facilities. ESO employs about 320 international staff members, Fellows and Associates in Europe and Chile, and about 160 local staff members in Chile.

The ESO MESSENGER is published four times a year: normally in March, June, September and December. ESO also publishes Conference Proceedings, Preprints, Technical Notes and other material connected to its activities. Press Releases inform the media about particular events. For further information, contact the ESO Education and Public Relations Department at the following address:

EUROPEAN
SOUTHERN OBSERVATORY
Karl-Schwarzschild-Str. 2
D-85748 Garching bei München
Germany
Tel. (089) 320 06-0
Telefax (089) 3202362
ips@eso.org (internet)
URL: <http://www.eso.org>
<http://www.eso.org/gen-fac/pubs/messenger/>

The ESO Messenger:
Editor: Peter Shaver
Technical editor: Kurt Kjær

Printed by
Universitätsdruckerei
WOLF & SOHN
Heidemannstr. 166
D-80939 München
Germany

ISSN 0722-6691

1466. D. Heath Jones, Ben W. Stappers, Bryan M. Gaensler: Discovery of an optical bow-shock around pulsar B0740-28. *A&A*.
1467. T.-S. Kim, R.F. Carswell, S. Cristiani, S. D'Odorico, E. Giallongo: The Physical Properties of the Ly α Forest at $z > 1.5$. *MNRAS*.
1468. L. Vanzi, L.K. Hunt, T.X. Thuan: Near-infrared properties of Blue Compact Dwarf Galaxies: the link between solar and low metallicity. *A&A*.

A Note from the New Editor

It is a pleasure to serve as editor of *The Messenger*, and to work with my colleague Kurt Kjær, the technical editor, in this endeavour. This task is made easier by the fact that *The Messenger* has been developed to such high standards over the years, and for this I am most grateful to my predecessors, in particular Marie-Hélène Ulrich who has served in this position for the last eight years.

PETER SHAVER

Contents

Catherine Cesarsky: United Kingdom Becomes Tenth Member of ESO 1

TELESCOPES AND INSTRUMENTATION

G. Monnet: Status of VLT 2nd Generation Instrumentation 2
R. Hanuschik and D. Silva: VLT Quality Control and Trending Services 4
Recent NAOS-CONICA Images 9
L. Germany: News from La Silla 10

REPORTS FROM OBSERVERS

G. Hasinger, J. Bergeron, V. Mainieri, P. Rosati, G. Szokoly and the CDFS Team: Understanding the sources of the X-ray background: VLT identifications in the *Chandra/XMM-Newton* Deep Field South 11
Carne Gallart, Robert Zinn, Frederic Pont, Eduardo Hardy, Gianni Marconi, Roberto Buonnanno: Using color-magnitude diagrams and spectroscopy to derive star formation histories: VLT observations of Fornax 16
Thomas Rivinius, Dietrich Baade, Stanislav Štefl, Monika Maintz, Richard Townsend: The ups and downs of a stellar surface: Nonradial pulsation modelling of rapid rotators 20
L. Pentericci, H.W. Rix, X. Fan, M. Strauss: The VLT and the most distant quasars 24
Daniel Harbeck, Eva K. Grebel, Graeme H. Smith: Evidence for external enrichment processes in the globular cluster 47 Tuc? 26

OTHER ASTRONOMICAL NEWS

Steve Warren: The UKIRT Infrared Deep Sky Survey becomes an ESO public survey 31
M. Jacob, P. Shaver, L. Dilella, A. Gimenez: Summary of the ESO-CERN-ESA Symposium on Astronomy, Cosmology and Fundamental Physics . . . 35
M. Sterzik: IAOC Workshop in La Serena: Galactic Star Formation across the stellar Mass Spectrum 40
Danielle Alloin and Luis Campusano: Astronomical Virtual Observatories discussed in Chile 40
Andreas Glindemann: Hunting for Planets – GENIE Workshop at Leiden University 40
Young Stars in Old Galaxies – a Cosmic Hide and Seek Game 41
A. Bacher and R.M. West: Information from the ESO Educational Office . . . 42
C. Madsen: ESO in the European Parliament 43
Rolf-Peter Kudritzki: Obituary Kurt Hunger 43
German Foreign Minister Visits Paranal Observatory 45

ANNOUNCEMENTS

The Very Large Interferometer: Challenges for the Future (A Jenam 2002 Workshop to be held at Porto, Portugal, on September 4–7) 46
Personnel Movements 46
ESO Fellowship Programme 2002/2003 47
List of Scientific Preprints (March–June 2001) 47
A Note from the New Editor 48